Value recovery from mine calcine tailings

by

Paul Mutimutema

Thesis presented in partial fulfilment
of the requirements for the Degree

of

MASTER OF ENGINEERING
(EXTRACTIVE METALLURGICAL ENGINEERING)

in the Faculty of Engineering
at Stellenbosch University

Supervisor
Dr Margreth Tadie

Co-Supervisor
Prof. Guven Akdogan

March 2021

DECLARATION

By submitting this thesis electronically, I declare that the entirety of the work contained therein is my own, original work, that I am the sole author thereof (save to the extent explicitly otherwise stated), that reproduction and publication thereof by Stellenbosch University will not infringe any third party rights and that I have not previously in its entirety or in part submitted it for obtaining any qualification.

Date: March 2021

PLAGIARISM DECLARATION

1. Plagiarism is the use of ideas, material and other intellectual property of another's work and to present is as my own.

2. I agree that plagiarism is a punishable offence because it constitutes theft.

3. I also understand that direct translations are plagiarism.

4. Accordingly, all quotations and contributions from any source whatsoever (including the internet) have been cited fully. I understand that the reproduction of text without quotation marks (even when the source is cited) is plagiarism.

5. I declare that the work contained in this assignment, except where otherwise stated, is my original work and that I have not previously (in its entirety or in part) submitted it for grading in this module/assignment or another module/assignment.

Initials and surname: P. Mutimutema

Date: March 2021

Abstract

As gold mining progresses, rich and free-milling ores which are metallurgically easy to process eventually get depleted. More metallurgically complex ores are encountered. These ores yield gold recoveries below 80% and are termed refractory ores.

The South African gold mining industry has left a legacy of abundant tailings dams – some of which are an environmental hazard due to the formation of acid mine drainage (AMD), discharge of metalloids, and or radioactive dust storms. Processing of tailings dams has slowly attracted the attention of investors as it is potentially cheaper to mine on the surface than shaft mining, in addition to having a lower exposure to risk associated with fatalities from mine shaft incidents.

The possibility of recovering gold from a calcine tailings heap was considered in this study. Due to the refractory nature of the host ore from which they were generated, a mineralogical characterization was performed to understand the nature and occurrence of the gold.

Fire assay revealed a gold grade of 2.96 ± 0.26 g/t. X-ray diffraction (XRD) and quantitative evaluation of minerals by scanning electron microscopy (QEMSCAN) both confirmed that silicates were the most abundant phase followed by iron oxide. Scanning electron microscopy (SEM) showed that gold existed in submicron and micron size, as free gold, and also as refractory gold associated with arsenic, sulfur and silicates like quartz and talc. These mineralogical findings influenced the selection of extraction routes for investigation to recover the gold. Therefore, ultrafine milling, microwave roasting, microwave assisted cyanide leaching and sodium hydroxide pre-leach treatment were the methods potentially considered to recover the gold.

Firstly, in order to confirm the degree of refractoriness of the tailings a series of direct cyanidation tests were conducted on the calcine tailings which resulted in average 17.3% gold recovery. Because of the confirmed high refractoriness, ultrafine milling of the original tailings (P_{80} — 53 µm) to P_{80} — 16 µm followed by cyanidation increased the gold recovery to 66.5%. Breaking of the host phases by ultrafine milling was beneficial.

Microwave roasting pre-treatment on the as received sample (original calcine tailings) proved effective as compared to the ultrafinely ground calcine tailings sample. A 43.7% gold cyanidation recovery was obtained for the as received sample after microwave roasting for 60 minutes. Addition of 6% water was also effective on the as received sample, and yielded a

42.6% gold cyanidation recovery after undergoing 30 minutes of microwave roasting. A cyanidation gold recovery of 68.4% was attained after 30 minutes of microwave roasting the ultrafine sample. Microwave assisted cyanidation had rapid kinetics. In 50 minutes, 56.8% gold recovery was attained on the ultrafine sample at a sodium cyanide dose of 8 kg/t.

Application of sodium hydroxide pre-leach treatment was beneficial by leaching gangue related elements in gold carrier phases (e.g. quartz and talc) into solution. Ambient temperature pre-leach at 1 M sodium hydroxide gave a 51.6% cyanidation gold recovery on the as received tailings sample after 24 hours. The ultrafine milled sample, after ambient pre-leach at 1 and 3 M sodium hydroxide, exhibited fast leaching rates, and maximum cyanidation gold recoveries of 71.9% and 77.6% respectively were obtained after 8 hours. Heat assisted pre-leach on a hot plate, however, did not result in improved gold cyanidation recoveries for both grinds and sodium hydroxide concentrations.

Based on the experimental findings, three process flowsheets were considered. The gold mass balance for each flowsheet was completed. The flowsheet which incorporated sodium hydroxide pre-leach treatment was chosen as the best as it achieved the highest cyanidation gold recovery of 77.6%.

Opsomming

Soos goudmynbou voortgaan, word ryk en vrymaalerts wat metallurgies maklik is om te prosesseer eventueel uitgeput. Meer komplekse metallurgiese erts word teëgekom. Hierdie erts bring goudherwinning onder 80% op en word weerbarstige erts genoem.

Die Suid-Afrikaanse goudmynindustrie het ’n erfenis van oorvloedige uitskotdamme –waarvan sommige ’n omgewingsrisiko is as gevolg van die formasie van suurmyndreinering (AMD), afskeiding van metalloïdes, en of radioaktiewe stofstorms. Prosessering van uitskotdamme het die aandag van beleggers stadig getrek omdat dit potensieel goedkoper is om op die oppervlak te myn as skagmynbou, saam met die laer blootstelling aan risiko geassosieer met noodlottighede van mynskaginsidente.

Die moontlikheid om goud te herwin van ’n kalsienuitskothoop is oorweeg in hierdie studie. As gevolg van die weerbarstige natuur van die gasheererts waarvan dit gegenereer is, is ’n mineralogiese karakterisering uitgevoer om die natuur en voorkoms van die goud te verstaan.

Vuuressai het ’n goudgraad van 2.96 ± 0.26 g/t getoon. X-straaldiffraksie (XRD) en kwantitatiewe evaluasie van minerale deur elektron mikroskopie skandering (QEMSCAN) het beide bevestig dat silikate die mees oorvloedige fase was, gevolg deur ysteroksied. Elektron mikroskopie skandering (SEM) het getoon dat goud bestaan het in submikron- en mikrongrotes, as vrye goud, en ook as weerbarstige goud geassosieer met arseen, swael en silikate soos kwarts en talk. Hierdie mineralogiese bevindinge het die keuring van ekstraksieroetes wat ondersoek is vir goudherwinning, beïnvloed. Daarom is ultrafyn malery, mikrogolfoond braaiery, mikrogolfoond-geassisteerde sianiedloging en seepsoda voorlogingsbehandeling die metodes wat potensieel oorweeg is om goud te herwin.

Eerstens, om die graad van weerbarstigheid van die uitskotte te bevestig, is ’n reeks direkte sianidisasietoetse uitgevoer op die kalsienuitskotte wat op gemiddeld 17.3% goudherwinning tot gevolg gehad het. As gevolg van die bevestigde hoë weerbarstigheid, het ultrafyn malery van die oorspronklike uitskotte (P_{80} — 53 µm) na P_{80} — 16 µm gevolg deur sianidisasie die goudherwinning tot 66.5% verhoog. Die breek van die gasheerfases deur ultrafyn malery was voordelig.

Mikrogolfbraaiingvoorbehandeling op die soos-ontvangde steekproef (oorspronklike kalsienuitskot) is as doeltreffend bewys in vergelyking met die ultrafyn gemaalde kalsienuitskotsteekproef. ’n 43% goud sianidisasie herwinning is verkry vir die soos-ontvangde

steekproef na mikrogolfbraaiing vir 60 minute. Byvoeging van 6% water was ook doeltreffend op die soos-ontvangde steekproef, en het ’n 42.6% goud sianidisasie herwinning opgebring na 30 minute se mikrogolfbraaiing. ’n Sianidisasie goudherwinning van 68.4% is verkry nadat die ultrafyn steekproef vir 30 minute in die mikrogolf gebraai is. Mikrogolf-geassisteerde sianidisasie het vinnige kinetika gehad. In 50 minute is 56.8% goud herwinning op die ultrafynsteekproef verkry by ’n natrium-sianieddosering van 8 kg/t.

Toepassing van seepsoda voorlogingbehandeling was voordeling by logings van aarsteen-verwante elemente in gouddraendefases (bv. kwarts en talk) in oplossing in. Omgewingstemperatuur voorloging by 1 M seepsoda het 51.6% sianidisasie goudherwinning op die soos-ontvangde uitskotsteekproef na 24 uur gegee. Die ultrafyn gemaalde steekproef, na omgewingsvoorloging by 1 en 3 M seepsoda, het vinnige logingstempo’s getoon, en maksimum sianidisasie goudherwinning van 71.9% 3 en 77.6% onderskeidelik verkry, na 8 ure. Hitte-geassisteerde voorloging op ’n warm plaat het egter nie tot verbeterde goud sianidisasie herwinning gelei vir beide male en seepsodakonsentrasies nie.

Gebaseer op die eksperimentele bevindinge, is drie prosesvloeidiagramme oorweeg. Die goudmassabalans vir elke vloeidiagram is voltooi. Die vloeidiagram wat seepsodavoorlogingbehandeling geïnkorporeer het, is gekies as die beste omdat dit die hoogste sianidisasie goudherwinning, van 77.6%, bereik het.

Acknowledgements

I would like to express my heartfelt appreciation to my Heavenly Father who gave me the grace to walk my Master's journey.

The following individuals and organizations to mention, made a tremendous impact to the completion of this project:

- Dr Margreth Tadie and Prof Guven Akdogan, my supervisors, who were always there to advise, guide and support me. Their contributions were invaluable.
- Flair Research who provided the funding for this work. I really appreciate them.
- Prof Johan De Swardt for the help concerning microwave modification and the related experiments.
- Prof Karen Hudson who helped me with my mineralogical characterization. Her contributions really set me going.
- Evelyn Manjengwa for proofreading my thesis prior to submission. Her comments and encouraging conversations were extremely useful.
- George Teke, Vitalis Chipakwe, Kieran Cairncross and Marnits Maree for their help in certain aspects of my experiments, results and discussion.
- Dr Margreth Tadie's research group for the presentations and support time we shared together.
- Stellenbosch University's Central Analytical Facility, SGS Barberton and XRD Analytical and Consulting for carrying out certain aspects of analysis on my samples.
- Department of Process engineering staff for the help in equipment setup and solution sample analysis.
- My mom and late dad for the being there for me through the years and helping me to rise in my career path. They have been a great inspiration to me.
- My wife and kids for their love, patience and understanding throughout this journey.

Table of contents

List of figures

List of tables

Nomenclature

AMD	Acid Mine Drainage
BIOX	Biological Oxidation
BTRP	Barberton Tailings Retreatment Plant
CAPEX	Capital Expenditure
COVID-19	Coronavirus Disease of 2019
EDS	Energy Dispersive Spectrometry
ICP-MS	Inductive Coupled Plasma Mass Spectrometry
ICP-OES	Inductive Coupled Plasma Optical Emission Spectrometry
OPEX	Operating Expenditure
PAR	Pan African Resources
PSD	Particle Size Distribution
QEMSCAN	Quantitative Evaluation of Minerals by Scanning Electron Microscopy
SEM	Scanning Electron Microscopy
XRD	X-Ray Diffraction
XRF	X-Ray Fluorescence

1.0 Introduction

1.1 Background

The South African gold industry has a history spanning over a century which has been accompanied by significant changes in technologies and processing methods. Processing technology has witnessed a dramatic improvement, from mercury amalgamation of coarse ores to cyanide leaching of fine ores (Naicker *et al.*, 2003; Tutu *et al.*, 2008; Weissenstein & Sinkala, 2011).

Gold mining activities have left vast amounts of mine waste. The mine waste exists in different sizes which have size distributions associated with sand dumps (coarse ores) to slimes dumps (fine ores) (Tutu *et al.*, 2008). South Africa has over 500 gold tailings dumps, (Janse van Rensburg, 2016), several of which have potential to be profitably reprocessed (Weissenstein & Sinkala, 2011). Gold lost to the dumps is attributed to inherent process inefficiencies (EcoPartners, 2010). In the past, up to 1993, gold lost annually to tailings in South African mines was considered equating to R8.5 billion (Metzner, 1993).

Mining is associated with a negative environmental and social legacy, with reported latent and external effects as reported in literature (Naicker *et al.*, 2003). The absence of adequate or relevant legal instruments and regulations governing operations, and mine closure, compound the challenges associated with earlier mining activity in the country.

Previously, mine closure was a process that entailed site abandonment without clear post-operational environmental, and social management plans in place (Limpitlaw & Briel, 2014). Toxic dust aerosols in the dry seasons, water pollution emanating from Acid Mine Drainage (AMD), and the resultant latent effects arising from mobilization of metalloids, are some of the environmental challenges associated with abandoned mines and their associated waste dumps (Janse van Rensburg, 2016). The social challenges associated with abandoned mines due to the proliferation of illegal mining activity are well documented (Minerals Council South Africa, 2020).

The gold mining industry has recently been experiencing challenges which have adversely affected production, led to several mine closures and job losses. Rising operational costs (labour and electricity), gold price slumps, and exhaustion of rich free milling ore bodies, are the most significant challenges (Minerals Council South Africa, 2019; Seccombe, 2018). As a result, the processing of refractory ores is increasingly becoming a preferred option. Refractory

ores are however, associated with low gold recoveries which lead to tailings deposits with significant gold content. However, the tailings (assay ranges of 0.5 – 1.9 g/t) also exhibit low gold recoveries (Dehghani *et al.,* (2009); Snyders *et al*., (2018)).

Considering the observed challenges confronting the gold mining industry, tailings recycling is a promising avenue in which value recovery can be undertaken at lower operational costs and risk. This ultimately awards another opportunity to improve the handling and final storage of the reprocessed tailings. Land previously committed to tailings storage can be rehabilitated for alternative uses such as real estate and farming activities (Pan African Resources, 2020a).

1.2 Problem statement

Historically, high sulphide ores were treated using calcination. The tailings contain a high content of sulfur and arsenic (if they are arsenopyrite bearing), and gold which is unrecovered. An example is the Barberton calcine tailings. The arsenic and sulfur in the tailings dump are a significant environmental and occupational safety concern. AMD acidifies water sources. The mobilization of arsenic into the atmosphere occurs as a result of very windy and dry conditions. Further, the leaching of arsenic into the soil, and eventually into surface and ground water sources is aggravated by AMD.

Most often the analysis of the tailings reveal that the gold head grade (0.5 – 1.9 g/t) is present in economically viable concentrations (Dehghani *et al*., (2009); Snyders *et al*., (2018)). The rise of pre-treatment methods for processing low grade and refractory ores (e.g. alkaline pre-leach pre-treatment, ultrafine milling), are a greenlight for recycling. The tailings recycling operations frequently confer additional economic, environmental, and social performance measures to the business model of the mining firms.

Most recently Pan African Resources (PAR) identified their tailings retreatment plans as a value accretive growth strategy (Pan African Resources, 2018, 2019a). The subject of this thesis has been devised as one of the key components of those initiatives.

1.3 Aims and objectives

The main aim of the research was to develop a processing strategy to recover gold from a refractory tailings dump. Several extraction and pre-treatment processes, from literature that have been demonstrated were investigated to achieve the aim. Three objectives were carried out.

The objectives sought to achieve the following:

i. Mineralogical characterization of the refractory tailings heap material to understand the gold size, nature, association and gangue phases.
ii. Develop a pre-treatment method to help recover the gold during cyanide leaching.
iii. Develop a method to aid direct cyanide leaching for improved recoveries.

1.4 Research approach

The study was divided into three phases based on the three objectives. In the first phase which relates to objective one, several mineralogical characterization tests were carried out which included:

- Fire Assay.
- Particle Size Distribution (PSD).
- X-Ray Diffraction (XRD).
- X-Ray Fluorescence (XRF).
- Chemical analysis – Inductively coupled plasma.
- Scanning Electron Microscopy (SEM).
- Quantitative Evaluation of Minerals by Scanning Electron Microscopy (QEMSCAN).

The mineralogical characterization findings influenced the selection of the pre-treatment method.

Phase two which fulfils objective two, was the development of a pre-treatment method that achieves high gold recovery. It was decided to investigate methods that expose gold grains either by a chemical or physical means. Both the chemical and physical methods were combined with ultrafine milling.

Sodium hydroxide pre-leach pre-treatment was considered to facilitate chemical alteration by alkaline dissolution of gold carrier phases (quartz and talc) within the tailings sample. During pre-leach pre-treatment, elements which constitute the gold carrier phases (gangue) are leached into solution thereby exposing gold surfaces prior to cyanidation. A full factorial experimental design was generated by varying particle size, temperature and sodium hydroxide concentration at two levels.

Microwave pre-treatment under specific conditions has shown some potential of achieving physical alteration (micro cracks) of minerals (Amankwah and Ofori-Sarpong, 2011). Though the equipment used in this study was not optimised for generation of micro-cracks, microwave

technology was applied to investigate whether physical alteration could be achieved, and thus pave the way for cyanide complexes to access previously encapsulated gold surfaces. Factors which were varied were particle size, time and water addition.

Phase three (objective three) entailed adopting microwaves to assist direct cyanide leaching. The effects of sodium cyanide concentration and particle size were investigated during the runs performed.

Based on the experimental results from phases two and three, three flowsheets were drawn, and their corresponding mass balances were performed. The flowsheet with the highest gold recovery was proposed.

1.5 Thesis structure

The thesis comprises of nine chapters. Chapter 1 introduces the research, outlines its background, problem statement and aims and objectives. The research approach to address the aim and objectives is mentioned. The thesis structure sheds light on the rest of the document.

Chapter 2 contains the literature review. The history of gold mining and the occurrence of gold in South Africa are highlighted. Mineralogy, refractory ores, and their processing routes are discussed. Previous findings concerning the investigated pre-treatment methods were explored. The leaching concept winds up the review.

Chapter 3 is the experimental section. The experimental design, reagents, equipment and procedure, analytical methods, and data interpretation are contained therein. Chapter 4 is the results and discussion section. Chapter 5 highlights gold mass balances for three proposed flowsheets. Chapters 6 and 7 contain the conclusions and recommendations respectively. Chapter 8 provides the list of references followed by the appendices in Chapter 9 which concludes the document.

2.0 Literature review

2.1 World gold mining and South Africa's contribution

Gold remains one of the world's most desired metals. This can be credited to its excellent properties some of which are corrosion resistant, malleable and electrical conductivity. This precious metal is generally inert thus making it useful for jewellery and multiple industrial applications (Minerals Council South Africa, 2018). Ninety-four countries in the world are actively involved in gold mining, and South Africa holds about 40% of the world's gold reserves (Butterman & Amey, 2005). South Africa's Witwatersrand basin is planet earth's greatest goldfield. This basin lies in the central part of the Kaapvaal Craton. This geological setting is the origin of a third of all gold that has ever been extracted on the planet (Tucker *et al.*, 2016). In 2007, China overtook South Africa as the planet's greatest annual gold producer. South Africa's gold mining now accounts for 4.2% of global annual production (Rashotte, 2019).

2.1.1 Gold mining in South Africa

The late 19th century gold rush gave birth to towns like Johannesburg (Egoli or City of Gold), Barberton and Pilgrim's Rest near the gold prospects (Minerals Council South Africa, 2019). The discovery of gold in South Africa has had a positive impact on the economy. Gold mining plays a pivotal role in the South African minerals market. Gold has been a vital contributor to the country's foreign exchange (Nattrass, 1995). A factor that distinguishes gold from a vast variety of other metals is that most of the gold that has ever been produced is still in existence (Habashi, 2005). This can be one of the reasons why gold bullions can be stored in a country's reserves. Gold bullions remain unaltered and maintain their state and market set value for ages.

Rising operational costs, falling ore grades, and fluctuating gold prices have been recently affecting the production of gold in South Africa. The declining ore grade has been a significant contributing factor in the search for more lucrative ore bodies. Typically, this has been associated with the exploitation of ore bodies that are situated at even greater depths. The result is not without a penalty. Higher operating costs and risks associated with mining at increasing depths have militated against the profitability of this enterprise (Minerals Council South Africa, 2019).

Several greenstone belts and geological sequences have hosted the precious metal in mineable quantities in South Africa. These are discussed in the next sections.

2.2 Gold occurrence in South Africa

2.2.1 The Kaapvaal craton

Foster and Piper (1993) named the tectonic and physiographic terranes in which Africa's Archaean rocks are preserved:

- Atlantic Rise of Cameroun, Gabon, and Congo extending southwards to the Malanje "Strip" of northern Angola.
- Guinea Rise of Guinea, Sierra Leone, and Liberia.
- Kaapvaal craton of South Africa.
- Kasai-Angola Massif of southern Zaire.
- North Zaire Massif stretching westwards into the Central African Republic.
- Reguibat Rise of Mauritania, Morocco and northwest Algeria.
- Tanzanian shield.
- Zimbabwe craton.

Southern Africa's continental nucleus is formed by the Zimbabwe and Kaapvaal cratons. In this research project, the focus will be on the Kaapvaal craton (Figure 2.1). The Kaapvaal craton took ~1 Ga to be formed and covers an area of ~$1.2*10^6$ km^2. This craton hosts tremendous extractable mineral wealth, and its formation can be divided into two geological time frames with both durations being approximately equal. The first phase, ~3.7 - 3.1 Ga ago, postulates the initial detachment of the continental geosphere of the craton from the mantle. The granitic greenstone belts of Barberton, Pietersburg and others originate from this era. The second phase, (~3.1 - 2.6 Ga) concludes with processes within the craton and its margin. It is in this period that sedimentary basins like Pongola, Ventersdorp, Witwatersrand, and others were formed (De Wit *et al.*, 1992).

Foster and Piper (1993) highlighted that Barberton, Murchison, Pietersburg, and Sutherland are the principal greenstone belts on the Kaapvaal craton. Postdating the granite-greenstone terrains' stabilization, the Kaapvaal craton became the foundation onto which the Pongola, Dominion, Witwatersrand, Ventersdorp, Transvaal, Soutpansberg and Waterberg sequences were formed. The layering was inconsistent, and mainly sedimentary in nature (Helmstaedt & Gurney, 2001). The Witwatersrand basin has been the principal goldfield in South Africa. A highly detailed review of the Witwatersrand is not included in this study since the primary focal point of the work will centre on the Barberton greenstone belt.

Figure 2.1: Map of Africa showing the Kaapvaal and other cratons of southern Africa (Phillips & Powell, 2015).

2.2.1.1 *Witwatersrand basin*

The Witwatersrand basin is the world's greatest gold field. Different geological processes have occurred over time to give birth to this basin (Robb & Meyer, 1995). The gold deposits cover an area of ~42 000 km^2 in the Gauteng, North-West and Free State provinces (Vermeulen, 2001). The year 1887 was the first full mining year of the basin with ~0.52 tonnes extracted, 3.85 tonnes the following year, and the highest annual peak was 989 tonnes in 1970 which accounted for 60% of global production (Sanders *et al.*, 1994; Werdmuller, 1986). The gold-rich conglomerate reefs of the Witwatersrand basin occur in seven major goldfields, and a few minor occurrences. The seven major goldfields are Welkom, Klerksdorp, West Wits, West Rand, Central Rand, East Rand and Evander (Tucker *et al.*, 2016). It is estimated that more than 120 mines have operated over a century of the Witwatersrand basin's history (Robb & Robb, 1998).

2.3 Barberton greenstone belt

2.3.1 Historical gold mining on the Barberton greenstone belt

Gold mining in the Barberton area can be traced back to 1884 during the time of the Barberton gold-rush. Barberton came to life after gold discovery by the Barber brothers in Reimer's Creek. This discovery came after a chain of successful operations in the nearby area which are Kaapsehoop-1881, Jamestown-1882 and Moodies Concession-1883 (Pearton & Viljoen, 2017). Mining in the goldfield matured from alluvial diggings to small individual workings which paved way for larger operations. With increasing depth in the operations, difficulties during beneficiation started to be encountered as the ore became more refractory. This came at a price on the beneficiation process as it became more sophisticated (Ward & Wilson, 1998).

There have been more than 350 gold occurrences on the Barberton greenstone belt. The bulk of these were small workings and ephemeral prospects (Anhaeusser, 1986). It is reported that the Barberton greenstone belt has yielded more than 375 tonnes of gold (Pearton & Viljoen, 2017). Three principal gold producing complexes on the Barberton greenstone belt have been the Agnes-Princeton, New Consort and Sheba-Fairview. Several gold mines have operated for over a century within the three complexes (Ward & Wilson, 1998).

Barberton Mines (Figure 2.2) is a collective name for three underground mines on the Barberton greenstone belt. These are Fairview, Sheba and New Consort mines. Barberton Mines is Pan African Resources (PAR) Group’s gold endeavour which processes 300 000 tonnes of ore per annum at an average head grade of 9.6 g/t. It is here where the biological oxidation (BIOX) process is made use of to treat their complex ores in an environmentally conserving manner (Pan African Resources, 2019b).

Pan African Resources has a tailings reprocessing plant in the Barberton area which was commissioned in 2013. The Barberton Tailings Retreatment Plant (BTRP) processes 1 200 000 tonnes of tailings per annum at an overall grade of 0.7 g/t (Pan African Resources, 2020b).

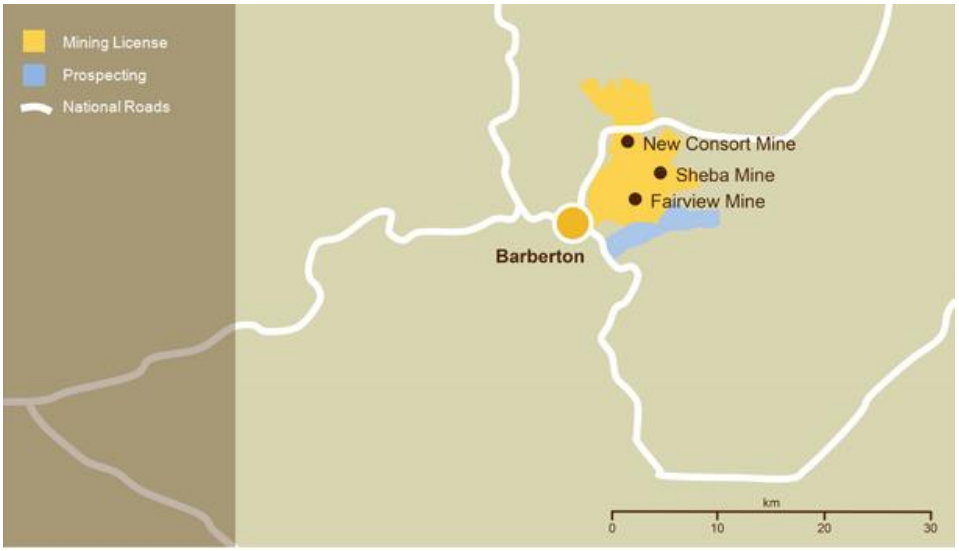

Figure 2.2: Map showing Barberton mines adapted from (Pan African Resources, 2019b).

2.3.2 Geological setting

The Barberton greenstone belt (Figure 2.3) is situated on the eastern side of the Kaapvaal Craton, South Africa (Lowe & Byerly, 1999). The Barberton greenstone belt stretches for ~120 km over a width of ~25 - 50 km. The greater part of the Barberton greenstone belt lies in the Mpumalanga province and a smaller portion of it overlaps into northern Swaziland (Anhaeusser, 1969; Ward & Wilson, 1998). The Barberton greenstone belt is an area of great geological significance in the study of the earth's ancient history. Rocks aging approximately 3.55 to 3.22 Ga have been discovered on this terrain making it one of the most intact and oldest geological environments on earth. These rocks comprise of sedimentary, shallow intrusive, and volcanic species (Lowe & Byerly, 2007). The greenstone belt sequence comprises of three stratigraphic units. In ascending order, the units include the following:

- Onverwacht Group, predominantly ultramafic and mafic volcanic rocks.
- Fig Tree Group, a metaturbiditic progression composed of cherts, greywackes and shales.
- Moodies Group, coarse-grained clastic sedimentary rocks, mainly sandstones and conglomerates (Lowe & Byerly, 1999; Visser, 1956).

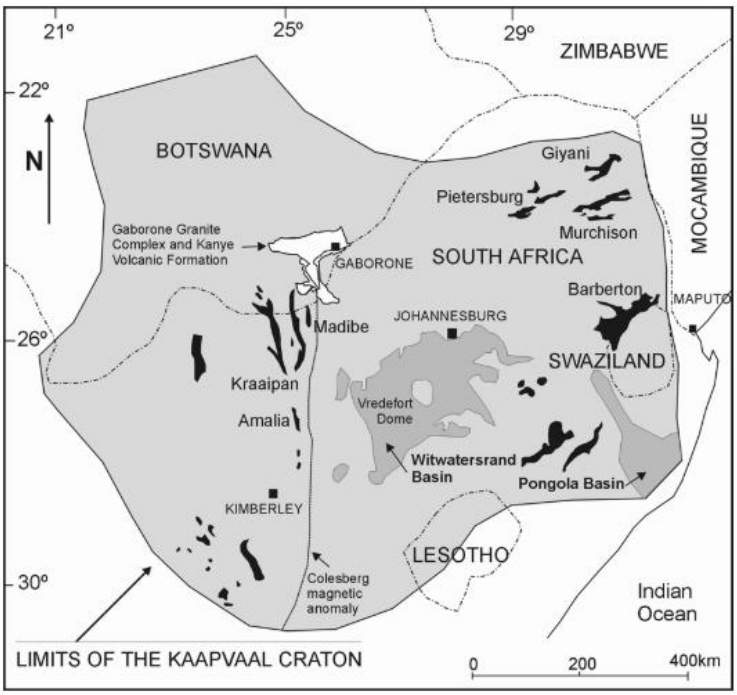

Figure 2.3: Map showing the Barberton greenstone belt (black shade) east of the Kaapvaal craton (Phillips & Powell, 2015).

2.3.3 Mineralogy of the Barberton gold deposits

Gold-bearing rocks in the Barberton greenstone belt range from greenstones (igneous rocks) to greywackes (sandstone), quartzites, and several cherts and shales. The wall-rock distortions accompanying the gold-bearing fractures within the Barberton greenstone belt are carbonisation, sericitisation, silicification and sulfidation (De Ronde *et al.*, 1992; Schouwstra & De Villiers, 1988). Gold mineralisation in the Barberton greenstone belt is concentrated in regions of severe folds and faults (Liebenburg, 1972). According to Brock and Pretorius (1964), hydrothermal activity was responsible for gold mineralisation in the Barberton greenstone belt. Nicolaysen (1962) outlined that gold mineralisation in the Barberton greenstone belt could be subdivided into two classes, gold encapsulated within sulfides and gold almost sulfide free.

Schouwstra and De Villiers (1988), Robertson (1989) and De Ronde *et al.* (1992) categorised the Barberton greenstone belt ores as free milling and partially to extremely refractory depending on the degree to which the gold is encapsulated within the related sulfides.

During the early days of the Barberton goldfield, there was almost no problem with refractoriness. With progression of time, the free milling ores were depleted, and the new ores

started presenting recovery problems due to refractoriness. The conventional method of cyanidation was posed with a challenge as it could no longer bring satisfactory recoveries.

2.3.4 Previous mineralogical investigations on Barberton gold deposits

The most common types of ores which are generally sulfidic in nature within the Barberton greenstone belt are (De Villiers, 1957):

- Pyritic ore.
- Ore with arsenopyrite and pyrrhotite.
- Antimony bearing ore.
- Lead bearing ore.

Gold deportment is most prevalent in ores containing pyrite, arsenopyrite, and pyrrhotite in the majority of the prime gold deposits in the Barberton greenstone belt whilst ores containing lead and antimony occur in minute quantities in a few mines or sections of a few mines (Feather, 1987).

Feather (1987) showed that pyrite is the most vital gold-bearing sulfide in the Barberton greenstone belt as it tends to occur with numerous ore minerals, arsenopyrite and pyrrhotite being the most valuable associations. Pyrite when oxidised in aqueous media can alter to goethite, hematite and or lepidocrocite.

Other researchers, Liebenburg and Schweigart (1966), divided the Barberton ores into three types which are:

- Unoxidized complex sulfide ore.
- Gold rich quartz veins with minute quantities of sulfide minerals.
- Weathered ore in the oxidised region, accounting for majority of the historical gold production.

Table 2.1 indicates the 65 ore minerals discovered from previous mineralogical investigations and 28 of them shown to be associated with gold.

Table 2.1: Ore minerals associated with gold deposits in the Barberton greenstone belt (modified after Barton (1982), Liebenburg (1972), Liebenburg and Schweigart (1966) and De Villiers (1957)).

ankerite	covellite§	Maucherite
angelsite	cubanite	melnikovite-pyrite*
native antimony§	electrum§	millerite§
argentite	enargite§	molybdenite
arsenopyrite§*	famatinite§	neodigenite§
azurite	franklinite	niccolite
berthierite	galena§	pentlandite
bindheimite	gersdorffite	pyrargyrite
metallic bismuth§	graphite	pyrite§*
bornite	goethite§	pyrrhotite§
bournonite	native gold*	safflorite
bravoite	hematite§	scheelite
cerussite	ilmenite	siderite
chalcocite§	jamesonite§	native silver§
chalcopyrite§	lepidocrocite	sphalerite§
chloanthite-skutterudite§	leucoxene§	stibnite§
chromite	linnaeite-violarite	tetradymite
cinnabar	loellingite§	tetrahedrite§*
cobaltite§	magnetite§	trevorite
native copper§	malachite	ullmanite§
corynite	marcasite	vallerite

*-main ore minerals, §-found with gold

The major mineralogical causes of refractoriness in the Barberton greenstone belt ores are (Swash, 1988):

- Sulfides (pyrite, arsenopyrite and pyrrhotite).
- Carbonaceous material.
- Gold tellurides (although rare).
- Submicroscopic gold.

The focus of the study within the context of this research is one of Pan African Resources' Barberton mines named the New Consort.

2.3.5 The New Consort Mine

2.3.5.1 *Introduction*

The New Consort gold mine is situated 15km north of Barberton town. It lies where the Jamestown schist belt blends with the greater part of the Barberton greenstone belt (Munyai *et al.*, 2011; Voges, 1986).

2.3.5.2 *Geological Setting*

The Consort Bar

Archaean rocks (~3.4 Ga) of the Onverwacht group cover the greater part of the Jamestown schist belt (Anhaeusser, 1972). Rocks of the Fig-tree group overlie the Onverwacht rocks in the eastern side of the Jamestown schist belt (Voges, 1986). The Consort Contact which lies between the base of the Fig Tree unit and the top of the Onverwacht unit, is denoted by a siliceous surface known as the Consort Bar (Pan African Resources, 2020c). The siliceous surface resulted from hydrothermal alteration. The Bar is a tough, dark brown fine-grained rock, averaging 60 – 180 cm in thickness although in other instances it reaches 24 m. The rock is associated with quartz, biotite, muscovite, rutile, apatite and sericite (Hearn, 1943).

Footwall rocks

The Footwall rocks is the term given to Onverwacht rocks which make contact with the base of the Consort Bar. These Footwall rocks consist of intercalations of amphibolites, chlorite schists, talc schists, tremolite-talc schists, chlorite-tourmaline schists, serpentine and antigorite schists. Shaly lens in the Footwall rocks have the same siliceous nature as of the Consort Bar (Hearn, 1943). The shaly lens are known as the Footwall lens (Pan African Resources, 2020d).

2.3.5.3 *Gold Mineralisation*

During the latter stage of the final intrusion of the De Kaap Valley Granite, hydrothermal solutions flowed through the Consort Bar and Footwall rocks. Silicates, sulfides and gold were deposited in the process (Hearn, 1943). Thus, gold mineralisation in the New Consort area mainly occurs in the Consort Bar and Footwall lens (Pan African Resources, 2020d).

The Consort Bar mineralisation is mainly characterised by sulfides as the main gold carriers with arsenopyrite being the main carrier and pyrrhotite to a lesser extent. Minute gold occurrences with silicates are present (Hearn, 1943; Voges, 1986).

Sulfides (arsenopyrite, chalcopyrite, and pyrrhotite) and iron arsenide (loellingite) are dominant in the Footwall lens mineralisation (Tomkinson and Lombard in (Otto *et al.*, 2007)).

Gold is found in arsenopyrite and as nuggets in Footwall lens cleavages (Pan African Resources, 2020c).

Arsenopyrite being the most important sulfide in both the Consort bar and Footwall lens mineralisation often occurs intermingled with other sulfides as shown in Table 2.2 (Otto *et al.*, 2007).

Table 2.2: Occurrence of arsenopyrite with related sulfides.

	Fine grained arsenopyrite	**Coarse grained arsenopyrite**
Chalcopyrite	Occurs along grain boundaries	
Pyrite		Occurs as flakes within
Pyrrhotite	Occurs along grain boundaries	Occurs as flakes within

An understanding of refractory ores is hereby delved into in the next section.

2.4 Refractory ores

Refractory ores (Figure 2.4) are complex ores that after milling yield low recoveries (<80%) during cyanidation (Yannopoulos, 1991). Amaya *et al.* (2013) considered ores with gold recoveries of 50 – 80% and < 50% as moderately refractory and highly refractory respectively. Sammut (2016) categorised refractory ores based on their carbon content into two classes which are single refractory (little or no carbon) and double refractory (> ~2 wt. % carbon). Refractory gold can exist in solid solution within a sulfide matrix or as discrete particles along grain boundaries of host minerals (Harbort *et al.*, 1996).

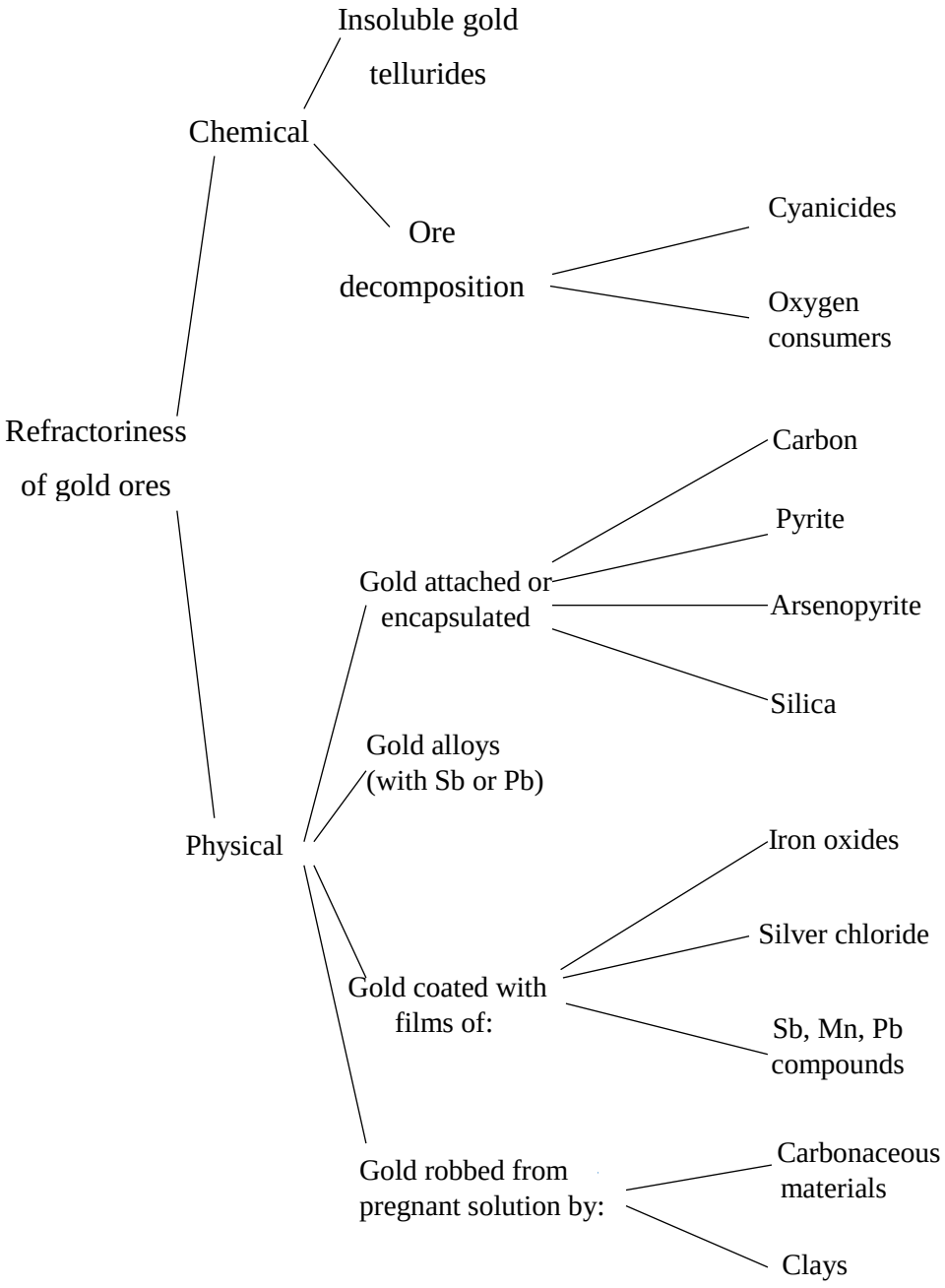

Figure 2.4: Classification of refractory gold ores, modified after (Yannopoulos, 1991).

According to Figure 2.4, refractory ores can be further classified according to their physical or chemical natures. Chemical refractoriness is mainly caused by insoluble gold tellurides, cyanicides and oxygen consumers. Cyanicides and oxygen consumers are ore constituents with a high affinity for cyanide and oxygen respectively. These ore constituents inhibit gold-cyanide complex formation and lead to gold precipitation in solution (Yannopoulos, 1991).

Physical refractoriness is the most common nature, which is mainly attributed to encapsulation, alloying, coating and preg-robbing of gold. Encapsulation relates to occlusion of gold in host phases like sulfides and silicates. When gold is alloyed (Sb, Pb) or coated, free cyanide ions cannot form complexes that dissolve the gold. Clay and carbonaceous materials strip gold from dissolved pregnant liquor (Yannopoulos, 1991).

Based on the descriptions of refractoriness discussed above, the New Consort ore is classified as physically refractory due to gold occlusion in arsenopyrite, pyrrhotite and silicates. However, the nature of refractoriness in the tailings might potentially be different from the host ore as this is influenced by the previous extraction process.

2.4.1 Key mineralogical features accounting for the refractoriness of gold ores

Figure 2.5 is an example diagram showing how gold encapsulation occurs in a host mineral.

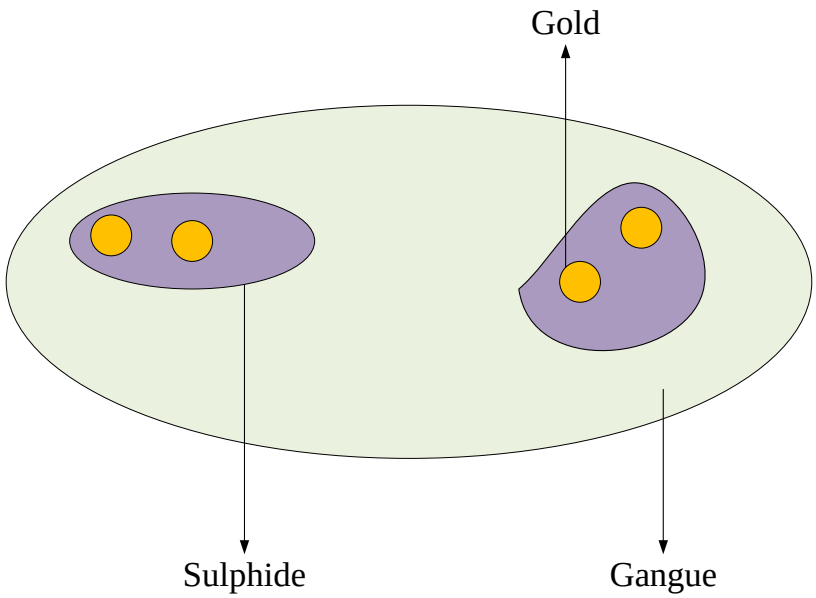

Figure 2.5: Gold encapsulated in a sulfide matrix. Redrawn after (Ellis, 2003).

Three key features that commonly account for the refractoriness of some gold ores include (Pooley, 1987):

1. The distribution of fine grained or submicron gold within host minerals like pyrite and arsenopyrite, thereby hindering cyanide ions access to gold surfaces.
2. The presence of cyanicides (sulfides, copper, arsenic and base metal ions) which compromise cyanide strength thus affecting gold dissolution.

3. The presence of minerals like ferrous ions, sulfide ions, thiosulfate and arsenite, which have a high affinity for oxygen which is salient for gold dissolution kinetics.

To achieve an increase in the recovery of gold from refractory ores by cyanidation it is necessary to pretreat the ores. A pre-treatment method will make the host lattice porous, eliminate cyanide and oxygen consumers, thus increasing chances for gold-cyanide complex formation to dissolve the gold (Komnitsas & Pooley (1989); Yannopoulos (1991)).

2.4.2 Processing of refractory ores

The existence and adoption of a universal extraction method is not practically possible owing to the variability in refractory ore properties. The variability arises from massive irregularities in the chemical, metallurgical and mineralogical properties. Consequently, the observations and conclusions drawn, following the processing of a specific refractory ore, are most relevant to that particular ore (Fraser *et al.*, 1991). Due to high operational costs, the general norm in the initial stages is to treat refractory concentrates generated from froth flotation concentration rather than treating the whole ore (Badri & Zamankhan, 2013).

Pre-treatment methods can be categorized as pyrometallurgical or hydrometallurgical (Iglesias & Carranza, 1994). Roasting, pressure oxidation (acidic and alkaline), biological oxidation, chlorination, and ultra-fine grinding are possible extraction methods that have been employed to process refractory ores (Fraser *et al.*, 1991). Table 2.3 shows several pre-treatment methods for gold ores or concentrates. Flotation, biological oxidation, gravity separation, pressure oxidation, ultrafine milling, and sodium hydroxide pre-leach are processes which are currently used in commercial metallurgical plants (Anderson & Twidwell, 2008; Anderson & McDonald, 2016; Das & Sarkar, 2018; Miller & Brown, 2005; Thomas, 2005). Microwaves are still being investigated at pilot plant level by the University of Nottingham's microwave process engineering department (Buttress *et al.* 2017). The use of ultrasound is still being demonstrated (Guo *et al.*, 2019). Roasting plants currently in use are however slowly being decommissioned (Anderson & McDonald, 2016).

Table 2.3: Pre-treatment methods, ores, or concentrates.

Pre-treatment method	**Phases in gold-bearing ore or concentrate**	**Reference**
Flotation	Sulfides, silicates, carbonate	Allan and Woodcock (2001), Yalcin and Kelebek (2011)
Biological oxidation	Silicates, sulfates, sulfides, oxides	Asamoah *et al.* (2018)
Gravity separation and Flotation	Sulfides, silicates, carbonate	Wang *et al.* (2019)
Pressure oxidation	Sulfides, silicates	Koslides and Ciminelli (1992)
Flotation and Ultrafine milling or Roasting	Sulfides, silicates	Ellis and Gao (2003)
Sodium hydroxide	Sulfides, silicates, oxides	Mesa Espitia and Lapidus (2015), Snyders *et al.* (2018)
Microwave roasting	Sulfides, silicates, oxides	Nanthakumar *et al.* (2007), Amankwah and Ofori-Sarpong (2011)
Conventional roasting	Sulfides, silicates	Dunn and Chamberlain (1997), Fernández *et al* (2010)
Ultrasound	Sulfides, silicates	Zhang *et al.* (2016), Guo *et al.* (2019)

Roasting, though associated with high energy costs, was one of the first pre-treatment options incorporated into metallurgical flowsheets to address refractoriness. However, emergent multi-stakeholder concerns on climatic and environmental issues continue to exert pronounced pressure on the discontinuation of roasting as a process option. The emission of acidic gases like (SOx) and particulates are a significant factor (Sammut 2016). Economic considerations have traditionally dominated decisions influencing the feasibility of pursuing a selected processing route. The current legislative and regulatory infrastructure also commands a significant degree of influence, as a result directing the capital expenditures and project related decisions. Organizational policy and stakeholder conversations reflect an increased focus on environmentally friendly thinking.

The New Consort Mine has applied roasting as a part of its process operations. This being the prior process involved in the generation of the calcine tails, it is now discussed in the next section in order to understand the chemistry that has resulted in the current tailings being investigated.

2.5 Roasting

Roasting is a thermal process occurring around 450 - 800°C initiating a reaction which facilitates the expulsion of volatile matter (Thomas & Cole, 2005). In refractory ores, the main target for roasting is to convert iron sulfides to porous iron oxides in order to expose the gold particles for cyanidation (Komnitsas & Pooley, 1989). Depending on the nature of the concentrates, roasting can either be a one stage or two-stage process. Pyritic concentrates are treated in a single-stage process while arsenopyrite concentrates are treated in a two-stage process (Fraser *et al.*, 1991).

A summary of the main reactions taking place during roasting are given below (Komnitsas & Pooley, 1989):

$$3FeS_2 + 8O_2 \rightarrow Fe_3O_4 + 6SO_{2(g)} \quad 1$$

$$12FeAsS + 29O_2 \rightarrow 4Fe_3O_4 + 3As_4O_{6(g)} + 12SO_{2(g)} \quad 2$$

$$2Fe_3O_4 + \frac{1}{2}O_2 \rightarrow 3Fe_2O_3 \quad 3$$

Reactions [1] and [2] constitute the first stage which is partially oxidizing to drive off most of the arsenic. As_4O_6 is condensed and collected as As_2O_3 (Komnitsas & Pooley, 1989). Reaction [3] is the second stage which aims to achieve an almost complete oxidation (~20% magnetite; ~80% hematite) of the impervious magnetite to a porous hematite. The product from roasting is a calcine which is chocolate brown in colour, the colour indicating complete or almost complete sulfide oxidation (Thomas & Cole, 2005).

Roaster off-gases are treated to recover metals escaping as calcine dust and poisonous species such as arsenic oxides and finally, to reduce SO_x gas emissions. Electrostatic precipitators are employed to remove metal calcine dust particles. Arsenic trioxide is separated from sulfur dioxide using wet scrubbers, bag houses or large chambers. Sulfur dioxide which can be vented depending on the concentration, can be directed to the production of off-gas sulfuric acid (Gossman, 1987).

2.5.1 Challenges encountered during roasting

The excessive exposure of arsenopyrite to highly oxidizing conditions leads to the formation of impervious iron arsenates (reaction [4]) which trap gold particles, thereby limiting their attack by cyanide ions (Gossman, 1987).

$$2FeAsS + 6O_2 \rightarrow 4FeAsO_4 + 2SO_{2(g)} \quad 4$$

$$Fe_2O_3 + As_2O_5 \rightarrow 2FeAsO_4 \quad 5$$

Abundance of oxygen leads to the formation of arsenic pentoxide which reacts with hematite to give a non-porous iron arsenate (reaction [5]) as well (Thomas & Cole, 2005). High temperatures above 800°C effect recrystallization of iron oxides leading to occlusion of gold (Gossman, 1987; Komnitsas & Pooley, 1989).

Due to the high heat generated by roasting reactions, fusion of iron sulfides and iron oxide phases sometimes occur. This occludes gold particles and cyanide ions cannot reach their surfaces for dissolution. This fusion also contributes to the residual sulfur (sulfide, sulfite and sulfate) and arsenic (arsenite and arsenate) in the calcine which are detrimental to cyanidation (Jha & Kramer, 1984; Yannopoulos, 1991).

Several potentially viable, pre-treatment methods were considered as options to treat the calcine tailings in this research (González-Anaya *et al.*, 2011; Nanthakumar *et al.*, 2007; Snyders *et al.*, 2018). Within the framework of this study, three pre-treatment methods were considered relevant to the tailings under study by virtue of their known technical benefits given the gold associations. These pre-treatment methods were factored in as a mechanism to circumvent any challenges encountered during previous roasting, and the associated refractory nature of the calcine tailings. Ultrafine milling, microwaves and sodium hydroxide pre-leach pre-treatment will be discussed. It must be noted however that the industrial application of microwave energy has not developed extensively as yet (Bradshaw, 1999).

2.6 Pre-treatment methods investigated

Advances in metallurgical technologies have yielded increased extraction efficiencies leading to gold tailings recycling (Bosch, 1987). The pre-treatment methods to be discussed will incorporate the literature of ores and tailings. This is premised on the fact that the tailings formed will exhibit some degree of similarity to the characteristics of the host ore.

2.6.1 Ultrafine milling

The economic use of ultrafine milling in mineral processing dates back to the 1990s (González-Anaya *et al.*, 2011).

Gold encapsulated in host minerals such as silicates and sulfides, and gold occurring in particle size ranges of 1 - 20 µm can be liberated by ultrafine milling of the ore. The resultant particle

size should be finer than P_{80} – 38 µm, to increase the liberation potential. The specific comminution energy required to ultrafine mill P_{80} – 75 µm to P_{80} – 3 µm usually goes beyond 250 kWh/t (Badri & Zamankhan, 2013; Corrans & Angove, 1991).

The high energy consumption (≥ 250 kWh/t depending with the ore type and target grind) associated with ultrafine milling pushes for treatment of concentrates with higher gold grades rather than whole ores. The ball mill, grinding media and electricity consumption costs need to be carefully examined against the gold grade for overall profitability (Corrans & Angove, 1991; Swash, 1988).

Ultrafine milling of gold occurring in the submicroscopic size range (< 1 µm) has not yielded significant improvements in the realized recovery. It follows therefore, that the achievement of higher gold recoveries can be realized in combination with another pre-treatment method (Corrans & Angove, 1991; Harbort *et al.*, 1996). Since ultrafine milling addresses physical refractoriness, combining it with a chemical pre-treatment method has potential to liberate the gold that is submicroscopic.

2.6.1.1 *Previous investigations on ultrafine milling*

Harbort *et al.* (1996) studied the effect of ultrafine milling on a pyrite concentrate. Findings of the study revealed a positive correlation between the grind size and subsequent cyanidation recoveries as detailed in Table 2.4.

Table 2.4: An examination of the effect of ultrafine milling on gold recoveries.

Sample	1	2	3
Grind size	P_{80} - 74 µm	P_{80} - 20 µm	P_{80} - 10 µm
Energy		17 kWh/t	42 kWh/t
Gold recoveries	23.4%	39.5%	70.2%

Based on the observed results in Table 2.4 it is can be seen that ultrafine milling effectively unlocked the occluded gold. Cyanide consumption was quite low, at P_{80} – 20 µm it was 1.44 kg/t and rose to 1.73 kg/t at P_{80} – 10 µm.

Ellis and Gao (2003) studied the feasibility of incorporating ultrafine milling of excess roaster feed (flotation pyritic concentrate) from P_{80} - 120 µm to P_{80} - 10 µm at Kalgoorlie Consolidated Gold Mines. Gold recoveries of 92% were achieved. They concluded that gold recovery and cyanide consumption peaked as particle size was reduced. The active cyanide consumer was found to be copper from chalcopyrite. Copper had been mechanically activated by the ultrafine milling process.

González-Anaya *et al.* (2011) achieved a relatively marginal increase in the gold recovery of a refractory arsenopyritic-pyritic flotation concentrate from 4.1% to 9.4 % by optimization of conventional cyanidation. However, ultrafine milling the concentrate from P_{80} - 46 µm to P_{80} - 4.6 µm resulted in a significant improvement in the recovery (67%) following cyanidation. Addition of 100 g/t lead nitrate caused a 58% reduction in cyanide consumption from 66.7 kg/t to 27.6 kg/t by forming lead sulfide which reduces the quantity of cyanicides in solution. Lead nitrate contributed to recoveries by improving the dissolution kinetics. A 67% cyanidation recovery was achieved in reaction time of 72 h. In the absence of lead nitrate, a longer reaction time 120 h was realised at the same cyanidation rate.

Celep and Yazici (2013) reported ultrafine milling of refractory silver tailings as a viable pre-treatment method. The tailings with a grind size of P_{80} - 100 µm and direct silver cyanidation recovery of 36% yielded a silver cyanidation recovery of 84% when ultrafine milled to P_{80} – 1.2 µm.

2.6.2 Microwaves

2.6.2.1 *Introduction*

Microwaves are electromagnetic waves with frequencies ranging from 0.3 – 300 GHz and they can be transmitted, absorbed or reflected as highlighted in Figure 2.6 (Mukendi *et al.*, 2000; Pickles, 2009a). A material's conductivity influences its response to irradiation. Poor conductors are transparent, semiconductors are good absorbers and good conductors are good reflectors (Xia & Pickles, 2000). Internationally recognised microwave irradiation frequencies in domestic and industrial applications are 2450 MHz and 915 MHz respectively (Pickles, 2009a).

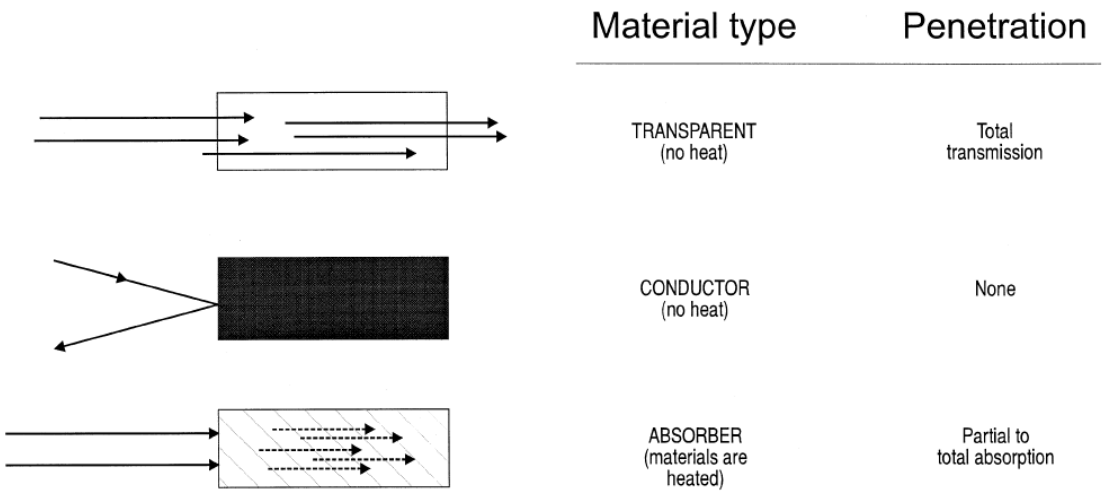

Figure 2.6: Interaction of irradiation with various types of materials. Adapted from (Haque, 1999).

For materials that exhibit slow heating responses to microwave irradiation at room temperature, coupling agents can be introduced to enhance reception (Pickles, 2009a). Microwave irradiation has excellent heating effects to most valuable minerals and poor heating effects compared to gangue minerals (Bradshaw, 1999). Sulfidic minerals are good microwave energy absorbers. This renders a high probability of micro cracks induction by microwaves on sulfidic refractory gold concentrates associated with transparent gangue minerals (Haque, 1999). The extent to which physical alteration achieved is dependent on grain sizes of absorbent minerals, mineralogy and microwave treatment conditions (Ali, 2010).

2.6.2.2 *Microwave heating versus conventional heating*

Figure 2.7 is a diagrammatic representation of how microwave and conventional heating occurs. During microwave irradiation, a metallurgical material is heated from within while during conventional heating, a metallurgical material is heated from without (Xia & Pickles, 2000).

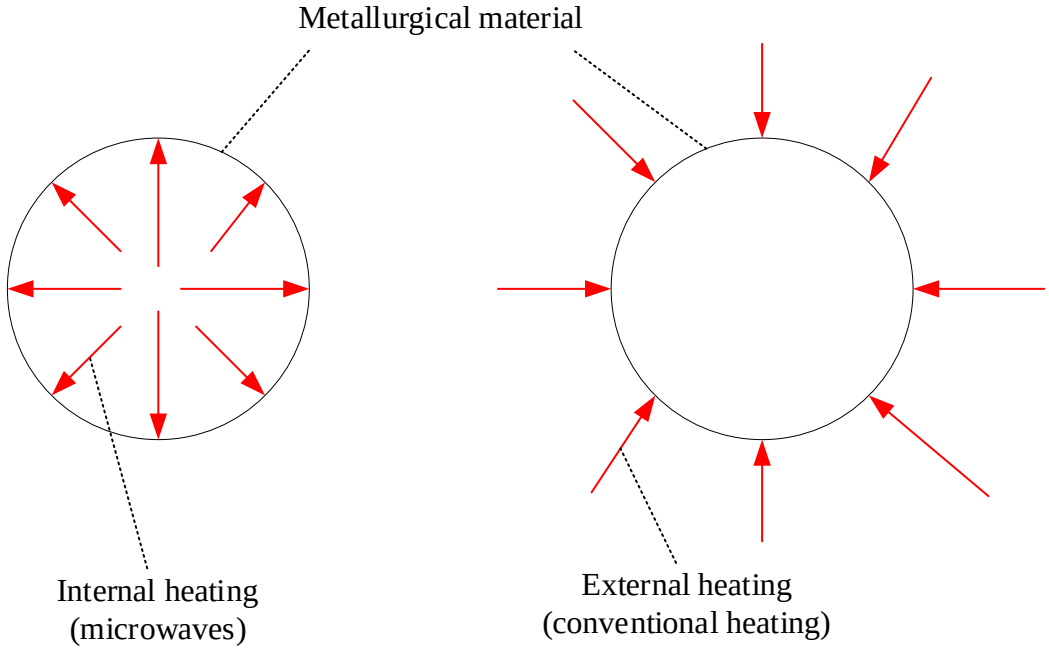

Figure 2.7: Microwave and conventional heating. After (Xia & Pickles, 2000).

Microwaves possess several rewarding heating characteristics as compared to conventional heating. These include swift heating, selective heating of materials, instantaneous irradiation turning on and off, heating of material body from within and reduced off gas volumes (Al-Harahsheh & Kingman, 2004; Haque, 1999; Xia & Pickles, 2000).

2.6.2.3 *History of microwaves in extractive metallurgy*

Since 1966, microwave irradiation has drawn the interest of many researchers in the field of extractive metallurgy due to its excellent heating capability (Al-Harahsheh & Kingman, 2004).

Research has been conducted for various applications such as coal desulfurization, comminution, drying, calcination and sintering, leaching, reduction and smelting, roasting, segregation processes and recycling of tailings (Amankwah & Ofori-Sarpong, 2011; Li *et al.*, 2020; Mukendi *et al.*, 2000; Pickles, 2009b). However, adoption of microwave energy for industrial applications has not advanced extensively in comparison to other available technologies. The observation is attributed to the drawbacks often encountered during scaling up from laboratory experiments and decommissioning already operational technologies (Bradshaw, 1999; Buttress *et al.*, 2017). Scaling up from laboratory experiments is met with a disadvantage of long residence times required to achieve uniform microwave roasting of huge quantities of metallurgical ores. This ultimately reduces plant throughputs and production targets are not satisfactorily met (Batchelor *et al.*, 2017). As of 2016, pilot scale studies for a plant that can microwave treat (assisted sorting) 150 t/h ore were ongoing (Buttress *et al.*, 2017).

2.6.2.4 *Principle of microwave heating*

When microwave radiation interacts with atoms and molecules of minerals, it causes minute displacement of stationary charges. This results in the generation of electric dipoles and subsequent polarization. Polarized molecules oscillate at the same rate due to rapid fluctuation in the electromagnetic fields. Intermolecular “friction” produces heat. Microwave radiation produces Alternating Current (AC) which interacts with mobile charges to give rise to electrical resistance heating (Pickles, 2009a).

Pickles (2009a) listed the factors that affect microwave energy interaction with metallurgical materials:

- Real and imaginary permittivities (ability to be electrically polarized).
- Thermal conductivity.
- Heat capacity.
- Temperature.
- Particle shape and microwave cavity.
- Bulk density of sample.
- Power level.

- Particle size.
- Sample mass.
- Presence of coupling agents (good absorbers that aid heating up of poor absorbers).
- Occurrence of chemical reactions or phase changes.

2.6.2.5 *Previous research done on microwave roasting in extractive metallurgy*

Haque (1987a,b) investigated the effect of microwave radiation on an arsenopyritic refractory gold concentrate. As and S vaporised as As_2O_3 and SO_2 respectively. Cyanidation of the calcine gave 98% gold recovery.

In another study by (Woodcock *et al.*, 1989), the suppression of As_2O_3 and SO_2 generation was achieved by microwave irradiation of arsenopyritic refractory gold concentrate in NaOH. Na_3AsO_4, Na_2SO_4 and $FeSO_4$ were produced in solution. Water washing of the microwaved residue to remove impurity elements and compounds at 75°C was followed by cyanidation which gave 99% gold recovery.

Nanthakumar *et al.* (2007) examined a double refractory gold ore that did not respond to direct microwave roasting. Oxidation of the carbonaceous matter was not achieved as the roasting temperatures failed to reach the minimum required temperature of 650°C. The researchers performed indirect microwave roasting. This entailed the introduction of a magnetite particle bed into the system as a coupling agent onto which the reactor crucibles containing the ore were placed. As a result, the preg-robbing nature of the ore was eliminated due to the oxidation of the carbon initially in the ore, as temperatures exceeded 650°C with this method. Both direct and indirect microwave roasting resulted in the elimination of sulfide sulfur via oxidation.

Amankwah and Pickles (2009) compared the effects of microwave energy with conventional roasting on a double refractory gold concentrate. Carbon and sulfide sulfur were the response measures. The results indicated that microwave energy eliminated 75% of carbon in less than 30 minutes whereas conventional roasting eliminated the same amount of carbon in over 7 hours. It was observed that both microwave and conventional roasting removed 90% and 75% sulfide sulfur respectively after 30 minutes. Microwave energy's superior roasting rates were attributed to excellent irradiation absorption by carbon and sulfide particles. Therefore, carbon and sulfide particles in microwave irradiation were at higher temperatures compared to conventional roasting. The researchers concluded that specific energy consumption was lower (12.8 kWh/kg) for microwaves than conventional roasting (45.8 kWh/kg). When Li *et al.* (2020) conducted chlorination roasting on refractory cyanide pellets of size ranging from 2 -

12 mm they concluded that microwaves consumed half the power and energy as compared with conventional roasting to yield the same gold recovery of 85%.

Ma *et al.* (2010) performed experiments on a refractory sulfidic gold concentrate wherein the crucibles were uncapped, partially capped and uncapped. Their findings indicated that oxidising conditions (uncapped crucible) were the most ideal for both arsenic and sulfur removal. At a temperature of 550°C arsenic and sulfur removal were 98% and 91% respectively.

Amankwah and Ofori-Sarpong (2011) conducted the microwave irradiation of a gold ore with the aim of reducing crushing strength and increasing gold recovery. The researchers also proved the principle of selective heating by irradiating the different constituents of the ore individually. Magnetite, hematite, aluminosilicate, and silica had 500°C, 150°C, 100°C and 40°C respectively after 5 minutes of irradiation. These different heating responses were shown to cause thermal stresses and micro cracks within the gold ore. The resultant micro cracks (Figure 2.8) reduced the crushing strength by 31.2%, and increased the rate of gold dissolution (95% recovery in 12 hours as compared to 92% in 24 hours) in the non-microwaved sample.

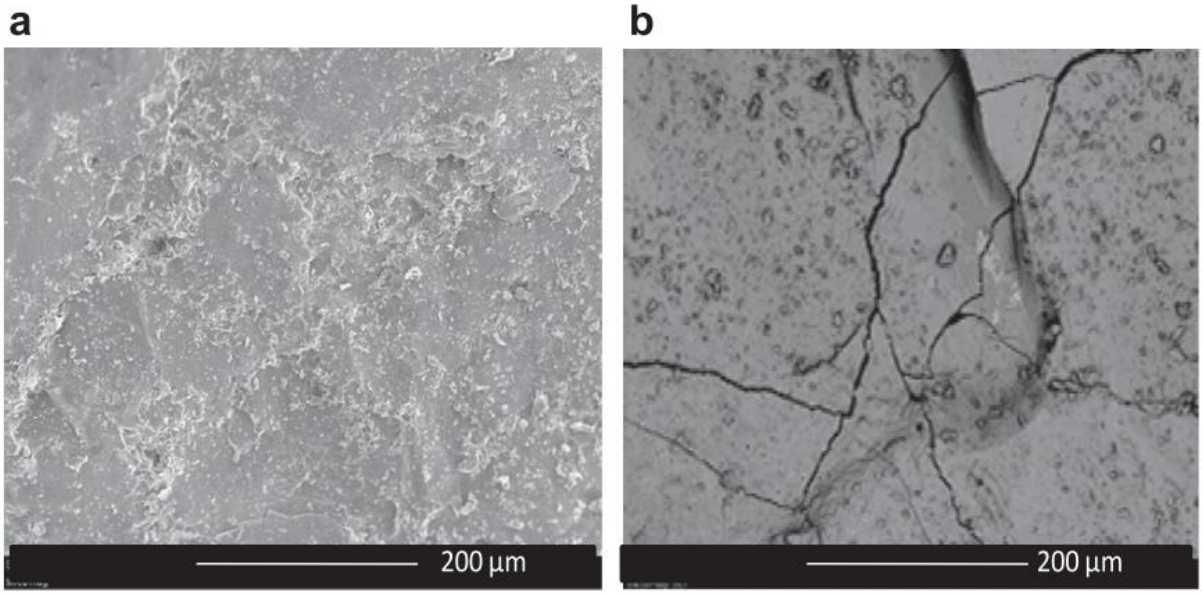

Figure 2.8: SEM image showing a sample in its original (a) and microwaved (b) state. Adapted from (Amankwah & Ofori-Sarpong, 2011).

Hu *et al.* (2017) employed water to aid microwave roasting of an arsenic sulfide gold concentrate. Water content was varied from 0%, 3%, 6%, 9%, 12% and 15%. They found out that 9% water content gave the highest sulfur removal of 88% and 75% gold recovery. Arsenic

elimination did not depend on water content with 95% being removed in all runs. It is worthy of note that crystalline water in different ore phases (like talc) can be lost when the stability temperature of the phase has been reached (Wesolowski, 1984).

2.6.2.6 *Principle of microwave assisted leaching*

Microwave assisted leaching involves the use of microwave irradiation to enhance a leaching process. A liquid and solid medium will yield different heating responses in the presence of microwave irradiation. The resultant temperature gradient generates large thermal convection currents from the surface of the irradiated solid. The thermal convection currents are responsible for continuous exposure of new surface area for the lixiviant as reaction products and layers diffuse into solution. This increases the kinetics of the reaction (Huang & Rowson, 2002; Krishnan *et al.*, 2007).

In a study by Harahsheh *et al.*, (2005) the mechanism for microwave assisted leaching is proposed to be localised heating of solid particles compared to the liquid phase for particles amenable to microwave absorption. It is postulated that the reaction interface has a higher temperature resulting in a lowering of the activation for the dissolution of valuable elements. This mechanism is however difficult to validate experimentally without sophisticated equipment.

Differential heating responses, as discussed earlier, in heterogeneous solids with different microwave absorption properties may also cause micro crack propagation which will further aid exposure of the valuable metal being leached. This phenomenon is achieved by heating at high power density and short exposure times (Ali & Bradshaw, 2011). The results can also be maximised by understanding particle size, texture and microwave treatment conditions of irradiation receptor constituents.

Batchelor *et al.* (2015) conducted experiments on copper, lead-zinc and nickel ores to better understand the influence of texture during microwave treatment. The work showed that a particle size of P(50) > 500 µm tended to have the best reception of microwaves when the absorbent phases constituted between 2 – 20 wt. % of the ore being treated.

2.6.2.7 *Previous research on microwave assisted leaching in extractive metallurgy*

Xia and Pickles (2000) investigated microwave assisted caustic leaching of electric arc furnace dust. They varied microwave power, caustic concentration and solid to liquid ratio. Their experiments indicated that high zinc recoveries were obtained by increasing microwave power

and caustic concentration. Decreasing solid to liquid ratios to a certain threshold yielded increased zinc recoveries. The investigation further revealed that microwave assisted leaching was more rapid and achieved higher zinc dissolution rates as compared to conventional heating. The researchers attributed the microwaves' superiority to superheating of the leachate, vigorous boiling behaviour, and irradiation interaction with solids in solution causing higher interfacial temperatures than conventional heating.

Mukendi *et al.* (2000) confirmed that microwaves contribute towards a higher gold recovery as compared to conventional heating (same bulk temperature of ~95℃) and ambient conditions. Leaching experiments were performed at 3.3 g/t NaCN on a refractory gold concentrate. Microwave assisted, conventional heating and ambient conditions leaching yielded gold recoveries of 48%, 38% and 23% respectively. The researchers demonstrated that doubling the NaCN concentration increased the recovery from 48% - 59% during microwave assisted leaching.

Huang and Rowson (2002) investigated microwave assisted decomposition of gold carriers pyrite and marcasite concentrates in nitric acid. Increasing temperature and acid concentration while reducing particle size were factors deemed most ideal for decomposition of both pyrite and marcasite. Marcasite readily decomposed as compared to pyrite.

Kim *et al.* (2017) compared autoclave and microwave assisted leaching experiments on matte from a secondary lead smelter. Their aim was to recover copper, nickel and zinc. For both operating temperatures (130℃ and 160℃) and nitric acid concentration (0.5 M HNO_3), microwaves had faster leaching kinetics, higher metal extractions, and a purer leach residue dominated by iron oxide.

Cho *et al*. (2020) investigated the upgrading of gold content in a sulfidic refractory flotation concentrate by microwave assisted leaching. Nitric acid was used as the lixiviant. The researchers reported that gold content could be upgraded after 20 minutes of leaching at 2 M nitric acid from 94.37 g/t to 132.55 g/t. The upgrade was concluded to be due to the dissolution of gold carrier phase (pyrite) as the overall mass loss of the concentrate was 40.5%.

2.6.3 Sodium hydroxide pre-leach

In 1989 the United States Bureau of Mines developed a process to treat ores containing arsenopyrite. The process involved dissolving and oxidising the arsenopyrite in alkaline conditions (Bhakta *et al.*, 1989). In instances where gold is in submicroscopic size and

encapsulated within host minerals, oxidation fuels the collapse of the crystal structure thereby facilitating enhanced recoveries (Jha & Kramer, 1984).

2.6.3.1 *Dissolution of minerals relevant to calcine tailings*

Dissolution of arsenopyrite

The sulfide (arsenopyrite) matrix hosting gold has to be dissolved to liberate the gold prior to cyanide leaching (Iglesias & Carranza, 1994). Arsenopyrite dissolves in alkaline aqueous solutions by the following equation (Sanchez and Hiskey in (Corkhill & Vaughan, 2009)):

$$FeAsS + 9H_2O \rightarrow FeOOH + H_2AsO_3^- + SO_4^{2-} + 15H^+ + 12e^- \quad 6$$

Iron oxyhydroxide, arsenite and sulfate are the dissolution products.

Dissolution of hematite

Ishikawa *et al.* (1997) reported that temperature and hydroxide concentration were influential for the dissolution of hematite (Fe_2O_3) in alkaline solutions. It was stated that an increase in temperature and hydroxide concentration effected an increase in hematite dissolution. The decomposition of hematite occurs by reduction in NaOH and is given by equation:

$$Fe_2O_3 + 2NaOH \rightarrow 2FeO_2^- + 2Na^+ + H_2O \quad 7$$

Dissolution of silicates

Silicates are a very abundant mineral group and often the gangue part of valuable ores. Dissolution of silicates is of great interest in extractive metallurgy. The kinetics of dissolution are influenced by reagent concentration and temperature (Crundwell, 2013, 2014a).

Crundwell (2014) proposed a three-step mechanism for silicates dissolution as illustrated in Figure 2.9: a) individual silicon or metal ions (depending on the silicate) react with hydroxyl ions across the Helmholtz double layer; b) tetrahedral silicate detaches into solution; c) products of a) and b) react with solution species to yield silicic acid (H_4SiO_4).

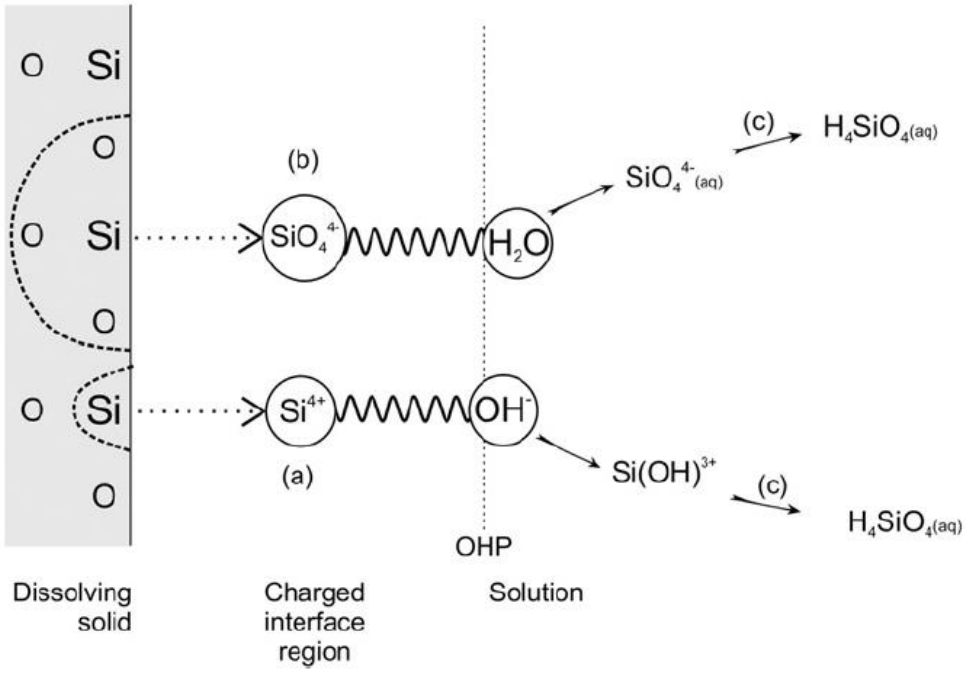

Figure 2.9: Proposed mechanism of silicate minerals dissolution. Adapted from (Crundwell, 2014b).

2.6.3.2 *Gold losses associated with alkaline dissolution*

Jeffrey and Anderson (2003) postulated that sulfur's reaction with sodium hydroxide yields sulfide sulfur, thiosulfate and polysulfide. The reactions are illustrated by equations 8 and 9 below:

$$4S + 6OH^- \rightarrow 2S^{2-} + {S_2O_3}^{2-} + 3H_2O \quad (8)$$

$$8(X-1)S + S^{2-} \rightarrow {S_X}^{2-} \quad (where\ X = 2\ to\ 5) \quad (9)$$

The sulfide and thiosulfate ions form strong and stable gold complexes by means of equations 10 and 11 (Jeffrey & Anderson, 2003):

$$Au^+ + S^{2-} \rightarrow AuS^- \quad (10)$$

$$Au^+ + 2{S_2O_3}^{2-} \rightarrow {Au(S_2O_3)^{3-}}_2 \quad (11)$$

Celep *et al.* (2011b) confirmed gold losses during alkaline sulfide leaching of a refractory antimonial ore. For the conditions investigated, gold losses were found to be 3 – 9%. The losses increased with increasing temperature and reagents (Na_2S and NaOH) concentration. Alp *et al.* (2010) reported 12.6% gold losses during KOH pre-leach pre-treatment of an antimonial refractory silver-gold ore. On the contrary, a study by Celep *et al.* (2011a) revealed that no gold was extracted during NaOH pre-leach pre-treatment of a refractory silver-gold ore. This

demonstrates that refractory ores do not always exhibit the same pre-leach pre-treatment characteristics. It was also observed that NaOH pre-leach pre-treatment is dependant on ore mineralogy as discussed earlier (section 2.6.3.1).

2.6.3.3 *Research on sodium hydroxide pre-leach*

Meng (2005), Celep *et al.* (2011a), Mesa Espitia and Lapidus (2015) and Snyders *et al.* (2018) studied the effect of NaOH for pre-treatment of refractory gold ores. In their experiments they did not utilise pressure as did Bhakta *et al.* (1989). Eliminating the use of pressure makes the pre-treatment process potentially economic as the costly infrastructure associated with pressure is avoided.

Meng (2005) established a process for treating carbonaceous refractory gold concentrates. As part of the process the following experimental parameters were employed 130 g/t NaOH, 400 g/L solids concentration and an initial temperature of 33°C for intensive alkaline leaching. This resulted in 97% and 47% oxidation of arsenic and sulfur respectively. Equations for decomposition of arsenopyrite and pyrite were postulated (Bhakta *et al.*, 1989; Meng, 2005)):

$$4FeAsS + 4FeS_2 + 12NaOH + 3O_2 + 6H_2O \rightarrow 4Na_3AsS_3 + 8Fe(OH)_3 \quad 12$$

$$2FeAsS + 10OH^- + 7O_2 \rightarrow Fe_2O_3 + 2AsO_4^{3-} + 2SO_4^{2-} + 5H_2O \quad 13$$

$$2FeAsS + 4NaOH + 7O_2 \rightarrow 2FeAsO_4 + 2Na_2SO_4 + 2H_2O \quad 14$$

$$2FeS_2 + 4NaOH + 3O_2 \rightarrow 2Na_2S_2O_3 + 2Fe(OH)_2 \quad 15$$

Celep *et al.* (2011a) investigated the use of NaOH pre-leach pre-treatment on a refractory antimonial ore. The gold in their study was associated with quartz and antimony sulfides which were the main reasons for refractoriness. In their investigation they varied NaOH concentration (0.5 M, 1 M, 3 M and 5 M), temperature (20°C, 40°C, 60°C and 80°C) and particle size (d_{80}: 50 µm, 15 µm, 5 µm). Gold recovery increased from 49% to 85% after pre-treatment. It was observed that no gold was lost to pre-leach liquor.

Mesa Espitia and Lapidus (2015) performed experiments on refractory arsenopyritic material at ambient temperature while varying NaOH concentration (0.1 M and 3 M), solids concentration (40 g/L and 200 g/L) and time (6 h and 48 h). They concluded that the higher NaOH concentration, the lower solids concentration and the greater contact time yielded the highest gold recovery of 81% up from 29% for thiosulfate leaching. An interesting phenomenon in this study was that increasing pre-leach pre-treatment temperature did not enhance gold recovery.

Snyders *et al.* (2018), while studying a refractory tailings heap, varied temperature (40°C, 60°C and 80°C), NaOH (1 M, 2 M and, 3 M) and time (8 h, 16 h and 24 h) in their experiments. Their study indicated that the highest temperature and concentration together with the least contact time produced the highest gold recovery. Direct cyanidation recovery was 7% and soared to 88% with pre-treatment.

2.6.4 Conclusions from pre-treatment methods investigated

Table 2.5 presents the pre-treatment methods to be employed and their effects on the causes of refractoriness.

Table 2.5: Pre-treatment methods and their effects on causes of refractoriness.

	Gold occluded	**Cyanide and oxygen consumers**
Ultrafine milling	✓	x
NaOH pre-leach	✓	✓
Microwave Roasting	✓	✓

It was understood that ultrafine milling can physically break host minerals' lattices to liberate gold particles that are greater than 1 µm. Ultrafine milling is limited to solve refractoriness that is chemical in nature. Sodium hydroxide pre-leach pre-treatment and microwave roasting can liberate gold that is encapsulated in host minerals and reduces the effect of cyanide and oxygen consumers. Water washing facilitates the removal of cyanide and oxygen consumers in both sodium hydroxide pre-leach pre-treatment and microwave roasting.

2.7 Leaching

Leaching involves dissolution of a valuable metal within an ore, concentrate, residue, scrap, or waste into aqueous phase by a leaching agent called a lixiviant. Common lixiviants include acids (sulfuric and hydrochloric), sodium cyanide and sodium hydroxide (Jackson, 1986; Woollacott & Eric, 1994).

A successful leaching process should produce a gangue that is almost free of the valuable metal and a pregnant liquor that is metal rich. The gangue is disposed of, and the metal is recovered from the pregnant liquor (Jackson, 1986).

2.7.1 Leaching mechanism

Four stages occur during a leaching process. The stages involve gaseous, aqueous and solid phases (Jackson, 1986):

i. Dissolution of gaseous phase into the aqueous phase.
ii. Diffusion of dissolved lixiviant reactant from the aqueous phase to the solid-aqueous interface.
iii. Reaction of dissolved lixiviant reactant with the solid at the interface.
iv. Diffusion of the solubilized reaction products from the interface into the bulk aqueous phase.

All four stages might have sufficient individual potential to be the slowest stage which affects the overall leaching rate. In other scenarios, two or more stages affect the overall leaching rate. Diffusion controlled stages ii and iv are usually the rate limiting steps (Jackson, 1986). Increasing the rate of the slowest stages will reduce the leaching time (Woollacott & Eric, 1994).

2.8 Leaching of calcine

Leaching in gold extraction is the dissolution of gold facilitated by a complexant and an oxidant in aqueous solution. Despite its toxicity cyanide has been preferred over other lixiviants due to its fairly low cost and efficaciousness (Marsden & House, 1992). Various processes for cyanide leaching have been developed namely intensive cyanidation, agitation leaching, heap leaching and vat leaching (Kappes, 2005; Marsden & House, 1992).

2.8.1 Cyanidation

2.8.1.1 *Chemistry of cyanide in aqueous solutions*

Cyanide salts dissociate in water to form metallic cations and cyanide anions (Marsden & House, 1992):

$$NaCN \rightleftharpoons Na^+ + CN^- \quad 16$$

Cyanide anions hydrolyse in water to form the most poisonous form of cyanide which is hydrogen cyanide (Dzombak *et al.*, 2006; Marsden & House, 1992):

$$CN^- + H_2O \rightleftharpoons HCN + OH^- \quad 17$$

HCN partially dissociates in water (Marsden & House, 1992):

$$HCN \rightleftharpoons H^+ + CN^- \; ; K_a\,(25℃) = 6.2\,x10^{-10}\,, pK_a = 9.2 \quad 18$$

At equilibrium, HCN dissociation is dependent on pH (Marsden & House, 1992). HCN is the dominant species in the pH regions of acidic to pH < 9.2 while CN^- species dominate at pH > 9.2 as illustrated in Figure 2.10 (Dzombak *et al.*, 2006). HCN is highly volatile in ambient

conditions owing to its low boiling point of 25.7°C hence cyanidation is most effective in alkaline pH > 10 to curb cyanide losses (Dzombak *et al.*, 2006; Marsden & House, 1992).

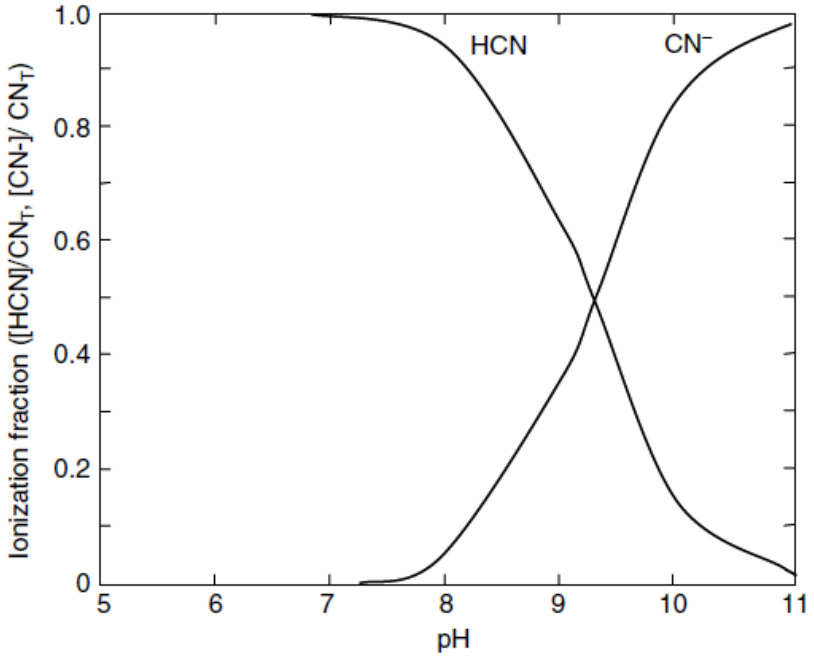

Figure 2.10: Free cyanide species distribution as a function of pH at 25°C (pKa = 9.2 at 25°C for HCN dissociation) after (Dzombak *et al.*, 2006).

2.8.1.2 *Dissolution*

Gold dissolution in alkaline conditions by cyanide has been the most common gold extraction method with over 120 years of application in South Africa (Deschênes, 2005; Hilson & Monhemius, 2006). Cyanide ions dissolve gold by formation of a gold-cyanide complex as proposed by Elsner's equation (equation [19]) to form a pregnant solution (Hilson & Monhemius, 2006).

$$4Au + 8\,NaCN + O_2 + 2H_2O \rightleftharpoons 4NaAu(CN)_2 + 4NaOH \qquad 19$$

2.8.1.3 *Mechanism of cyanidation*

Oxygen is dissolved into the solution. Free cyanide ions and dissolved oxygen move to the solid-aqueous interface where they are both adsorbed onto the surface. Oxygen consumes electrons at the cathodic site (metal surface) while gold donates electrons at the anodic site. Cyanide ions dissolve the gold at the reaction interface by forming a gold-cyanide complex which is desorbed from the reaction interface into the bulk solution (Deschênes, 2005; Yannopoulos, 1991). Figure 2.11 shows the mechanism of cyanidation.

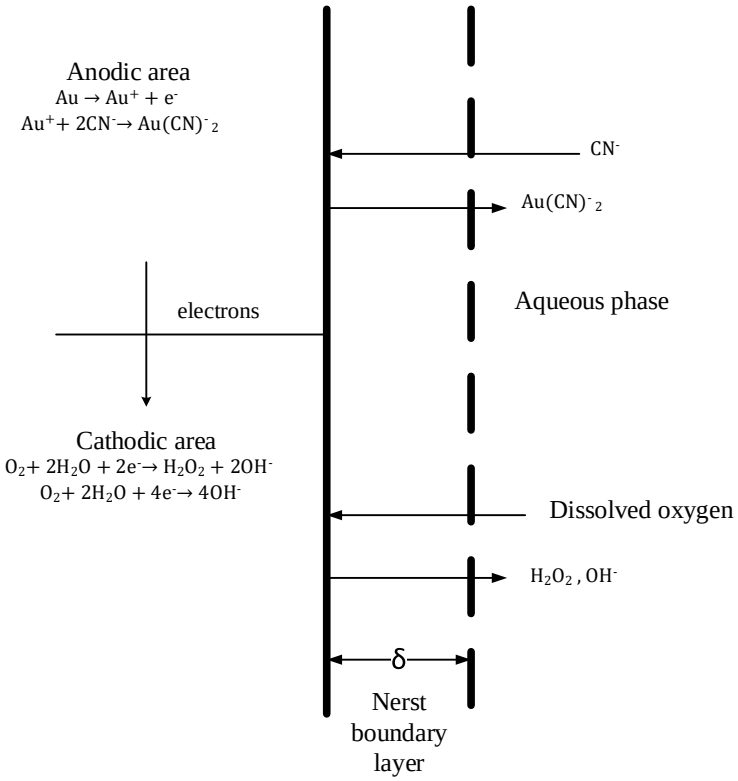

Figure 2.11: Cyanidation of gold. Redrawn after (Habashi, 1967).

2.8.1.4 *Parameters influencing cyanidation*

Oxygen

Air sparging has been used as a source of oxygen with beneficial gold recoveries comparable to those yielded by chemical oxidizing agents like bromine, chlorine, potassium permanganate and sodium peroxide. Adequate oxygen supply is advantageous as it helps increase the rate of reaction and gold liberation while conserving cyanide by side reactions with potential cyanicides (Yannopoulos, 1991).

Cyanide concentration

At ambient conditions and atmospheric pressure, cyanide concentration does not affect the rate of cyanidation. It is controlled by oxygen (Yannopoulos, 1991).

Alkali additions

Bases (CaO, NaOH and Na_2CO_3) are added to the cyanide solution to curb cyanide hydrolysis and neutralize any form of acidity in the ore. However, their use must be carefully monitored as they are beneficial to a certain threshold beyond which they start retarding gold dissolution (Yannopoulos, 1991).

Cyanicides

Cyanidation is diffusion controlled, however, cyanide and oxygen consumers tend to influence the rate of gold recovery. Cyanicides form stable cyanide complexes, thus diminishing the quantity of free cyanide to form the desired gold complexes. Sulfides, copper, arsenic, zinc, antimony, and base metal ions (Fe^{2+}, Fe^{3+}, Mn^{2+} and Ni^{2+}) are typical cyanicides (Yannopoulos, 1991).

Cyanicide reactions as indicated by Yannopoulos (1991):

$$S^{2-} + CN^{-} + 0.5O_2 + H_2O \rightarrow CNS^{-} + 2OH^{-} \quad 20$$

$$Fe^{2+} + 6CN^{-} \rightarrow Fe(CN)^{4-}_{6} \quad 21$$

$$2Cu^{2+} + 7CN^{-} + 2OH^{-} \rightarrow 2Cu(CN)^{2-}_{3} + CNO^{-} + H_2O \quad 22$$

$$ZnO + 4NaCN + H_2O \rightarrow Na_2Zn(CN)_4 + 2NaOH \quad 23$$

$$Ca_3(AsS_3)_2 + 6NaCN + 3O_2 \rightarrow 6NaCNS + Ca_3(AsO_3)_2 \quad 24$$

Three main factors which contribute to low leaching recoveries of gold from various minerals (Lorenzen & van Deventer, 1992):

i. Existence of gold in sub microscopic sizes ‘locked’ in host minerals which require fine grinding to unlock the gold.
ii. Existence of conductive minerals associated with gold which propels galvanic interactions between the gold and minerals.
iii. Release of sulfide ions into the leach slurry which consumes cyanide and dissolved oxygen. The resultant products passivate the gold surface halting all electron movement.

2.9 Summary of literature review

South Africa has a strong background of gold mining, which boasts of more than a century of production. The large inventories of gold tailings stockpiles are potential feed material for gold tailings reprocessing. As high-grade ores are depleted and the economics of shaft mining become unattractive, investor confidence can potentially be secured by exploring value creation in tailings recycling and reprocessing. Further, the negative environmental legacies associated with the tailings can potentially be redressed.

The occurrence of gold in South Africa on the Kaapvaal craton was mentioned in the review. In this regard a description of the mineralogy of the Barberton green stone belt (eastern side of Kaapvaal), with special emphasis to the New Consort was considered. Extensive work on the mineralogy of the New Consort area has been undertaken by independent researchers (Anhaeusser, 1972; Hearn, 1943). The New Consort is one of the three principal gold complexes on the Barberton greenstone belt that also has refractory ore. Gold was found to be mainly associated with arsenopyrite, and pyrrhotite and silicates to a lesser extent.

Refractory material can either be moderately refractory (50 – 80% gold recovery) or highly refractory (< 50% gold recovery), either physical or chemical refractory, and either single refractory (little or no carbon) or double refractory (> 2 wt. % carbon). Typically, the gold can be encapsulated in a host matrix (sulfides or silicates) or surrounded by cyanide and oxygen consumers in the host ore.

The occurrence of gold in both scenarios affects cyanidation recoveries hence, the need for pre-treatment to increase recoveries. Consequently, processing routes and conclusions drawn for a particular refractory material, are valid only for that material as another specimen may behave differently. The different behaviours arise from extensive irregularities in the chemical, metallurgical and mineralogical properties of refractory material. Processing of refractory material is therefore quite complex. As a result, pre-treatment and methods of pre-treatment were covered in the literature review. The methods looked at the physical, chemical, and radiation-based interventions. Leaching fundamentals were also considered.

Microwave treatment of metallurgical materials has attracted the attention of many researchers. Microwaves are proposed to have the potential to be more effective and environmentally friendly due to a reduced quantity of emissions and no combustion fumes generated compared to conventional roasting methods (Xia & Pickles, 2000). Based on the literature considered thus far, the scope for further exploration of microwave assisted leaching on refractory metallurgical material still exists. The findings in the literature review were used to assist the experimental design. In the sections that follow, an examination of the potential of extracting locked value in gold calcine tailings was undertaken.

3.0 Experimental

In this section a detailed discussion of the sample preparation, calcine tailings characterization and gold recovery tests conducted during the research is covered.

3.1 Sample preparation

Sample preparation entailed three major steps namely cone and quartering, riffle splitting and rotary splitting which are illustrated in Figure 3.1.

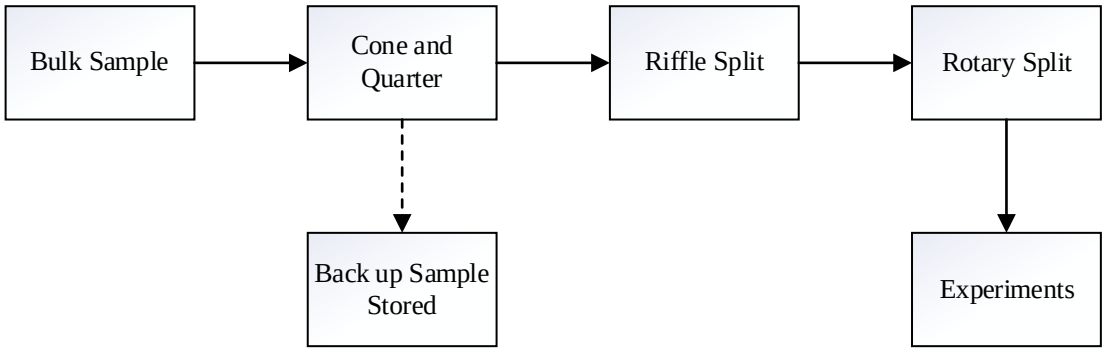

Figure 3.1: Diagrammatic representation of sample preparation procedure.

The first step entailed blending approximately 113 kg of the Barberton calcine tailings sample. Blending was achieved by cone and quartering. Diagonally opposite halves were stored for back up while the remaining two halves were riffled and split in a rotary splitter into 500 g representative aliquots. Ninety aliquots were generated and stored for the planned experiments.

3.2 Sample characterisation

Several tests which include, Fire Assay, Particle Size Distribution (PSD), X-Ray Diffraction (XRD), X-Ray Fluorescence (XRF), Chemical analysis – Inductively coupled plasma, Scanning Electron Microscopy (SEM) and Quantitative Evaluation of Minerals by Scanning Electron Microscopy (QEMSCAN) were carried out to characterise the sample. Figure 3.2 outlines a summary of characterisation methods that were used for the research.

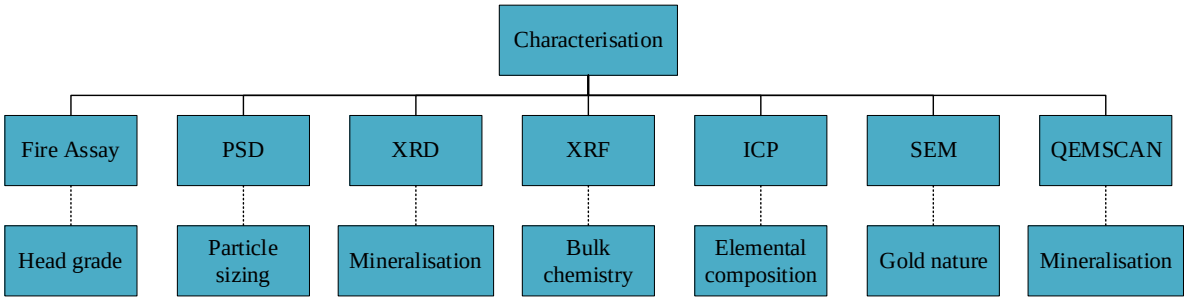

Figure 3.2: Summary of characterisation methods used.

3.2.1 Fire assay

The gold head grade of the calcine tailings sample was determined by lead fusion fire assay and gravimetric finish at SGS Barberton Laboratory on nine representative aliquots weighing 50 g each.

3.2.2 Particle Size Distribution (PSD)

The Particle Size Distribution (PSD) was determined for a 20 g composite as received tailings sample, at the Stellenbosch University Process Engineering Analytical laboratory. The Micromeritics Saturn Digisizer 5200 Laser Diffraction Particle Size Analyser was used for this analysis. This analysis gives information on the fineness of the grind of the sample.

3.2.3 X-Ray Diffraction (XRD)

XRD was performed at the XRD Analytical and Consulting Company (Pretoria) to determine the different phase constituents of the as received tailings sample. A 50 g composite as received tailings sample was used for the analysis. The sample was prepared using a back-loading preparation method. It was analysed with a PANalytical Aeris diffractometer with a Pixcel detector and fixed slits with Fe filtered Co-Kα radiation. The phases were identified using X'Pert Highscore plus software.

3.2.4 X-Ray Fluorescence (XRF)

XRF was conducted on 50 g composite as received tailings sample using a PANalytical Axios Wavelength Dispersive spectrometer at the Stellenbosch University Central Analytical Facility. This analysis enables for the chemical composition of the sample to be characterised.

3.2.5 Chemical analysis – Inductively Coupled Plasma (ICP)

A trace elemental analysis was determined on three composite as received tailings samples weighing 20g each. The samples were digested by six parts nitric acid and one-part hydrogen peroxide in a MARS microwave digester. The solutions were analyzed using the instruments Agilent 7900 Inductive Coupled Plasma Mass Spectrometry (ICP-MS) and Thermo ICap 6200 Inductive Coupled Plasma Optical Emission Spectrometry (ICP-OES) at the Stellenbosch University Central Analytical Facility.

3.2.6 Scanning Electron Microscopy (SEM)

Within the context of this research, SEM was deemed as the best method to determine the occurrence of the gold in the as received tailings sample. SEM was conducted at the Stellenbosch University Central Analytical Facility. Selected tailings samples were also analysed using SEM.

3.2.6.1 *Sample mounting prior to analysis*

Six cylindrical stubs were mounted on a glass plate by adhesive tape. The stubs were half filled with a composite as received tailings sample. Epoxy resin was poured on top of the sample into the stubs. The glass plate was placed into an oven for drying and hardening at 40°C for 24 hours. After drying, the stubs were detached from the glass plate and individually polished using 9 µm, 3 µm and 1 µm grits. The polished mounts were carbon coated to render their surfaces conductive using a Quorum Q150T E coater.

3.2.6.2 *SEM analysis*

The gold particle size and associations were investigated by SEM. The samples were then loaded in a Zeiss MERLIN Field Emission Scanning Electron Microscope for analysis. A Zeiss 5-diode Back Scattered Electron (BSE) Detector (Zeiss NTS BSD) and Zeiss SmartSEM software generated BSE images. An Oxford Instruments X-Max 20 mm^2 detector attached to the SEM and Oxford Aztec software chemically quantified the samples by semi-quantitative Energy Dispersive X-Ray Spectrometry (EDS) and generation of corresponding EDS maps.

3.2.7 Quantitative Evaluation of Minerals by Scanning Electron Microscopy (QEMSCAN)

QEMSCAN analysis on the as received calcine sample was performed at the University of Cape Town Centre of Minerals Research. About 500 g of the as received calcine sample were split into four size particle size ranges which include +75 µm, -75+38 µm, -38+25 µm and -25 µm. Two polished sections were prepared for each size fraction. The sections were

analysed by a QEMSCAN 650F with two Bruker EDS detectors. Bulk mineral analysis and trace mineral search were measured on each section.

3.3 Gold recovery tests

3.3.1 Introduction

Direct cyanide leaching, ultrafine milling, microwave pre-treatment, microwave assisted cyanide leaching and sodium hydroxide pre-leach pre-treatment were the tests carried out in this study. The selected pre-treatment methods used were ultrafine milling, microwave roasting and sodium hydroxide pre-leaching, discussed in section 2.6. All gold recovery tests except for microwave tests, were conducted at Stellenbosch University's Department of Process Engineering. The microwave tests were carried out at Stellenbosch University's Department of Electrical and Electronic Engineering. These tests are described in detail in this section. Figure 3.3 provides a schematic illustration of the sequence of the tests conducted.

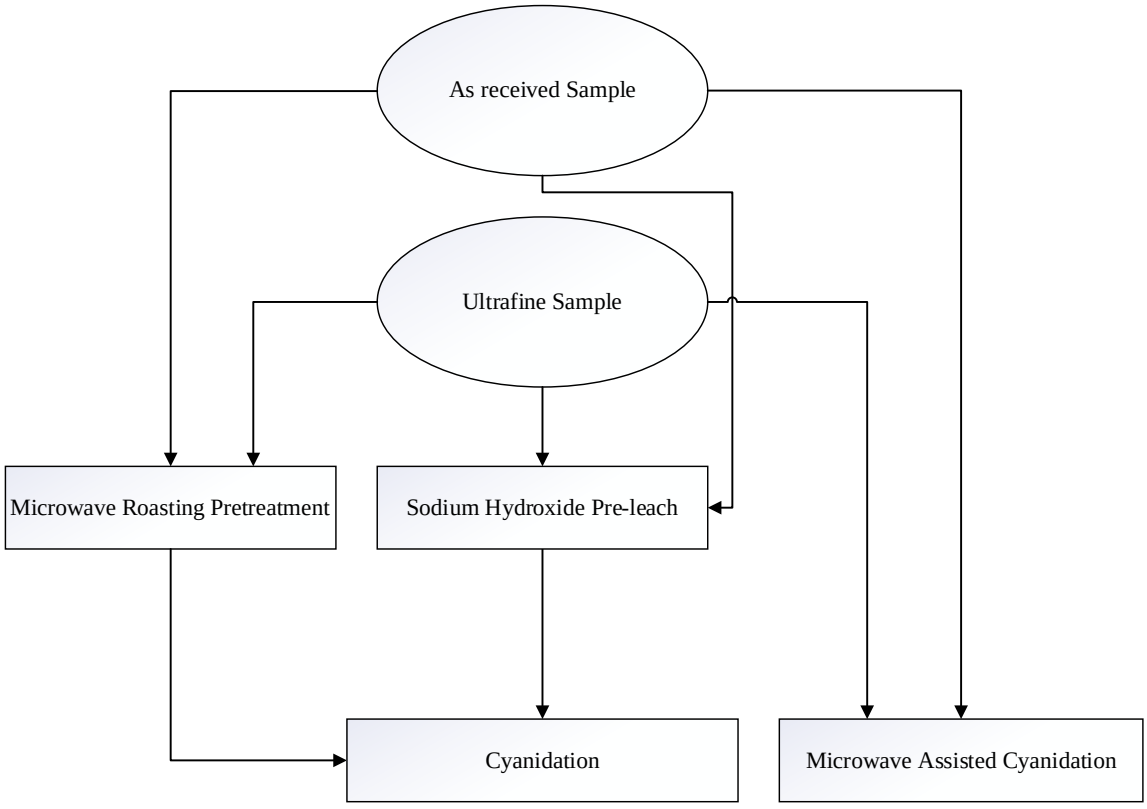

Figure 3.3: Gold recovery tests done on the as received and ultrafine samples.

3.3.2 Experimental design

3.3.2.1 *Microwave roasting pre-treatment*

The effects of time, particle size, and water addition during microwave roasting pre-treatment were investigated. The experimental runs are detailed in Table 3.1. Microwave power (1 kW), water load volume (300 ml), reactor volume (1 L) and sample mass (60 g) were kept constant in all runs. The water load served the purpose of preventing excessive reflection of microwaves which damages the magnetron.

Table 3.1: Microwave roasting experiments.

Run	Time	Particle size	Water addition
1	30min	AR	--
2	30min	AR	6%
3	60min	AR	--
4	30min	Ultrafine	--

AR = As received = P_{80} – 53 µm, Ultrafine = P_{80} – 16 µm

Amankwah and Pickles (2009) explored the impact of microwave roasting on a refractory gold concentrate. The researchers observed that 90% of cyanicides were oxidised after 30 minutes of microwave roasting. Since refractory ores do not behave the same and respond differently to microwave irradiation, Amankwah and Ofori-Sarpong (2020) performed roasting experiments with a duration of 60 minutes. Lower and upper limits of 30 and 60 minutes were defined in the study.

The influence of the moisture content during microwave roasting was considered by other researchers. Hu *et al.* (2017) for example, reported that a 9% water addition gave the highest microwave roasting temperature after 30 minutes. The researchers however noted that a further increase in the water resulted in a decrease in temperature. Interestingly, in this study, a 6% water addition gave the highest temperature after 15 minutes of microwave roasting. Addition of water to beyond 6% resulted in a decrease in temperature. Therefore, an addition of 6% water was also investigated. The water investigation is highlighted in Appendix A.

Pickles (2009a) mentioned particle size as a factor influencing the interaction of metallurgical materials with microwaves. As a result, a comparison of the finer grind of the tailings vs the as received sample was considered in the study.

3.3.2.2 *Microwave assisted cyanidation*

Experiments were conducted varying particle size, sodium cyanide concentration and solids concentration. Table 3.2 outlines the 6 experiments done. Microwave power, stirrer speed and reactor volume were kept constant during all experiments.

Table 3.2: Microwave assisted cyanidation experiments.

Run	[NaCN]	Particle size
1	2 kg/t	AR
2	2 kg/t	Ultrafine
3	4 kg/t	AR
4	4 kg/t	Ultrafine
5	8 kg/t	AR
6	8 kg/t	Ultrafine

AR = As received = P_{80} – 53 µm, Ultrafine = P_{80} – 16 µm

3.3.2.3 *Sodium hydroxide pre-leach pre-treatment*

A full factorial design with three factors investigated at two levels was employed. Temperature, reagent concentration and particle size were the factors considered. The design (2^3) gave 8 runs as shown in Table 3.3. Stirrer speed, leaching time, reactor volume and solids concentration were kept constant for all pre-leach pre-treatment runs.

Table 3.3: NaOH pre-leach experimental design.

Run	Temperature	[NaOH]	Particle size
1	Ambient	1 M	AR
2	Ambient	3 M	AR
3	Ambient	1 M	Ultrafine
4	Ambient	3 M	Ultrafine
5	80°C	1 M	AR
6	80°C	3 M	AR
7	80°C	1 M	Ultrafine
8	80°C	3 M	Ultrafine

AR = As received = P_{80} – 53 µm, Ultrafine = P_{80} – 16 µm, Ambient (uncontrolled room temperature)

Snyders *et al.* (2018) worked with temperatures 40°C, 60°C and 80°C, and sodium hydroxide concentrations of 1 M, 2 M and 3 M while treating refractory material from a tailings dump. The researchers showed the existence of a positive correlation between temperature and sodium hydroxide concentration, and the gold recovery for the shortest pre-leach pre-treatment time of 8 hours. For the purpose of this study, lower and upper limits were ambient conditions and

80°C respectively. Similarly, for the sodium hydroxide concentration, lower and upper limits of 1 M and 3 M were selected.

Jackson (1986) noted that increasing surface area during leaching resulted in an increase in the leaching rate. This influenced working with ultrafine grind and the as-received grind of the tailings sample. The as-received grind and the ultrafine grind were considered as the lower and upper limits respectively.

González-Anaya *et al.* (2011) employed 25% solids concentration while leaching refractory material in cyanide. It was decided to keep the solids concentration at 25% in all cyanidation and pre-leach runs to minimise saturation of solutions by the refractory calcine material for this research.

3.3.3 Reagents

Sodium cyanide (98% assay) supplied by Alfa Aesar was used for all cyanide leaching experiments. For all pre-leach pre-treatment runs, sodium hydroxide pellets (97% assay) from Science World were used. Quick lime (95% purity) used for pH control during cyanide leaching was supplied by Science World.

3.3.4 Cyanidation

Gold dissolution in cyanide was investigated by running two 24-hour bottle roll experiments on the composite as received tailings sample. The procedure was carried out to investigate the degree of refractoriness. Furthermore, the effect of particle size reduction on the as received tailings sample was explored using direct cyanidation. The ultrafine milling procedure is discussed in the next section (3.3.5).

3.3.4.1 *Conditions*

The experimental conditions defined for this section are detailed in Table 3.4 below.

Table 3.4: Experimental conditions for cyanidation procedure.

Parameter	Description	Measure
1	Time	24 hours
2	Temperature	Ambient (uncontrolled room temperature)
3	Solids density	25%
4	pH range	10.5 - 11.0
5	NaCN concentration	2 kg/t
6	Rolling speed	195 rpm

3.3.4.2 *Equipment and procedure*

The cyanide leaching experimental setup comprised of a mechanical roller (Figure 3.4), HCN detector, 2 L Schott bottle.

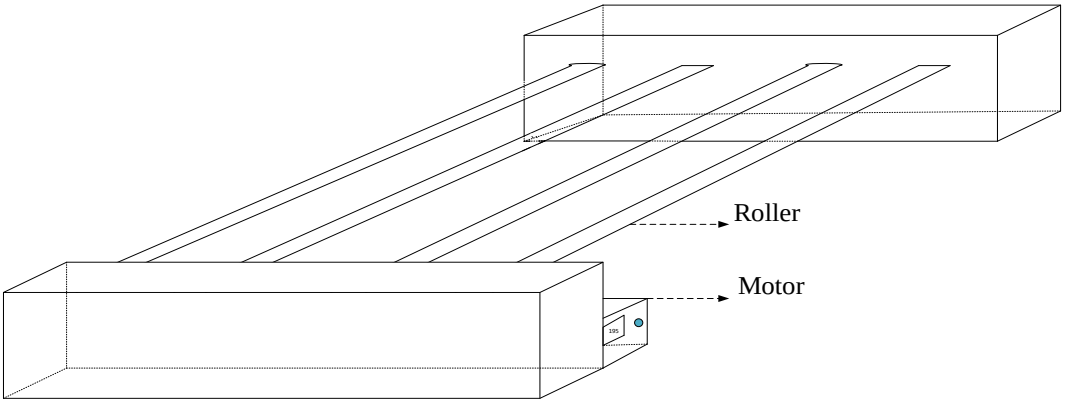

Figure 3.4: Mechanical roller drawing.

A volume of ~180 ml deionised water and a mass of ~60 g of the feed sample was added to the Schott bottle. The pH was adjusted and maintained at 10.5 - 11 by adding lime. A mass of ~0.12 g NaCN (98%) granules supplied by Alfa Aesar, was added to the pulp and the mechanical roller was switched on to start leaching. Solution samples were collected at predetermined intervals of 1, 2 and 24 hours, and analysed for gold using ICP OES. After 24 hours the mechanical roller was switched off. The pulp was water washed and filtered. The filter cake was oven dried at 50°C. The dry tailings were weighed and sent for gold fire assay.

3.3.5 Ultrafine milling

3.3.5.1 *Equipment and procedure*

Ultrafine milling was performed by a pulverizer machine. The setup consisted of a vibrator, pulverizer vessel and grinding components (two hollow cylindrical rings and a cylindrical block). Grinding components were positionally placed in the pulverizer vessel. A 100 g composite aliquot of the as received tailings sample was poured into the pulverizer vessel and the lid was closed. The vessel was clipped into its position, and the machine was turned on for a period of 120 seconds. After 120 seconds, the machine was switched off and the vessel emptied. A 20 g representative aliquot of the sample was sent for particle size analysis. The pulverizing process was repeated until about 7 kg of ultrafine sample were generated.

3.3.6 Microwave roasting pre-treatment

3.3.6.1 *Equipment and procedure*

A 1 kW, 2.45 GHz Samsung model domestic use microwave oven was used. 300 ml water load and approximately 60 g representative aliquots of the feed sample were used for microwave roasting experiments. The roasting setup is schematically represented in Figure 3.5.

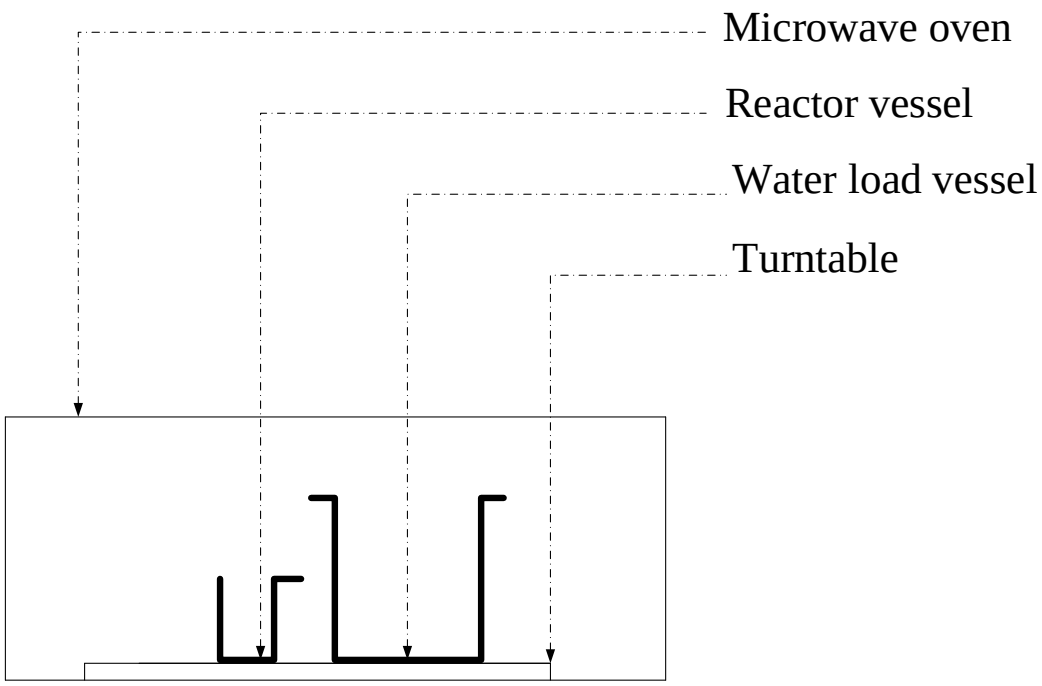

Figure 3.5: Microwave roasting pre-treatment setup.

The feed sample was placed in a 100 ml Duran glass beaker. The microwave oven was set for the intended duration and switched on. After roasting was complete, the sample was left to cool. After cooling, the sample was weighed, labelled, and stored prior to cyanidation.

For the test with the addition of 6% water, ~3.6 ml of deionised water was poured into the sample. The sample was thoroughly stirred until the moisture was evenly distributed within the sample. The 100 ml Duran glass beaker was positioned on the turntable of the microwave together with the 300 ml water load. The water load served to prevent the excessive reflection of microwaves which is harmful to the magnetron.

The microwave oven was switched on and set to run for 10 minutes to volatilise off all the moisture. After 10 minutes the sample was left to cool before water washing it in 200 ml deionised water at 200 rpm for 5 minutes. The pulp was filtered using a vacuum filter pump and the filtrate (wash water) was analysed for Au and S. The filter cake was oven dried at 50°C. The dry sample was microwaved again for the remainder of the set time (20 minutes). When the roasting time had expired, the sample was left to cool then weighed, labelled, and stored prior to cyanidation.

Cyanidation of the microwave roasted calcine followed the same cyanidation procedure described in section 3.3.4.

A 3 g composite of the cyanidation tailings was taken for SEM analysis, to investigate physical changes that might have resulted from the pre-treatment.

3.3.7 Microwave assisted leaching

3.3.7.1 *Microwave modification and safety*

Microwave modification poses a danger of irradiation leakages. The human body absorbs microwave irradiation and is vulnerable. Eyes and male reproductive organs are the most susceptible when exposed to high power levels for a lengthy period. Experts have set maximum leakage limit to 5 milliwatts per square centimetre (mW/cm^2) at 5 cm away from the aperture. The irradiation has a short wavelength, at 50 cm away, the irradiation falls by 100 times to 0.05 W/cm^2 (World Health Organization, 2005).

Microwave modification procedure

Three holes were drilled on the roof top of the microwave oven for the condenser, stirrer and sampling ports. An Al bush was made to seal the sampling port during operation. The turntable was removed and replaced by a stationary hollow bottom Teflon block. A Teflon lid was

designed with corresponding extension pipes to link the lid and the holes while curbing reactor leaks into the oven or atmosphere. After modification, the oven was inspected for radiation leaks by a Holaday microwave survey meter. Al tape was used to seal off small apertures along the edges that had resulted from drilling vibrations. The radiation leaks from the holes were maintained to below the recommended threshold of 5 mW/cm^2 (World Health Organization, 2005).

3.3.7.2 *Equipment and leaching procedure*

The microwave assisted leaching experimental setup consisted of a modified 1 kW, 2 450 MHz Samsung model microwave oven, an overhead stirrer, a Graham condenser and a 100 mm flange 1 L reactor vessel. Liquids volume and solids mass were 600 ml and 100g respectively. Liquids to solids ratio was 6:1. A schematic of the experimental setup is shown in Figure 3.6.

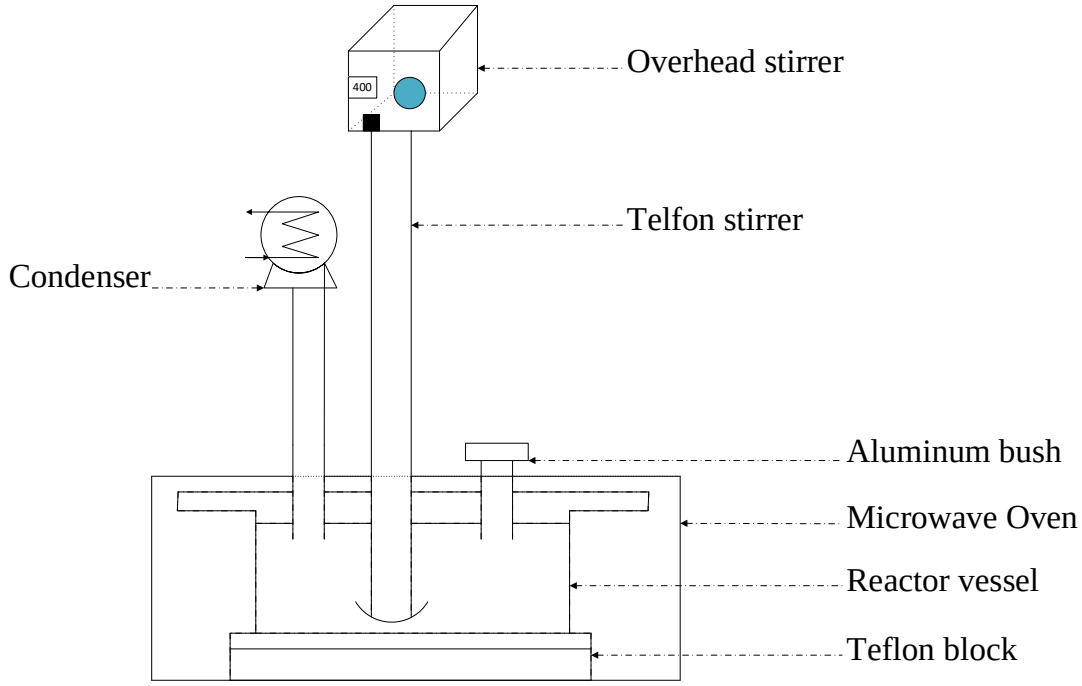

Figure 3.6: Modified microwave oven.

The first step of sample preparation entailed achieving the required solids concentration. The step was followed by preconditioning and pH adjustment. The reactor was then placed on a Teflon block at the geometric centre of the microwave oven. The stirrer height was adjusted to achieve uniform stirring, switched on and set to 400 rpm. After 3 minutes, the stirrer was switched off and pH of the pulp was measured. Lime was used to adjust the pH to the range of pH 10.5 – pH 11. As a safety precaution an HCN detector was positioned next to the microwave during the leaching operation.

The required NaCN concentration was added to the pulp. Leaching commenced when the pulp was agitated and irradiated simultaneously. A syringe and extender pipe were used to draw aliquots during sampling. Filtration was achieved by use of 0.22 µm syringe filters. These solution samples were collected at predetermined intervals of 10, 30 and 50 minutes. The solutions were analysed for Au. When the set time had lapsed, the overhead stirrer was switched off, and the oven door was opened to allow rapid cooling of the pulp. The pulp was washed with deionised water, filtered and oven dried at 50℃. The dry residue (tailings) was then weighed, labelled, and set aside for the fire assay.

A 3 g composite of the tailings was taken for SEM analysis, to investigate physical changes that might have resulted from the pre-treatment.

3.3.7.3 *Limitations of microwave experiments, equipment and context of study*

The equipment used for the microwave experiments was not optimised and had several limitations which include:

- Inability to accurately measure temperature against time. Ideally, this would help to understand if uniform heating was attained.
- Not all microwave heating was used to heat the sample as some of the microwave energy heated the water load which was necessary to protect the equipment.
- The set up did not quantify both the absorbed and reflected power.
- A retrofitted domestic applicator is not designed to vary power density. Increasing the power density above a material's critical power density and reducing residence time leads to energy savings and should be a consideration for any further work in this area.

Finally, in these tests irradiation of 60 g of sample for 60 mins (maximum time for tests) at 1 kW results in use of 16 700 kWh/t. This microwave energy input is far greater than the recommended economic limit around 5 kWh/t for industrial application (Batchelor et al., 2015). In the design of the experiment not all the 16 700 kWh/t is utilised on the sample. Attention for this work will however only focus on the potential to unlock gold which is presented by microwave roasting on the calcine tailings prior to cyanidation.

3.3.8 Sodium hydroxide pre-leach pre-treatment procedure

3.3.8.1 *Equipment and pre-conditioning*

A 200 mm flange, 5 L reactor, overhead stirrer and hot plate were used for the pre-leach pre-treatment setup (Figure 3.7). The required volume of deionised water was poured into the reactor followed by the required NaOH mass to constitute the desired concentration according to the experimental design in section 3.3.2.3. The overhead stirrer was switched on and adjusted to 700 rpm to help rapidly dissolve the NaOH pellets. Once the pellets were dissolved, the overhead stirrer was switched off, and the required mass of the feed sample was introduced to the reactor for ambient temperature tests.

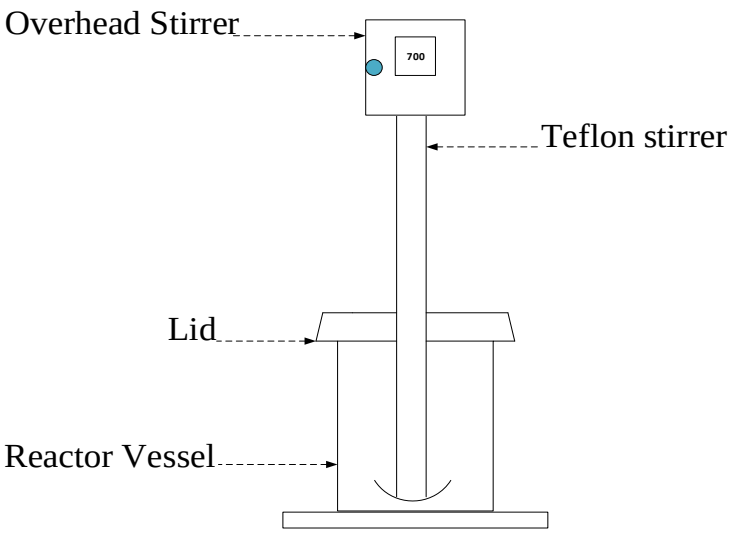

Figure 3.7: Ambient NaOH pre-leach pre-treatment apparatus.

For hot plate assisted leaching, the sodium hydroxide solution was heated to 80°C before the feed sample was added into the reactor. The reactor was insulated by a geyser blanket to curtail heat losses. Once the sample was added, the pre-leach pre-treatment procedure was the same for both ambient and 80°C tests. Figure 3.8 shows the equipment for the hot plate pre-leach pre-treatment setup.

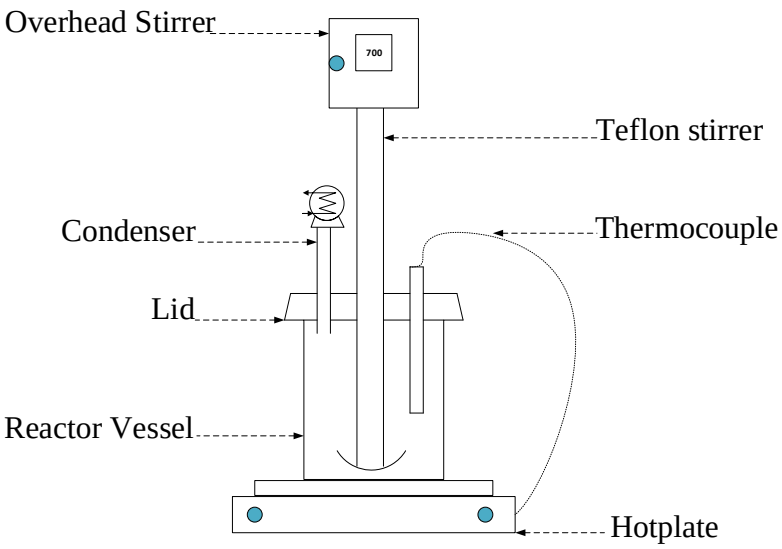

Figure 3.8: Hot plate NaOH pre-leach pre-treatment setup.

3.3.8.2 *General procedure for NaOH pre-leach pre-treatment*

The overhead stirrer was switched on. The stirrer height was adjusted to ensure homogeneous stirring at the same time preventing settling. Solution samples for Au, As, Al, Fe, S, Si and Zn analyses were drawn at 4 hours by means of a syringe and extender pipe. The solutions were filtered from the pulp using 0.22 µm syringe filters into labelled falcon tubes. At the end of the experiment, the overhead stirrer (and the hot plate for 80°C tests) was switched off.

The pulp was washed with deionised water, filtered, and oven dried at 50°C. The dry pre-leach residue was weighed, homogenised by crushing lumps, and rotary split to obtain a representative sample for gold fire assay. Cyanidation of the pre-leach residue followed the same cyanidation procedure described in section 3.3.4 except that there was no pH control required. The pH of the pre-leached pulp was highly alkaline < 11.

A 3 g composite of the tailings was taken for SEM analysis, to investigate physical changes that might have resulted from the pre-treatment.

3.3.9 Repeatability

3.3.9.1 *Microwave roasting pre-treatment*

Three repeat runs were carried out to confirm repeatability. The conditions were 30 minutes microwave roasting of the ultrafine sample with no water addition. The procedure is discussed

in section 3.3.6. Cyanidation of the microwave roasted residues followed the same procedure as in section 3.3.4.

3.3.9.2 *Microwave assisted leaching*

Microwave assisted cyanide leaching on the ultrafine sample at a sodium cyanide dosage of 8 kg/t for 50 minutes was repeated three times. Section 3.3.7 discussed the leaching procedure.

3.3.9.3 *Sodium hydroxide pre-leach pre-treatment*

Repeatability of sodium hydroxide pre-leach pre-treatment was checked by performing three repeats at 80℃ on the ultrafine sample at a sodium hydroxide dosage of 3 M. The pre-leach residues were cyanide leached. Experimental procedures for pre-leach pre-treatment and cyanide leaching are contained in sections 3.3.8 and 3.3.4 respectively.

3.3.10 Analytical methods

All solutions collected during pre-leach pre-treatment and cyanidation runs were analysed by ICP-OES and ICP-MS. Pre-leach pre-treatment solutions were analysed for Au, As, Al, Fe, S, Si and Zn while cyanidation solutions were analysed for Au only. Pre-leach pre-treatment feed and solid residues were sent for fire assay together with cyanidation feed and tailings. SEM was performed on the tailings to examine the transformations resulting from pre-treatment methods.

3.3.11 Data interpretation

The leaching efficiency of each run was calculated using Equation 25:

$$Leaching\ efficiency\ (\%) = \frac{V_L * C_L}{M_F * C_F} * 100 \qquad 25$$

Where V_L = Volume of leachate in reactor (L)

C_L = Concentration of leachate (µg/L)

M_F = Mass of feed sample used (g)

C_F = Concentration in feed sample (µg/g)

Due to irregularities observed from fire assay head samples for each run, a decision was made to use the calculated head grade (from the tailings grade) rather than the measured head grade. The calculated head grade was determined by maintaining the gold balance at the end of a leaching test as:

Gold (feed) = Gold (solution) + Gold (tailings)

This gold balance resulted in equation 26 for the measured head grade:

$$C_F * M_F = (C_T * M_T) + (V_L * C_L) \quad 26$$

Where C_F= Concentration in feed sample (mg/kg)

M_F= Mass of feed sample used (kg)

C_T= Concentration in tailings sample (mg/kg)

M_T= Mass of tailings (kg)

V_L= Volume of leachate in reactor (L)

C_L= Concentration in leachate (mg/L)

4.0 Results and discussion

The chapter is divided into two parts. The first part entails a detailed discussion of the findings based on the sample characterization while the second covers the findings from the gold recovery tests.

4.1 Sample characterization

The results of sample characterization tests which include fire assay, Particle Size Distribution (PSD), X-Ray Diffraction (XRD), X-Ray Fluorescence (XRF), chemical analysis (ICP), Scanning Electron Microscopy (SEM) and Quantitative Evaluation of Minerals by Scanning Electron Microscopy (QEMSCAN) are presented in this section.

The sample used for the study was excavated from the calcine tailings dam shown in Figure 4.1 at the New Consort mine. The material used for the study is reddish in colour. A combination of hematite and ferrian amounting to approximately 40 wt. % contributes to the reddish colour.

Figure 4.1: New Consort mine calcine dump. Taken during July 2019 site visit.

4.1.1 Head grade

Nine 100 g as received samples underwent fire assaying to determine the head grade. Table 4.1 presents results obtained from fire assay. The average head grade is 2.96 ± 0.26 g/t.

Table 4.1: Fire assay results.

Sample	Assay (g/t)
HG1	3.19
HG2	3.52
HG3	2.71
HG4	2.83
HG5	2.82
HG6	2.83
HG7	3.21
HG8	2.78
HG9	2.78
Average	2.96 ± 0.26

This grade is very high when compared to the average grade of South African dumps which is 0.5 g/t (Naicker *et al.*, 2003). The Evander and Elikhulu Tailings Reprocessing plants within the Pan African Resources group, have been processing tailings with head grades averaging between 0.28 and 0.30g/t while achieving recoveries that allow the operations to remain viable and dilute the overall gold cost of production (Pan African Resources, 2019a).

Potential exists to expand the gold revenue base by exploiting the New Consort tailings dump which has an estimated stockpile of 270 000 tonnes. The pursuit of the process is contingent on the development of a process with high recoveries and favourable economics.

4.1.2 Particle Size Distribution (PSD)

The particle size analysis of the as received sample is illustrated in Figure 4.2. The raw data is presented in Appendix B.

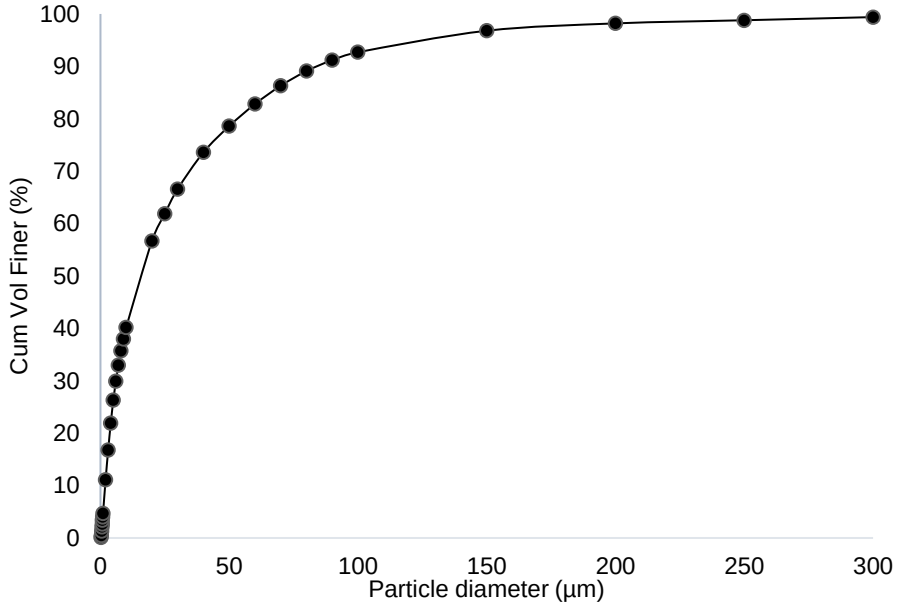

Figure 4.2: Particle size distribution of the composite as received calcine tailings sample.

The calcine tailings sample has a P_{80} – 53 µm and P_{50} – 16 µm which is finer than typical gold cyanidation tailings which are usually P_{75} – 75 µm (Muir *et. al*, 2005). Due to the refractory nature of the host ore, milling to P_{80} – 53 µm might have yielded increased gold recoveries.

4.1.3 X-Ray Diffraction (XRD)

XRD analysis was performed to determine the phase constituents of the composite as received calcine tailings. The results of the analysis are shown in Table 4.2.

Table 4.2: XRD results of the composite as received calcine tailings sample.

Mineral phase	**Wt.%**
Quartz (SiO_2)	22.4
Hematite (Fe_2O_3)	12.2
Magnesiohornblende, ferrian ($Ca_2[Mg_4(Al,Fe)]Si_7AlO_{22}(OH)_2$)	25.5
Clinochlore ($Mg_5Al(AlSi_3O_{10})(OH)_8$)	5.8
Biotite ($K(Mg,Fe)_3(AlSi_3O_{10})(F,OH)_2$)	10.2
Anorthite ($CaAl_2Si_2O_8$)	14.7
Talc ($Mg_3Si_4O_{10}(OH)_2$)	7.5
Calcite ($CaCO_3$)	1.8

The spectrum is illustrated in Figure 4.3. The results indicated that the major non-metallic and metallic oxides in the sample are silica and hematite, respectively making up 37% of the sample. Hematite in the calcine tailings is a roasting product from the host refractory arsenopyritic ore. Hematite is readily heated by microwaves whereas quartz does not heat up

(Amankwah & Ofori-Sarpong, 2011). The metals magnesium and aluminium are distributed in magnesiohornblende-ferrian, biotite and clinochlore. The silicate minerals quartz, magnesiohornblende-ferrian, clinochlore, biotite, anorthite and talc constitute 86% of the ore. The absence of arsenic and sulfur related phases largely points out to the efficiency of the roasting process which oxidized most of the arsenopyrite in the host ore leaving probably very little amounts which XRD could not detect.

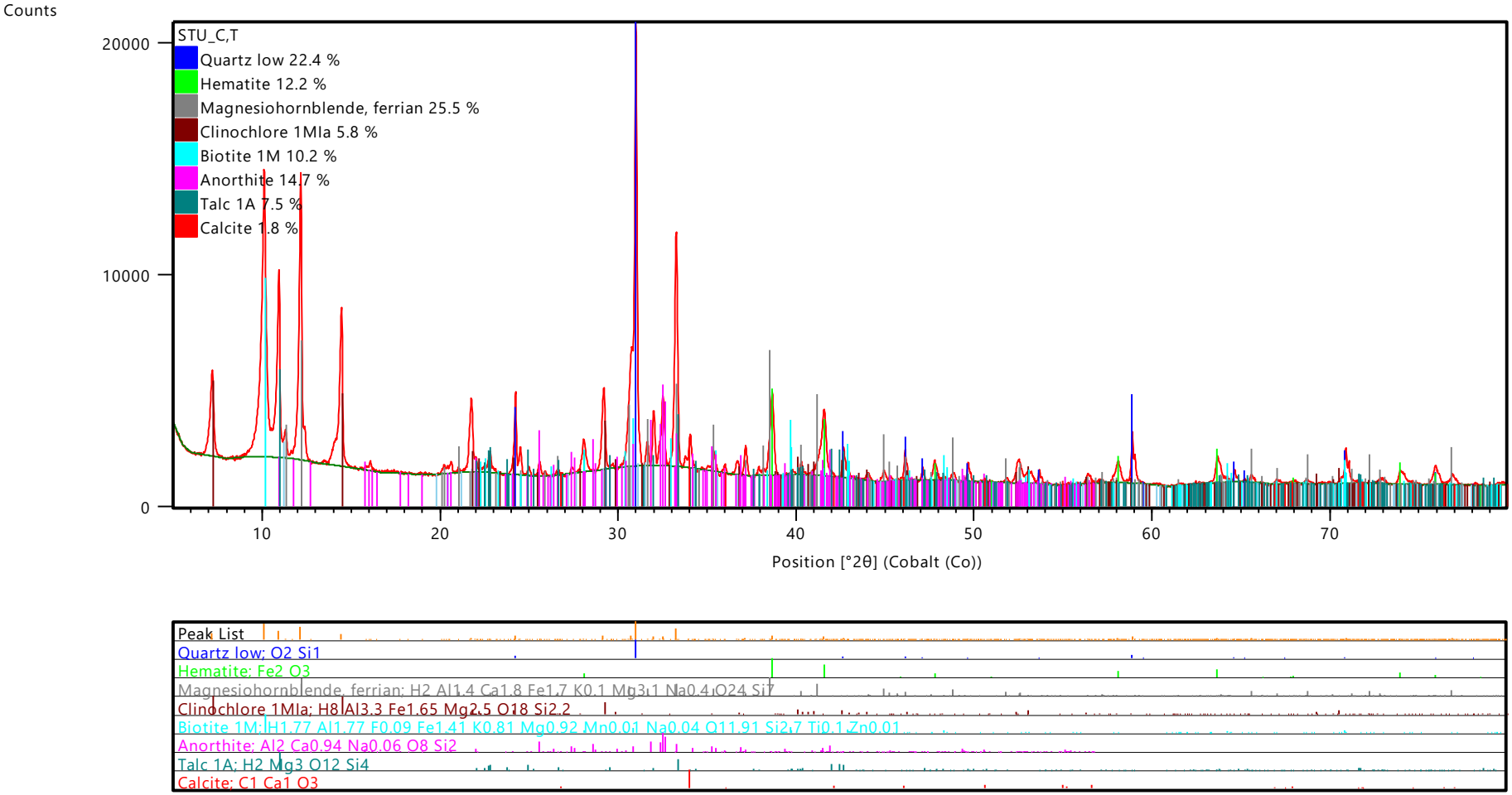

Figure 4.3: XRD spectrum of the composite as received calcine tailings sample.

4.1.4 X-Ray Fluorescence (XRF)

XRF was used to quantify the bulk chemistry of the composite as received calcine tailings sample. The results are shown in Figure 4.4.

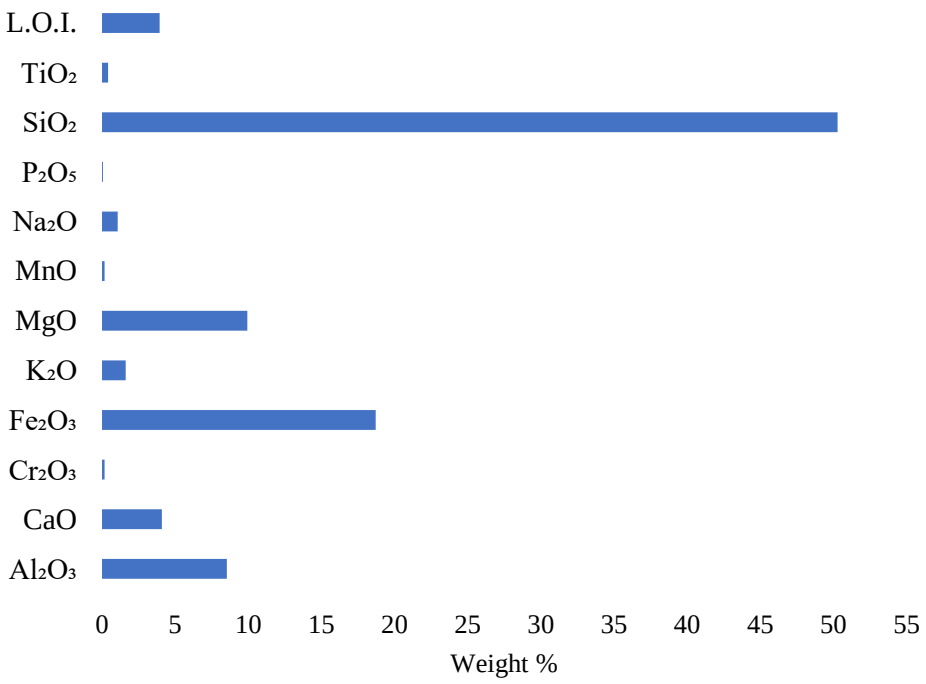

Figure 4.4: XRF results of the composite as received calcine tailings sample.

Silicon and iron are the major elements in the sample. Significant amounts of sodium, magnesium, potassium and aluminium were detected, and these are likely to be associated with the dominant silicate phases in the sample detected through XRD. Calcium is mainly hosted in calcite and silicate minerals. Loss on ignition (LOI) represents the elements (sulfur, arsenic, etc.) that were volatised in the process of attaining the XRF reading temperature of 1000°C.

4.1.5 Chemical analysis – Inductive Coupled Plasma (ICP)

A nitric acid-hydrogen peroxide digestion was performed on three composites of the as received calcine tailings samples. The solutions from the digestion were also analysed by ICP-MS and ICP-OES for trace elements (Table 4.3).

Table 4.3: ICP-MS and ICP-OES results of trace elements

Cu	**Cr**	**Co**	**Ba**	**Ni**	**Sb**	**As**	**S**
mg/kg	mg/kg	mg/kg	mg/kg	mg/kg	mg/kg	mg/kg	mg/kg
165	919	87	128	664	54	4 106	5 173
V	**Na**	**Sr**	**Zn**	**Sn**	**Pb**	**Mn**	**P**
mg/kg	mg/kg	mg/kg	mg/kg	mg/kg	mg/kg	mg/kg	mg/kg
84	897	35	314	2	120	922	261

Percentage deviation ranges from 2.8% – 12.0%.

Arsenic and sulfur are present in significant quantities as 4 106 ± 246 mg/kg and 5 173 ± 620 mg/kg respectively. These two elements are cyanide consumers and environmental contaminants. Copper and zinc are also cyanide consumers though they occur in relatively low proportions of 165 ± 11 mg/kg and 314 ± 25 mg/kg.

4.1.6 Scanning Electron Microscopy (SEM)

The objectives of the Scanning Electron Microscopy analysis on the as received calcine tailings sample were:

1) Identify the gold and its form.
2) Identify the gold associations.

4.1.6.1 *Gold particle size*

The gold particles detected by SEM analysis within the tailings sample were found to be ranging from nanometre to micron size. Figure 4.5 illustrates both nanometre (505.7 nm) and

micron (7.4 µm) gold particles. The 505.7 nm gold particle was the smallest size detected by SEM.

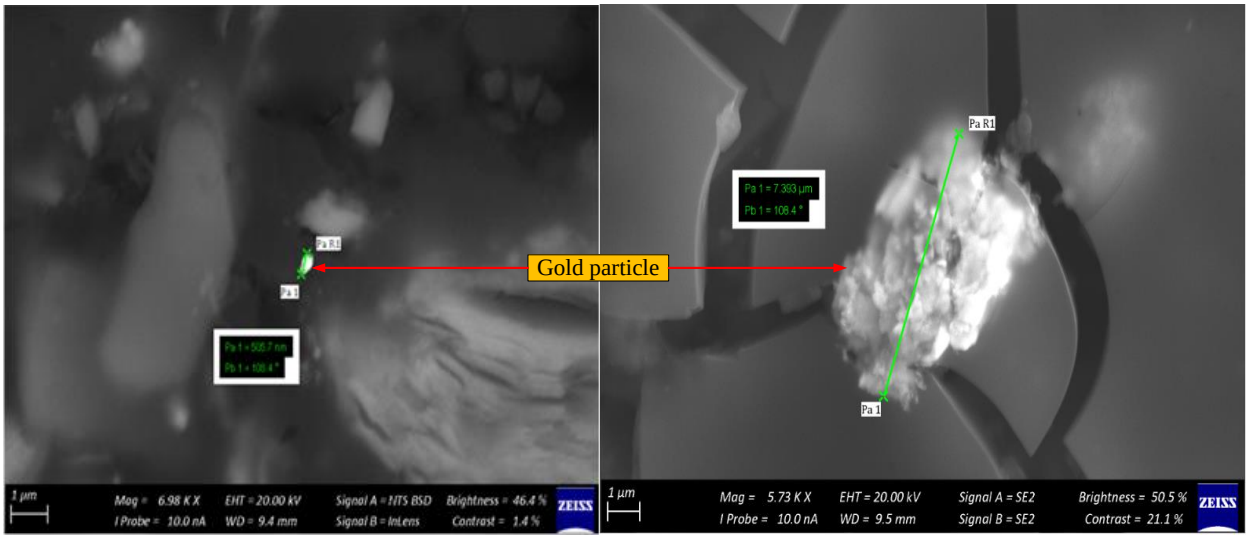

Figure 4.5: Image of the nanometre and micron gold particle detected by SEM.

4.1.6.2 *Encapsulation of gold*

Gold was found to be in association with gangue minerals, quartz and talc. Figure 4.6 displays an electron image, corresponding Energy Dispersive Spectrometry (EDS) spectra and overlay chemical maps. These show a gold particle occluded in a silicate matrix.

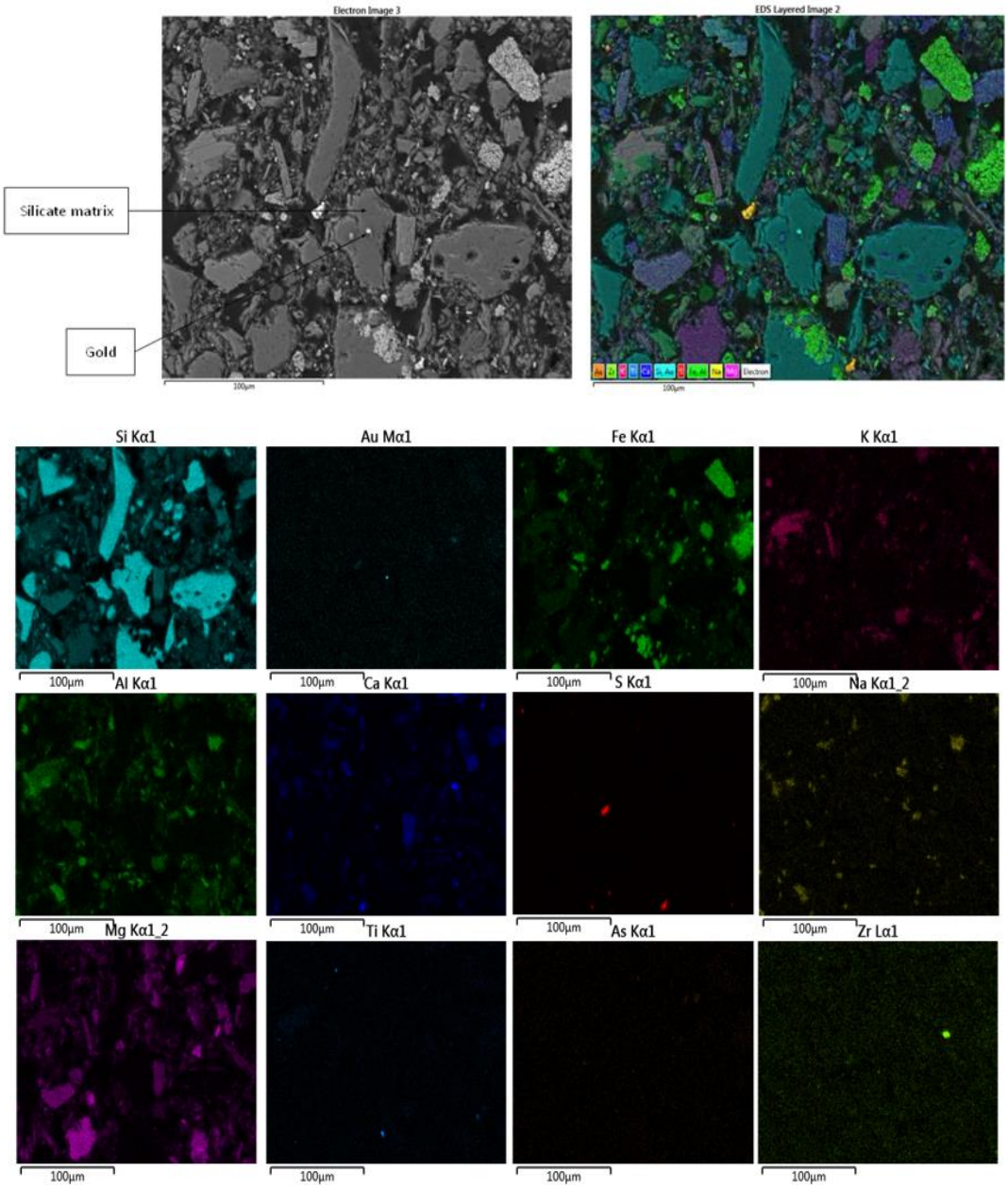

Figure 4.6: Electron image, EDS layered image and overlay chemical maps showing gold encapsulated in a silicate matrix.

The silicate matrix in which the gold particle is occluded is likely to be quartz due to the dominance of Si in the overlay maps. Further, no other elements occur within this grain.

The electron image in Figure 4.7 shows a gold particle encapsulated in a mineral matrix. The EDS image and the corresponding overlay maps (Figure 4.7) shed more light on the gold occlusion and association.

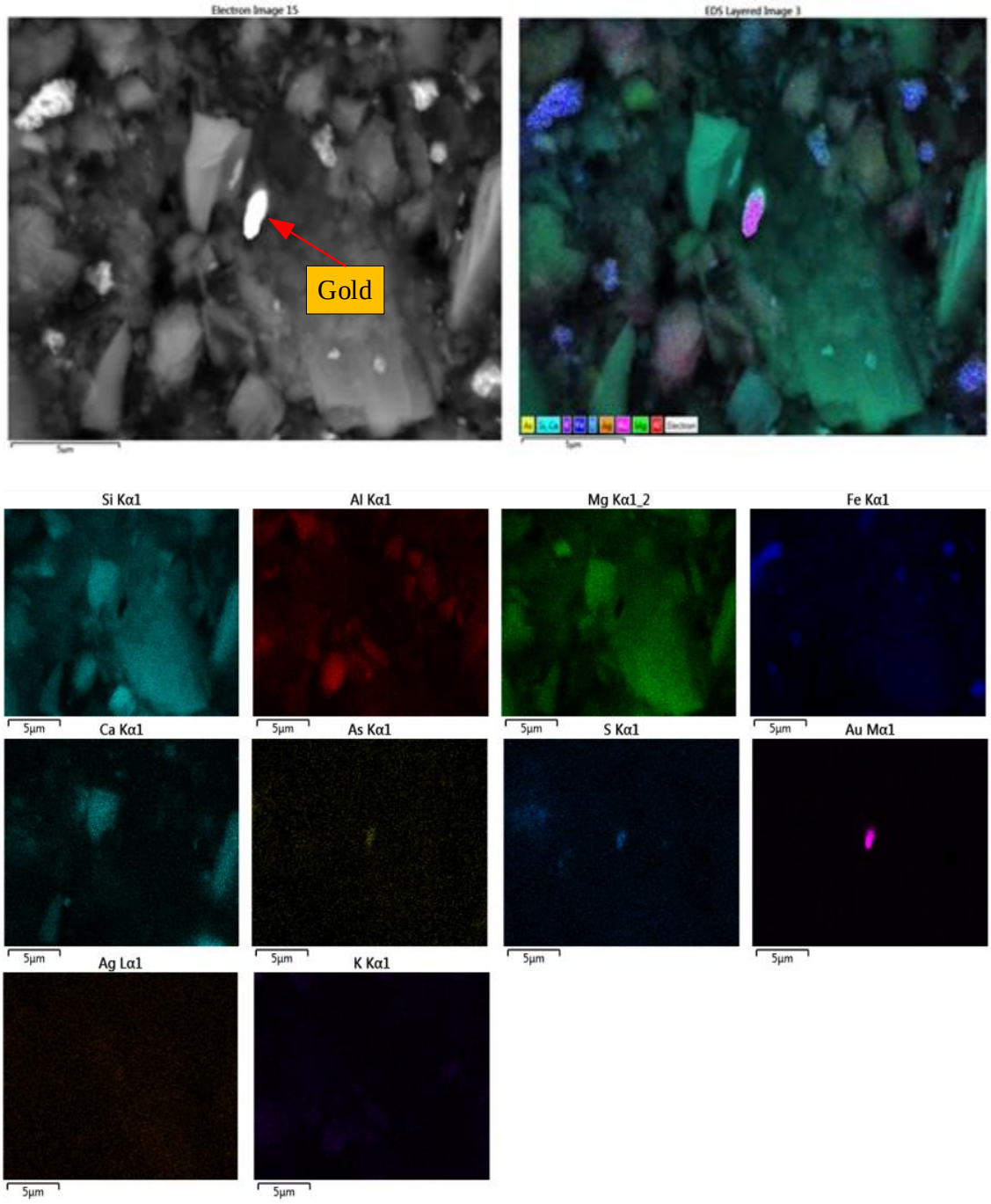

Figure 4.7: Electron image, EDS image and chemical overlay maps.

Gold exists in association with sulfur and arsenic inclusion in a silicate matrix as was observed in the chemical overlay maps in Figure 4.7. The absence of iron in the sulfur and arsenic association with gold is likely to be as a result of incomplete arsenopyrite oxidation during roasting of the host ore. It could also be due to the coalescence of arsenic and sulfidic roasting products with gold into porous walls (Swash & Ellis, 1986).

The silicate matrix in Figure 4.7 is in close resemblelance to talc due to the abundance of Mg and Si and no other association.

4.1.6.3 *Free gold*

Figure 4.8 shows the electron image, EDS layered image and overlay maps respectively confirming the occurrence of free gold in the as received tailings sample. The observation is based on the fact that there is no other element associated with the gold particle in the images and maps.

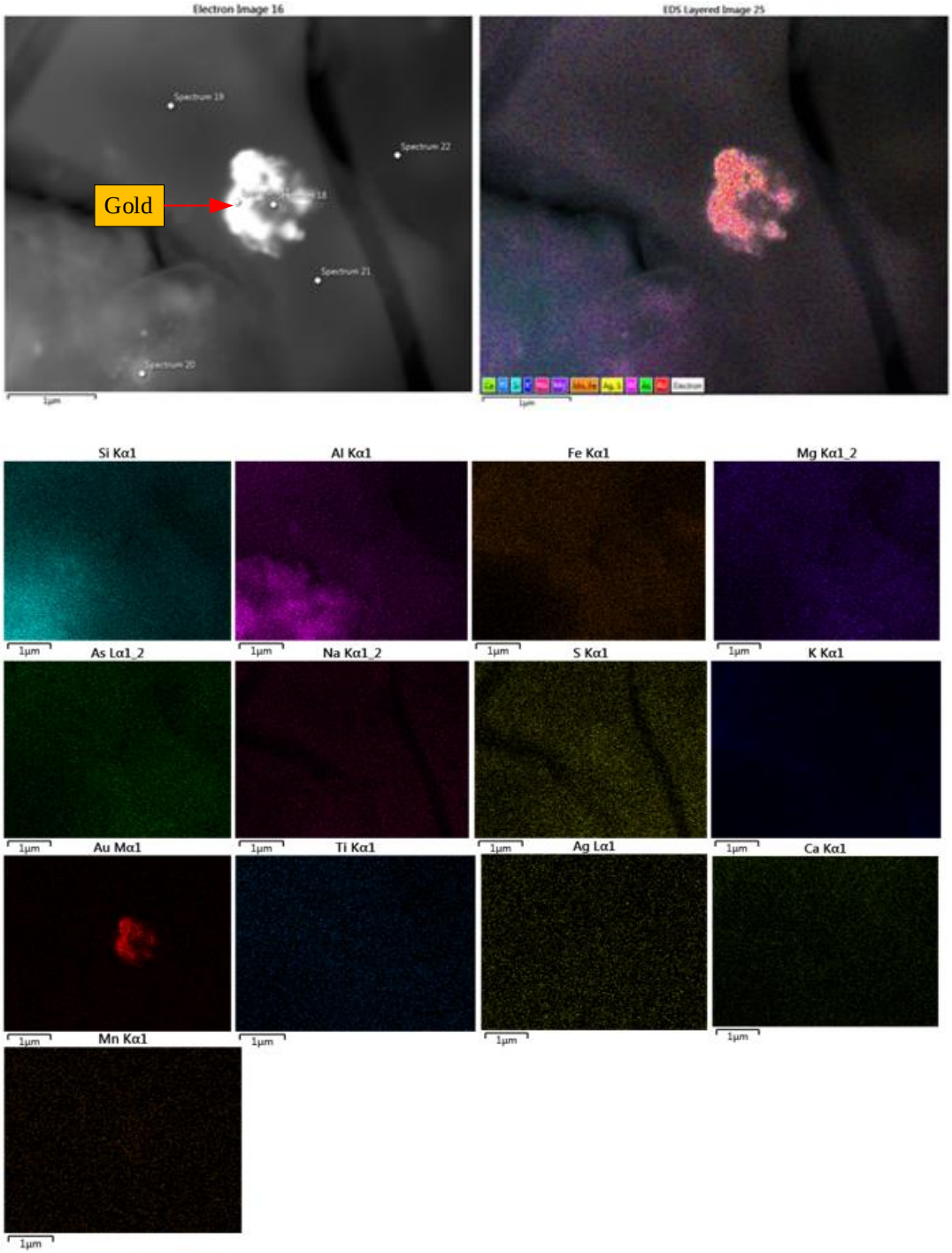

Figure 4.8: Electron image, EDS image and chemical overlay maps of free gold.

4.1.6.4 *Sulfide phase*

The SEM analysis confirmed the possible occurrence of a sulfide phase of interest in the as received tailings sample. Spectrum 13 is shown in the electron image in Figure 4.9 (circled in red), has very similar As, Fe and S mass percentages to arsenopyrite (FeAsS). Arsenopyrite in the tailings points to left over unoxidized particles during prior roasting.

Spectra 14 and 17 are iron oxide phases. Spectrum 15, 16 and, 18 are iron-silicate phases. These spectra are generally iron-rich gangue phases.

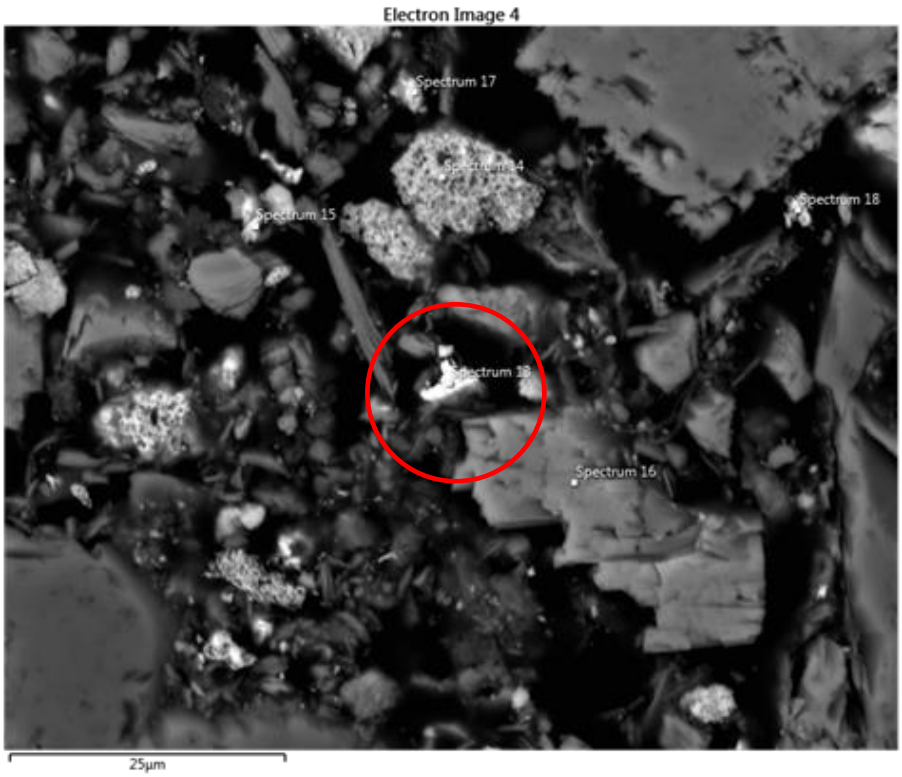

Figure 4.9: Electron image of phases in the as received tailings.

Figure 4.10 and Table 4.4 represent the weight percentages and elemental peaks for spectrum 13 respectively.

Table 4.4: Individual spectra chemical weight percentages.

Spectrum Label	Spectrum 13	Spectrum 14	Spectrum 15	Spectrum 16	Spectrum 17	Spectrum 18
O		25.58	27.75	40.62	20.29	31.36
Mg				9.54		
Al			2.20	0.53		
Si			6.25	26.50		11.30
S	18.24					
Ca				1.39		
Fe	32.13	74.42	63.80	21.40	79.71	57.34
Ni						
As	49.63					
Total	100.00	100.00	100.00	100.00	100.00	100.00

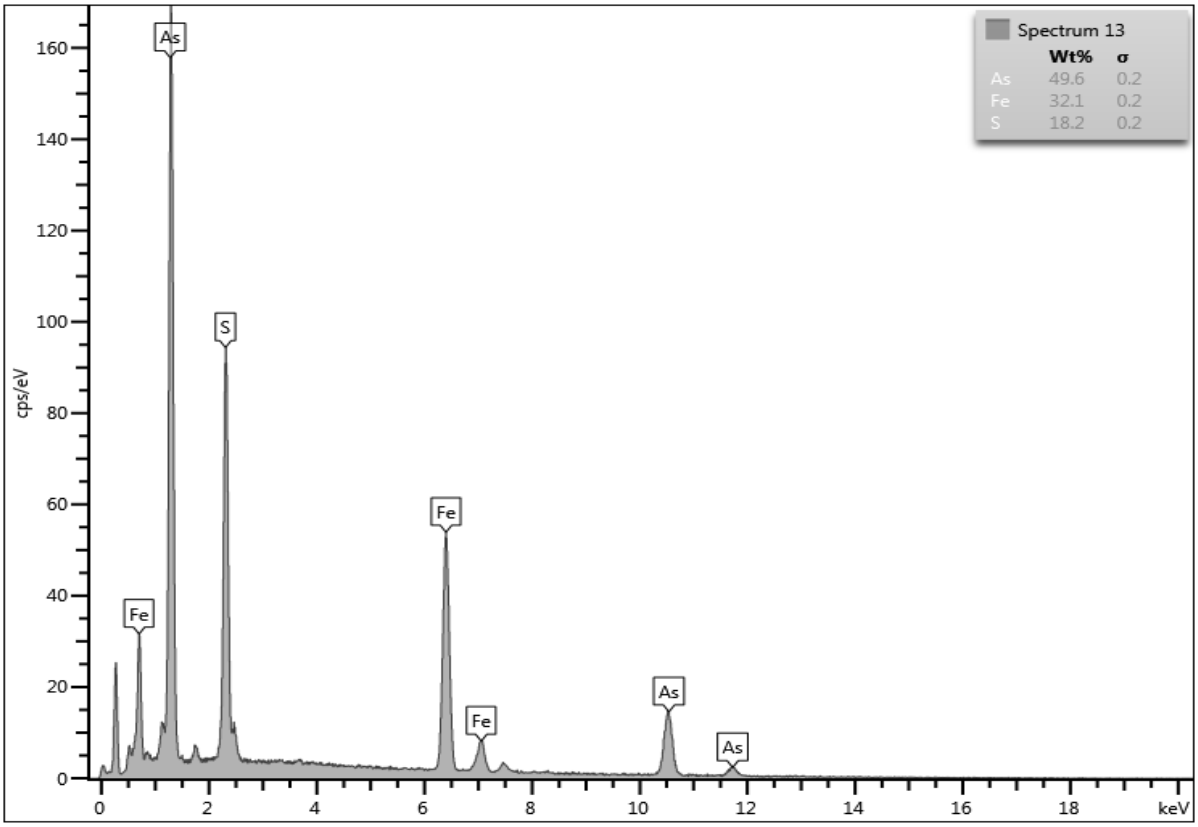

Figure 4.10: Peaks for spectrum 13.

4.1.6.5 *Metallurgical implications*

Submicroscopic gold

Ultrafine milling cannot effectively unlock gold that is < 1 µm. Additional pre-treatment which further alters the gold carrier phases can help to complement ultrafine milling for higher cyanidation gold recoveries (Corrans & Angove, 1991; Harbort *et al.*, 1996).

Gold occluded in a quartz grain

Gold occluded within a quartz grain is another cause of refractoriness since the lixiviant cannot percolate and dissolve gold that is encapsulated. Occlusion in quartz is typical of calcine. Owing to the oxidation of the host sulfide mineral during roasting, unlocked gold sometimes becomes occluded in the molten quartz.

Quartz is inactive when irradiated by microwaves as compared to other phases like hematite and arsenic carrying sulfides. When exposed to microwaves it is anticipated that differential expansion due to absorption of microwaves from hematite and sulfides may cause associated more brittle quartz to experience cracking (Amankwah & Ofori-Sarpong, 2011; Batchelor *et*

al,. 2015; Haque, 1999). Micro crack propagation might also be dependent on the relative amounts of the different phases for differential heating.

Quartz can also be decomposed by alkaline pre-leach pre-treatment, thus unlocking occluded gold surfaces (Crundwell, 2014b; Snyders *et al.*, 2018). The Si in quartz can be leached into solution during alkaline pre-leach pre-treatment.

Gold association with sulfur and arsenic in a talc matrix

The refractoriness in this scenario is twofold. The talc matrix shields gold surfaces from dissolution by lixiviant, and sulfur is a cyanide and oxygen consumer (Yannopoulos, 1991). The association of gold with arsenic and sulfur has been previously encountered by researchers Swash and Ellis (1986) who highlighted that during roasting, arsenic and sulfur oxidation products diffuse together with fused submicroscopic gold particles to porous walls.

Sulfur and arsenic can be leached into solution by alkaline pre-leach pre-treatment while the talc phase can be decomposed as well (Crundwell, 2014b; Mesa Espitia & Lapidus, 2015; Snyders *et al.*, 2018).

The existence of free gold

This gold should be readily dissolved by cyanide during cyanidation unless passivation of the gold surface is encountered (Bas *et al.*, 2015). Passivation of gold surfaces usually results from the pre-treatment method by film formation on gold surfaces due to decomposition of the surrounding phases (Yannopoulos, 1991).

Arsenopyrite phase

Numerous researchers have demonstrated the effectiveness of alkaline pre-leaching in decomposing arsenic bearing minerals (Darban *et al.*, 2011; Mesa Espitia & Lapidus, 2015; Snyders *et al.*, 2018). In addition, arsenopyrite is a good microwave irradiation absorber (Haque, 1999). This would help facilitate propagation of micro cracks due to thermal stresses arising from differential heating responses of the ore constituents during microwave roasting (Amankwah & Ofori-Sarpong, 2011).

Gold association with hematite

Gold in calcine tailings is usually expected to be in association with hematite due to oxidation of the host arsenopyrite during roasting. Hematite becomes the porous gold carrier. However, when all SEM analyses were done on the calcine tailings sample, there was no gold association with hematite that was observed.

Summary of gold association as confirmed by SEM

Table 4.5 shows a summary of the gold associations as detected by SEM. SEM was able to qualitatively give gold mineral associations.

Table 4.5: Gold association as detected by SEM.

Gold association			
Phases		**Elements**	
Quartz	Talc	Arsenic	Sulfur
✓	✓	✓	✓

4.1.7 Quantitative Evaluation of Minerals by Scanning Electron Microscopy (QEMSCAN)

QEMSCAN analysis was performed on the as received calcine tailings to reveal the bulk mineralogy and base metal mineral proportions. The bulk mineralogy QEMSCAN results are presented in Table 4.6. The associated graph is shown in Appendix C.

Table 4.6: Bulk mineralogy mass (%).

Mineral	**+75 µm**	**-75+38 µm**	**-38+25 µm**	**-25 µm**
Base metal minerals	0.3	0.6	1.0	1.7
Quartz	32.5	20.9	18.1	12.4
Feldspar	12.9	12.0	10.8	6.7
Pyroxene	3.8	3.8	3.4	5.9
Amphibole	15.5	22.2	21.1	18.1
Mica	13.3	12.3	11.6	13.4
Chlorite	6.8	7.1	7.2	14.0
Serpentine	1.1	1.3	1.0	0.8
Talc	2.6	3.6	2.6	3.8
Fe oxides	10.2	15.0	21.5	21.0
Rutile/Anatase	0.3	0.3	0.3	0.4
Dolomite	0.2	0.5	0.4	0.5
Apatite	0.2	0.1	0.1	0.2
Others	0.5	0.6	0.7	1.1

The dominant phases in all four size fractions are silicates (quartz, feldspar, amphibole and mica) and iron oxides. The results are consistent with XRD analysis which confirmed an abundance of silicates and hematite. Base metal minerals, rutile, dolomite and apatite occur in the calcine tailings in significantly low quantities. Gold grains could not be detected during

QEMSCAN analysis due to the submicroscopic size of the gold being below the detection limit of the instrument. Quantification of gold associations could therefore not be done.

The relative proportions of the base metal minerals are shown in Table 4.7 and the graph is illustrated in Appendix C.

Table 4.7: Base metal minerals.

Mineral	**+75 µm**	**-75+38 µm**	**-38+25 µm**	**-25 µm**
Chalcopyrite	22.7	17.0	13.2	17.5
Pyrrhotite	55.6	61.1	56.9	63.8
Pyrite	8.6	8.3	6.8	3.4
Pentlandite	0.1	0.3	0.2	0.4
Arsenopyrite	10.7	11.9	20.2	13.0
Sphalerite	0.9	0.1	0.0	0.2
Galena	0.7	0.1	0.2	0.4
Other Sulfides	0.0	0.6	1.1	0.7
Loellingite	0.8	0.4	1.3	0.7

After mineralogical characterisation was complete, the next phase of test work focused on gold recovery. The results obtained for the direct cyanide leaching, microwave pre-treatment, microwave assisted leaching and sodium hydroxide pre-treatment will be discussed in the following sections. Discussion of a simple high level possible economic contribution analysis from the test results concludes the chapter.

4.1.8 As received sample

The extent of refractoriness on the calcine tailings was investigated by direct cyanidation. The tests were done in duplicate for 24 hours by means of bottle rolls. Solution samples were collected at 1, 2 and 24 hours, and analysed for gold by ICP-OES. The cyanidation gold recoveries are shown in Figure 4.11 and the raw data is presented in Appendix D.

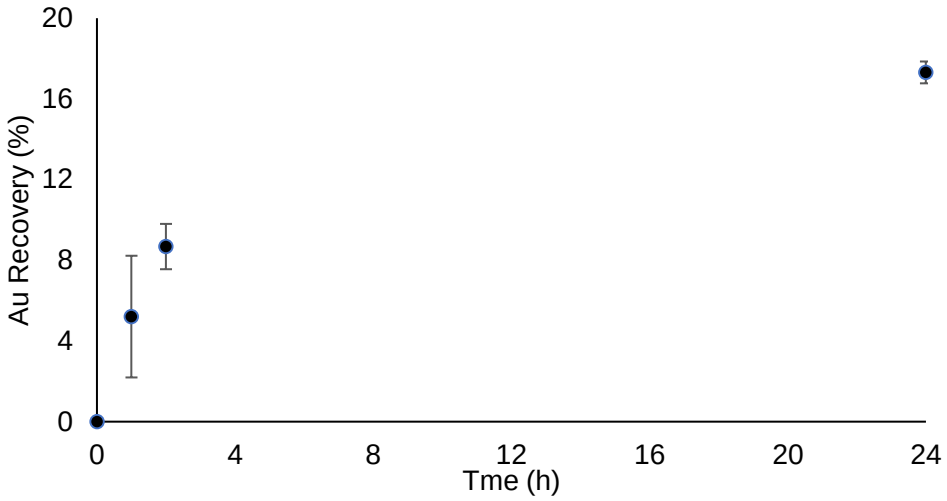

Figure 4.11: Repeat tests results of direct cyanidation of the as received sample. (25% solids, 2 kg/t NaCN, pH 10.5 – pH 11, 195 rpm, 25°C).

The test results indicated an average gold recovery of 17.3 ± 0.54%. The poor recovery classifies the calcine tailings in the category of highly refractory material (Amaya *et al.*, 2013). The recovery also serves to give an indication of the amount of free gold within the calcine tailings sample as refractory gold cannot be leached by conventional cyanide leaching. This recovery will serve as the benchmark to compare the effectiveness of ultrafine grinding, pre-treatment methods and microwave assisted leaching on the calcine tailings.

4.1.9 Ultrafine milling Particle Size Distribution

Figure 4.12 is a graphical representation of the particle size distribution of the ultrafine milled as received tailings sample. Data used to generate the curve is presented in Appendix E.

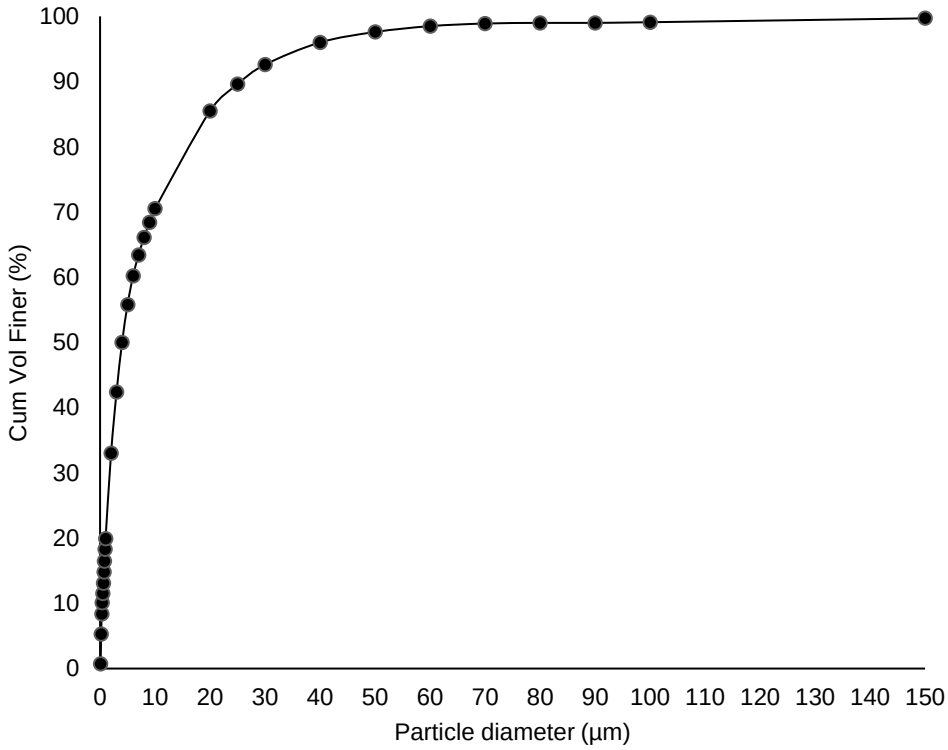

Figure 4.12: Particle size analysis of the ultrafine milled sample.

The as received calcine tailings sample was pulverised for 120 seconds to yield a P_{80} - 16 µm and P_{50} - 4 µm from P_{80} - 53 µm. This substantial size reduction is beneficial to eliminate physical refractoriness of the sample in instances where the gold is coarse (>1 µm). Eliminating the physical barriers expose gold surfaces for lixiviant attack (Corrans & Angove, 1991; Pooley, 1987; Yannopoulos, 1991).

4.1.10 Effect of ultrafine milling on cyanidation

Unlocking occluded gold brought about by ultrafine milling the calcine tailings sample was investigated by 24-hour bottle roll experiments. This was conducted in duplicate. Solution samples were collected at 1, 2, 8 and 24 hours, and analysed for gold by ICP-OES. The leaching recoveries are displayed in Figure 4.13 and the raw data in Appendix F.

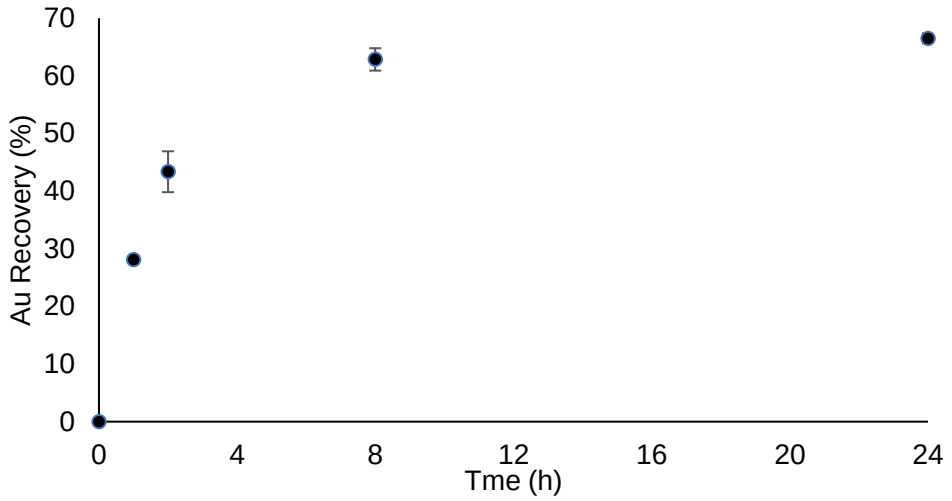

Figure 4.13: Repeat tests results of direct cyanidation of the ultrafine sample. (25% solids, 2 kg/t NaCN, pH 10.5 – pH 11, 195 rpm, 25°C).

The average gold recovery after 24 hours was 66.5 ± 0.87%. The results indicated that ultrafine milling of the composite as received calcine tailings was instrumental in improving gold recovery. This also proved that part of the gold in the tailings sample existed in a physical refractory nature. The breaking of the host matrix by ultrafine milling effectively exposed gold surfaces for cyanide attack (Yannopoulos, 1991).

4.1.11 Microwave roasting pre-treatment

The effect of microwave roasting pre-treatment on the calcine tailings to increase cyanidation gold recoveries was investigated. Four calcine tailings samples (3 as received and 1 ultrafine) were microwave roasted and cyanide leached. Solution samples were collected at 1, 8 and 24 hours, and analysed by ICP-OES for gold. The leaching curves showing gold recoveries are displayed in Figure 4.14 and other data is presented in Appendix G.

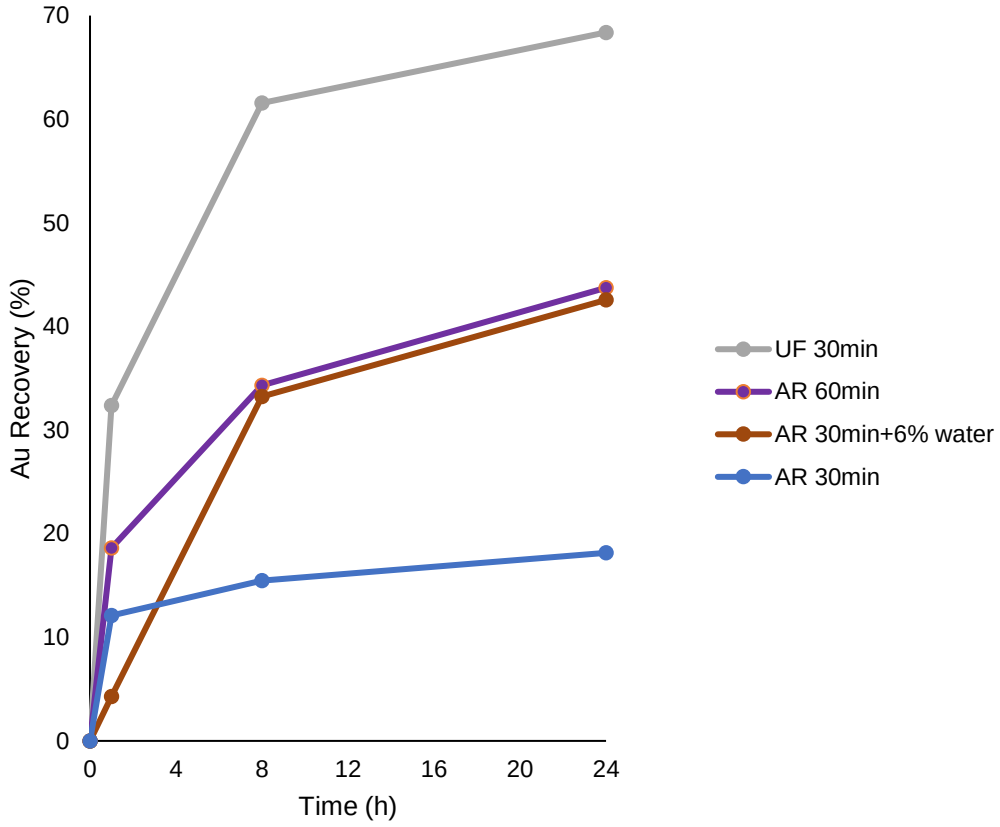

Figure 4.14: Cyanidation of microwave roasted samples. (UF – ultrafine, AR – As received, Ambient (uncontrolled room temperature), 25% solids, 2 kg/t NaCN, pH 10.5 – pH 11, 192 rpm).

Gold recoveries of 68.4% was obtained for the ultrafine sample after 24 hours of cyanidation. However, considering that the direct cyanidation gold recovery on the ultrafine sample was 66.5%, microwave roasting of the ultrafine sample did not perform as expected. Further investigation (time and microwave treatment conditions) of microwave roasting on the ultrafine sample is recommended.

Microwave roasting pre-treatment generally improved gold recovery on the ‘as received’ sample. The highest gold recovery effected by microwave roasting on the ‘as received’ sample was 43.7% after a roasting time of 60 minutes. This recovery was 2.5 times more than the direct cyanidation recovery of 17.3% of the as received sample. The increase suggests the possibility that micro cracks were induced (either quartz or talc) in the as received sample by microwave irradiation thereby exposing occluded gold surfaces for cyanide attack. The micro cracks result in enhanced lixiviant percolation as noted by Amankwah and Ofori-Sarpong (2011). It cannot however be concluded that only micro-cracks were specifically responsible for the increase in

recovery due to the equipment not being optimised for generation of microcracks, as discussed in section 3.3.7.3.

Microwave roasting the as received sample for 30 minutes yielded 18.2% cyanidation gold recoveries. Doubling the roasting time gave 43.7% cyanidation gold recoveries. These recoveries highlighted that a longer roasting time allowed for greater alteration of the as received sample as a result of micro crack propagation on the as received sample.

Water was added to improve microwave heating of the as received sample. A 42.6% cyanidation gold recovery was achieved after a total of 30 minutes microwave roasting on the as received sample with a 6% water addition. A 24.4% increase in gold recovery was attained as compared to microwave roasting the as received sample without water addition for 30 minutes. A 6% water addition before microwave roasting and a water washing step after 10 minutes of microwave roasting (discussed in section 3.3.6.1) are attributed to have effected an increase of in cyanidation gold recoveries as explained below.

Water addition

Water has excellent microwave absorption characteristics and as it evaporates during roasting, it leaves behind micro-holes due to expansion of steam. Hu *et al.* (2017) observed that generation of the micro-holes in gold hosting phases increases the porosity of the sample and specific surface area thereby exposing gold surfaces for cyanide leaching. Though it was not specifically searched for this process could account for increased recoveries.

Water washing step

Following analysis by ICP-OES of the water wash solution, no gold was detected, and 484.4 mg/L of sulfur were extracted from the sample. The observed results suggest that microwave treatment roasting the calcine, converting the S still left in the calcine into water soluble SO_2, and so enhancing subsequent cyanidation of the Au. Cyanidation is enhanced as the quantity of sulfur, which is a cyanide and oxygen consumer is reduced, thereby leaving more free cyanide ions to form gold complexes and yield a higher gold recovery (Lorenzen & van Deventer, 1992).

Despite limitations (section 3.3.7.3), the tests managed to show that microwaves have the potential to unlock encapsulated gold. It is possible that cyanidation recoveries might be increased by use of optimized equipment.

4.1.11.1 *Scanning Electron Microscopy (SEM) of the cyanidation tailings*

Tailings generated from cyanidation of the 30 minute microwave roasted ultrafine sample were analysed using SEM. An electron image for the tailings analysis is displayed in Figure 4.15.

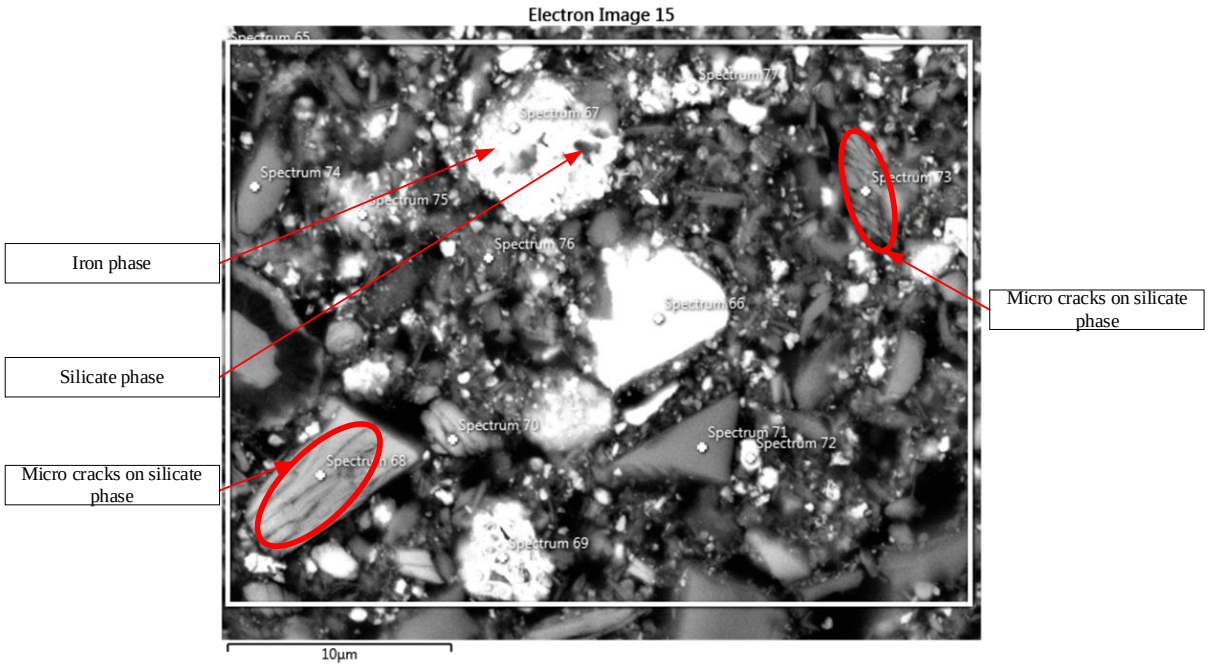

Figure 4.15: SEM analysis of cyanidation tailings of microwave roasted calcine.

Spectrum 68 and 73 are silicate phases in the electron image which indicate micro cracks. The micro cracks might have been facilitated by microwave pre-treatment due to differential heating responses within the carrier matrix. Spectrum 67 shows a shiny iron phase which is perceived to have been exposed by the gradual "peeling off" of the silicate phase (dark shade within the iron phase). The micro cracks and gradual "peeling off" improve lixiviant percolation and access to exposed gold surfaces during cyanidation. A summary of the spectra in the electron image is displayed in Appendix K.

4.1.11.2 *Repeatability*

The result of repeatability tests of microwave roasting pre-treatment followed by cyanidation was examined. Three cyanidation repeat runs were carried out for ultrafine samples after undergoing 30 minutes microwave roasting. The results for the repeatability tests are shown in Figure 4.16 and Table 4.8. Other generated data used are presented in Appendix G.

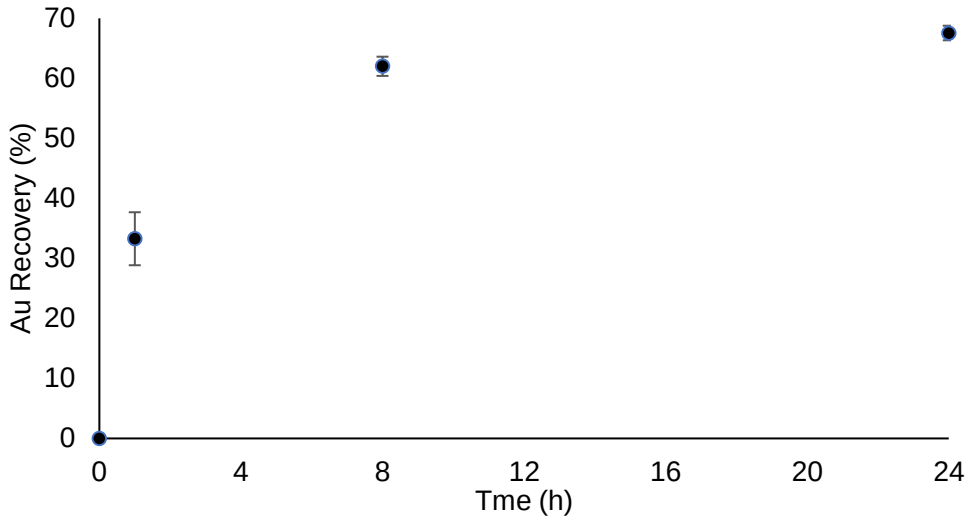

Figure 4.16: Repeats of cyanidation of microwave roasting pre-treatment (30 mins, Ultrafine). (Ambient-uncontrolled room temperature, 25% solids, 2 kg/t NaCN, pH 10.5 – pH 11, 192 rpm).

Table 4.8: Repeatability data on cyanidation of microwave roasted calcine.

Time (h)	**1**	**8**	**24**
Repeat 1 (%)	34.7	62.0	68.7
Repeat 2 (%)	36.8	63.6	67.8
Repeat 3 (%)	28.3	60.4	66.3
Average (%)	33.3	62.0	67.6
Standard Deviation (%)	4.42	1.60	1.22

For the three repeats, it was observed that the error limit decreased as the leaching time increased. At 1, 8 and 24 hours, the error limits were 4.42%, 1.60% and 1.22%. Repeatability improved as residence time was increased. This could be due to the heterogeneity of the microwave roasted calcine samples which triggered different cyanidation responses at the beginning of the leaching runs.

The repeatability of microwave pre-treatment followed by cyanidation was considered to be very high with an error limit of 1.22%.

4.1.12 Microwave assisted leaching

Microwaves were used to aid direct cyanide leaching for improved recoveries on the as received and ultrafine samples. Six microwave assisted cyanide leaching runs were performed. Solution samples were collected at 10, 30 and 50 minutes, and were analysed for gold by ICP-OES. The leaching results are illustrated in Figure 4.17. Appendix H contains further data.

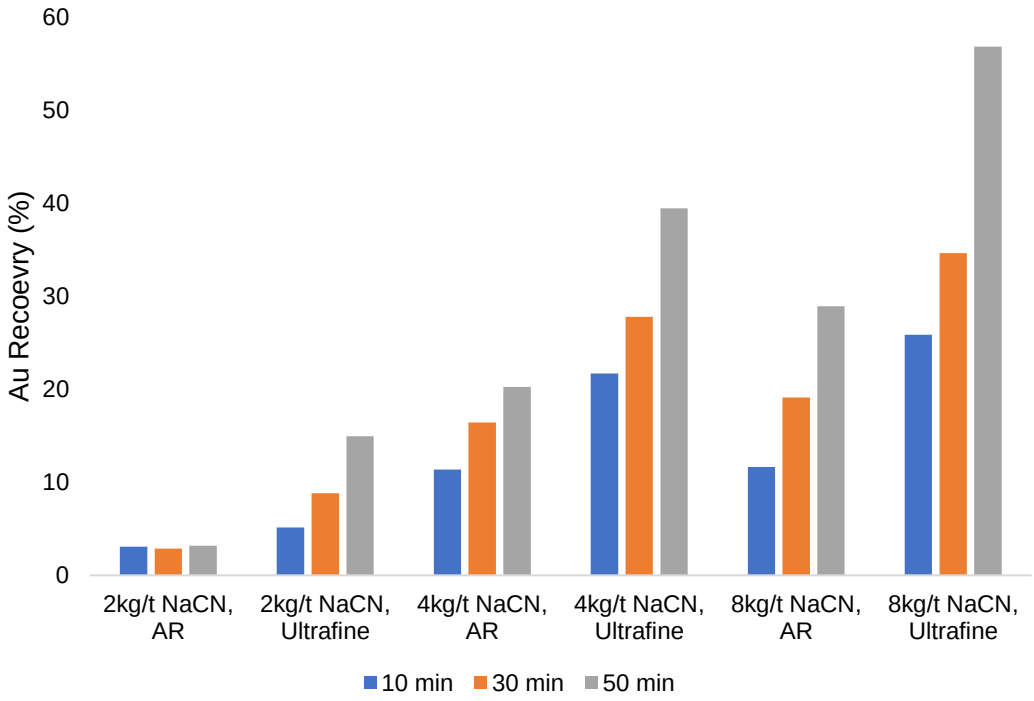

Figure 4.17: Microwave assisted leaching progression with respect to time (pH 10.5 – pH 11, 400 rpm). Key AR-As received.

Leaching at 2 kg/t NaCN for both the as received sample and ultrafine sample yielded low gold recoveries of 3.2% and 15.0% respectively. Increasing the NaCN dosage to 4 kg/t and 8 kg/t effected low gold recoveries of 20.3% and 29.0% respectively on the as received sample. It was observed that increasing the NaCN dosage during microwave assisted leaching of the as received sample produced a gradual increase in gold recoveries though recoveries were still very low. Cyanicides consume free cyanide ions thus hindering gold cyanide complex formation (Pooley, 1987; Yannopoulos, 1991).

Increasing the NaCN dosage to 4 kg/t on the ultrafine milled sample had a significant effect on the gold recovery. The attained recovery was 39.5%. Further, doubling the NaCN to 8 kg/t gave a 17.4% increase in gold recovery to 56.9%. The significant improvement in gold recovery brought about by 8 kg/t NaCN in the ultrafine milled sample, highlights the benefits of the rapid kinetics associated with microwave assisted leaching. According to Huang and Rowson (2002) and Krishnan *et al.* (2007), thermal convection currents are generated by differential heating responses of the various ore constituents. These convection currents facilitate the rapid removal of reaction products from the solid-liquid interface. This allows rapid exposure of unreacted surfaces for continuous lixiviant attack. The vigorous nature (microwave heating and

stirring) of the leaching was considered to be effective in washing away any passivated gold surfaces thus exposing them for cyanide action.

Gold recovery increased considerably as NaCN dosage increased on the ultrafine milled sample. This also points out to chemical refractoriness of the sample to a greater extent (Pooley, 1987; Yannopoulos, 1991). Microwave heating is suspected to have aided dissolution of ultrafine milled gangue phases as in depiction given in Figure 2.9 which could have been through localised heating of gangue phases. Therefore, increasing the cyanide dosage increases the availability of free cyanide ions thus helping ease the competition for free cyanide ions. More gold complexes are formed which ultimately increases gold recovery.

Mukendi *et al.* (2000) carried out microwave assisted cyanide leaching tests on a different refractory material containing 35% pyrite, 13% arsenopyrite and 5% pyrrhotite which resulted in 59% gold recoveries. However, in the current study microwave assisted leaching of the as received sample (86% silicates, 12% hematite) yielded a 29% gold recovery. This might be indicative that the current material is relatively more refractory than that of Mukendi *et al.* (2000) as the recovery could only be upgraded to 57% by ultrafine milling. Mukendi *et al.* 2000's material had a large quantity of sulphides which are better microwave absorbers than silicates which dominate refractoriness in the current study's material (Amankwah & Ofori-Sarpong, (2011);Haque, (1999)).

4.1.12.1 *Scanning Electron Microscopy (SEM) of microwave assisted leaching tailings*

Cyanidation tailings of microwave assisted leaching of the ultrafine sample at 8 kg/t NaCN for 50 minutes were analysed by SEM. Figure 4.18 shows an electron image of the SEM results.

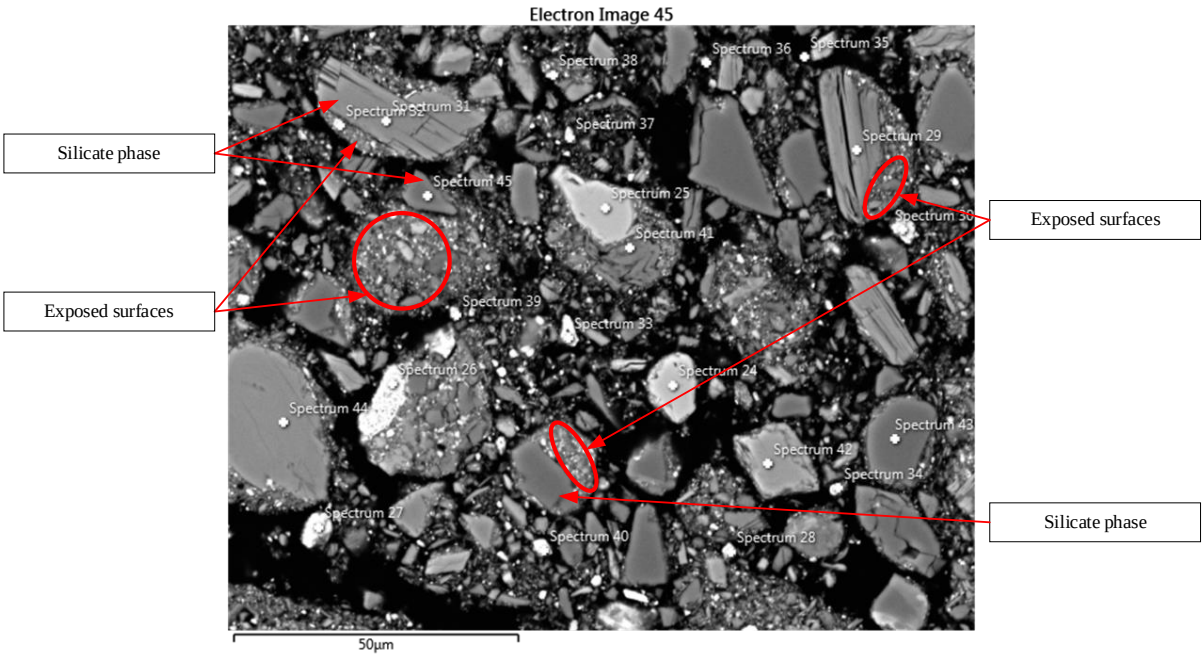

Figure 4.18: SEM analysis of microwave assisted cyanidation tailings.

Owing to the abundance of silicates in the sample, encapsulation causing refractoriness is attributed to them. The electron image indicates the effectiveness of the treatment method which induced mechanical defects on the silicate phases. “Peeling off” or washing off of the silicate phases as seen in the image exposes fresh surfaces for possible extraction of gold during cyanidation. An example of this phenomena is spectrum 31 (barrier) and spectrum 32 (exposed surface) which are silica and iron dominated respectively. The faster the washing away, the faster the gold-cyanide complex formation and the higher the recoveries attained.

Individual spectra compositions for the highlighted phases are in Appendix L.

4.1.12.2 *Repeatability*

Repeatability runs were performed on the ultrafine sample at a NaCN dosage of 8 kg/t. The results obtained are illustrated in Figure 4.19 and Table 4.9. Appendix H contains raw data generated during the runs.

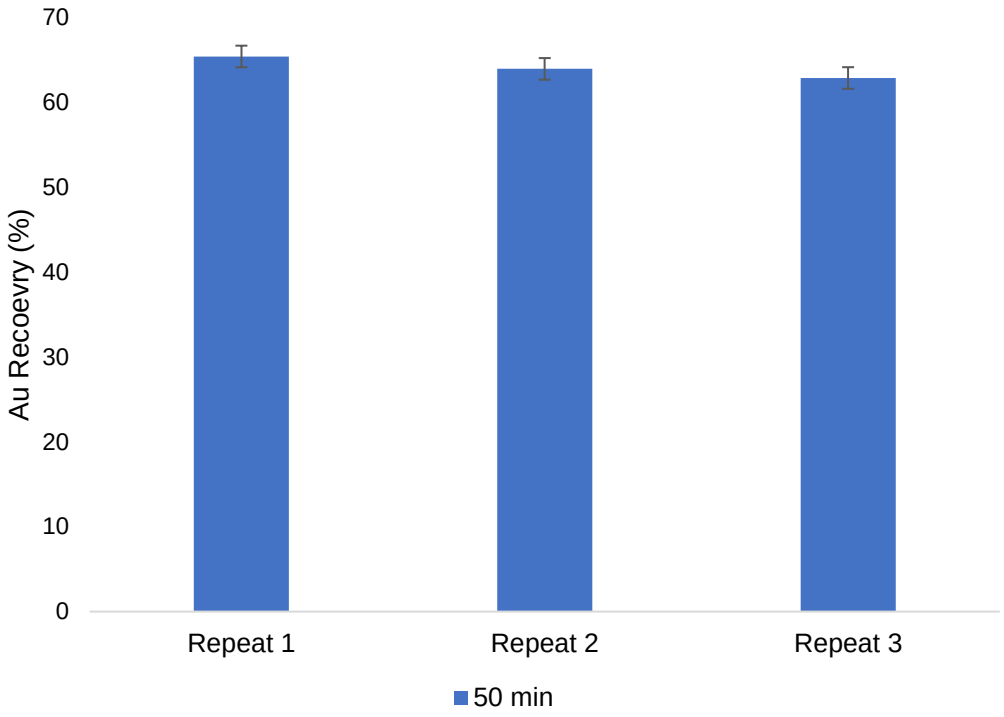

Figure 4.19: Repeats of microwave assisted leaching. (8 kg/t NaCN, liquids: solids ratio 6:1, pH 10.5 – pH 11, 400 rpm).

Table 4.9: Data on repeats of microwave assisted leaching.

Repeat 1 (%)	65.4
Repeat 2 (%)	63.9
Repeat 3 (%)	62.9
Average (%)	64.1
Standard Deviation (%)	1.27

An average gold recovery of 64.1 ± 1.27% was achieved after 50 minutes of microwave assisted cyanidation. The repeatability of microwave assisted leaching proved to be very high with an error limit of 1.27% at 50 minutes.

4.1.13 Sodium hydroxide pre-leach pre-treatment

Eight NaOH pre-leach pre-treatment runs were performed as described in section 3.3.2.3. Pre-leach pre-treatment solution samples were collected at 4 hours. These were analysed by ICP-OES for impurities that included Al, As, Fe, S, Si and Zn. Results of the analyses are shown in Figure 4.20. Gold extraction during the pre-leach pre-treatment experiments was also monitored, Figure 4.21 and Figure 4.22 displays the extraction during each run. Assays and other leaching data for all pre-leach runs are contained in Appendix I.

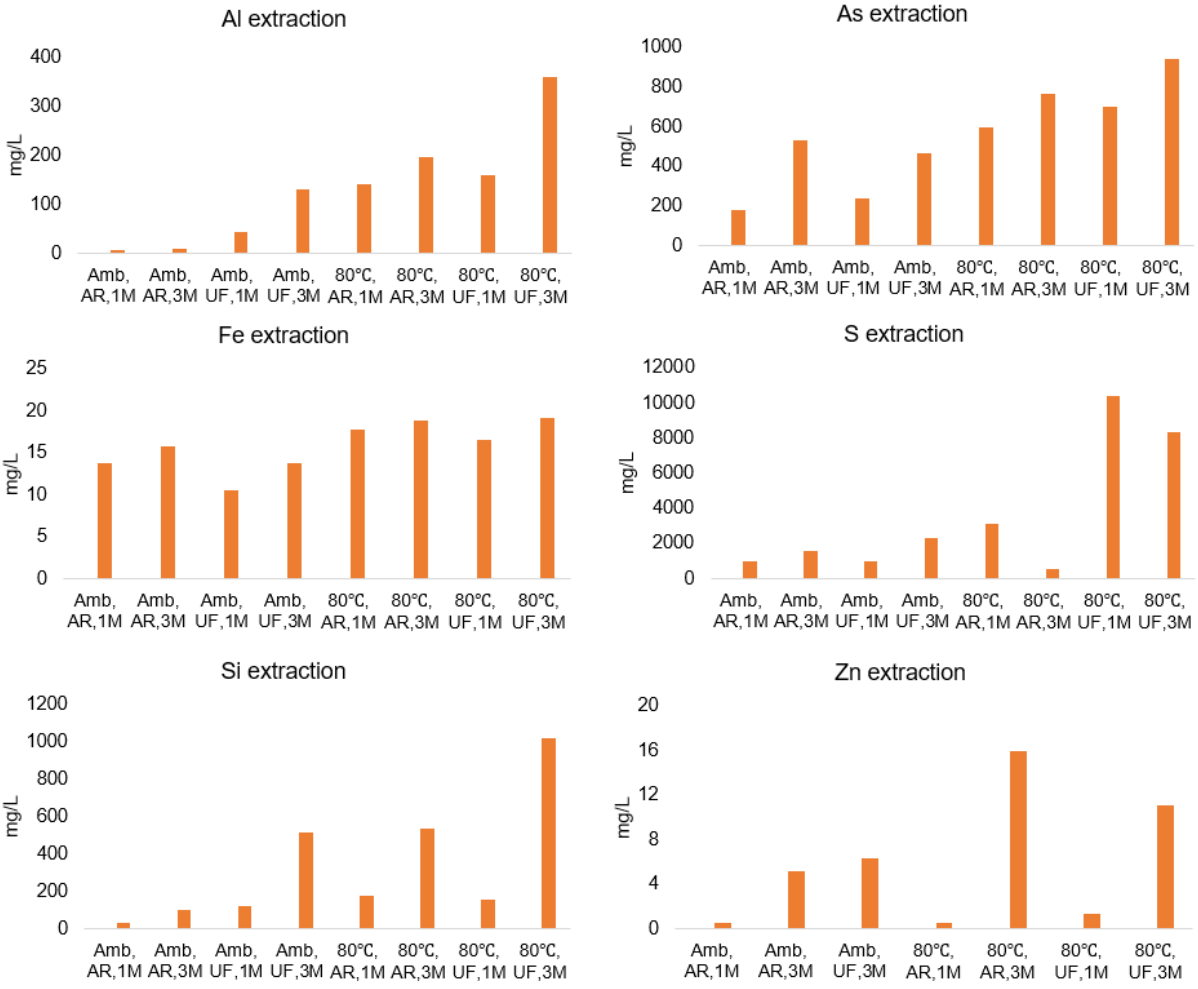

Figure 4.20: Impurity elements Al, As, Fe, S, Si, and Zn. Key Amb-ambient (uncontrolled room temperature), AR-As received, UF-ultrafine. (25% solids, 700 rpm).

4.1.13.1 *Gold leaching during NaOH pre-treatment*

Figure 4.21 indicates gold leaching during the 80°C pre-treatment runs.

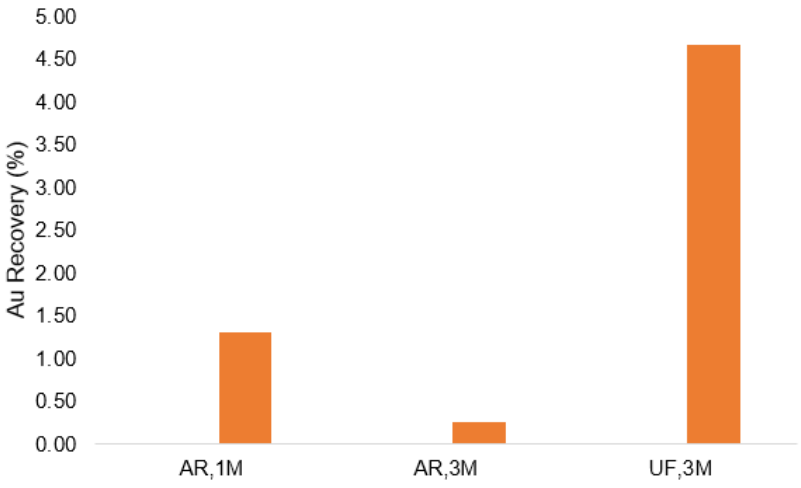

Figure 4.21: Gold extraction during 80°C NaOH pre-leach runs. Key AR-As received, UF-ultrafine. (25% solids, 700 rpm).

It was observed that the highest gold leaching (4.7%) during NaOH pre-treatment was associated with a high Al, As, S and Si extraction (in Figure 4.20) for ultrafine grind at 3 M NaOH and 80°C for 4 hours. These elements Al and Si, As and S correlate with silicates and sulfides respectively. It was evident that, breaking both the silicate and sulfide matrices exposed gold for extraction. Jeffrey and Anderson (2003) postulated that the sulfide and thiosulfate ions formed during alkaline pre-leach pre-treatment of sulfidic refractory ores are highly capable of forming stable gold complexes with the exposed gold. Equations 8 - 11 discussed in section 2.6.3.2 provide an insight into the mechanism of gold extraction during NaOH pre-leaching.

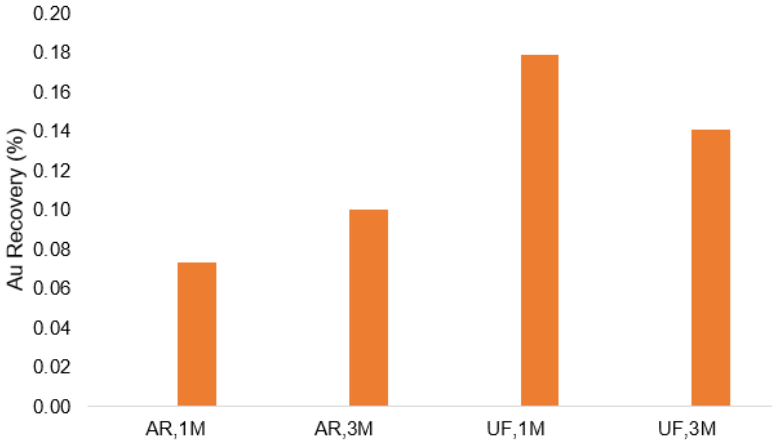

Figure 4.22: Gold extraction during ambient (uncontrolled room temperature) NaOH pre-leach runs. Key AR-As received, UF-ultrafine. (25% solids, 700 rpm).

For all ambient pre-leach pre-treatment conditions (Figure 4.22), the gold extraction was less than 1% which highlighted that ambient temperature did not enhance gold extraction compared to higher temperature pre-treatment.

In general, impurity elements leached into solution during the pre-leach pre-treatment have environmental consequences. Their safe disposal on a plant scale is a priority, and recycling of the effluent water if possible, can be a good option.

4.1.13.2 *Cyanidation of NaOH pre-leach pre-treatment residues*

The pre-leach pre-treatment residues were subjected to 24-hour cyanidation experiments to investigate the effectiveness of the treatment on gold dissolution. The cyanidation experiments were performed as discussed in section 3.3.4. Solution samples were generated at 8 and 24 hours. They were analysed by ICP-OES for Au. The solid residues were fire assayed for Au.

The cyanidation gold recoveries obtained are illustrated in Figure 4.23. The assay and leaching data are contained in Appendix I.

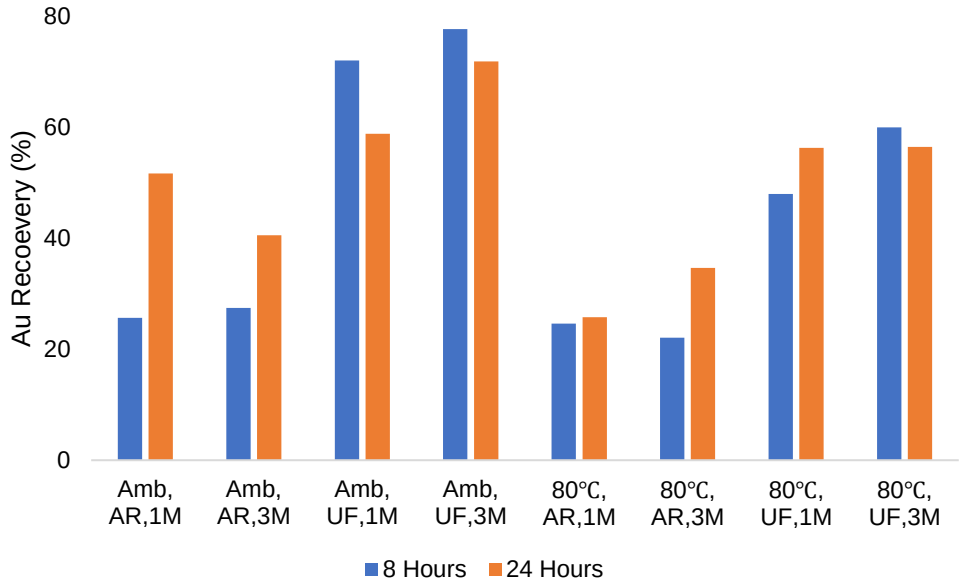

Figure 4.23: Gold recovery during cyanidation of NaOH pre-leached residues. Key Amb-ambient (uncontrolled room temperature), AR-As received, UF-ultrafine. (25% solids, 2 kg/t NaCN, pH 10.5 – pH 11, 192 rpm).

Ambient temperature pre-leach pre-treatment was instrumental in effecting an increase in gold recovery on the as received sample. A cyanidation gold recovery of 51.6% was the highest obtained for the as received sample after pre-leach pre-treatment conditions of ambient temperature and 1 M NaOH concentration. Comparing this recovery with 17.3% of direct cyanidation on the as received sample, breaking of the silicate and sulphide matrices (as seen in Figure 4.20) done by NaOH pre-leach pre-treatment, proved essential to increase gold recovery in the calcine tailings sample. As confirmed by SEM results in section 4.1.6, gold is locked up in a quartz and talc matrices, and associated with arsenic and sulfur.

Crundwell (2014) proposed a three-step mechanism of alkaline dissolution of silicates (discussed in section 2.6.3.1) to form H_4SiO_4. As silicates are dissolved they expose gold surfaces that were previously encapsulated for gold-cyanide complex formation.

Darban *et al.* (2011) investigated the alkaline dissolution of orpiment (As_2S_3), an arsenic bearing mineral. The researchers discovered that hydroxyl ion interaction with the orpiment surface led to alteration of the arsenic sulfur bond. This alteration yielded new reaction products which are believed to expose gold surfaces prior to cyanidation. Mesa Espitia and Lapidus (2015) reported that during NaOH pre-leach pre-treatment of sulfidic refractory material,

arsenic and hydroxyl ions form complexes which facilitate distortion of the host matrix, thereby aiding gold dissolution during thiosulfate leaching.

Ambient temperature pre-leach pre-treatment on the ultrafine sample was beneficial to cyanidation as it increased kinetics and gold recovery. For both tests (1 and 3 M), it was observed that most of the gold was dissolved within 8 hours and that prolonging to 24 hours caused the gold to precipitate from the solution. Alternative research has confirmed that pre-leached residues exhibit faster leaching rates as compared to the as received sample (Mesa Espitia and Lapidus, 2015). Free cyanide ions concentration in solution could have decreased beyond 8 hours and thus causing gold precipitation to occur. Increasing the NaOH concentration from 1 M to 3 M during pre-leach pre-treatment was beneficial as it yielded an increase in gold recovery from 71.2% to 77.6% after 8 hours of cyanidation.

It was generally observed that, temperature (80°C) assisted pre-leaching for both the grinds and NaOH concentration was not effective in increasing the gold during cyanidation. For all four tests, gold recoveries declined when compared to the test samples conducted at ambient conditions. A plausible cause of this would be explained as follows. At 80°C, the quantity of impurity elements that are leached into solution for both grinds (Figure 4.20) is generally higher than that of ambient temperature. Most probably, during cooling after the 80°C pre-leach pre-treatment, precipitation of some of the impurity elements on to solid interfaces could have occurred. Water washing of the cool pre-leach residue did not manage to eliminate the impurity elements that were stuck on to the solid interfaces. This phenomenon led to cyanidation inefficiencies as the potentially exposed gold surfaces from pre-treatment were coated by the impurity elements. Some of the impurity elements like sulfur and arsenic are cyanide consumers as well. On the contrary, impurity elements leached in to solution for ambient pre-treatment remained in solution, and were efficiently eliminated by water washing. Cyanidation performed better as gold surfaces were well exposed and the quantity of cyanide consumers was deemed very little if present.

Refractory ores will tend to behave differently. Researchers Mesa Espitia and Lapidus (2015), also concluded that temperature assisted NaOH pre-leach pre-treatment did not improve impurity removal prior to thiosulfate gold leaching.

Dehghani *et al*. (2009) while working on sulfidic tailings that were fine milled and roasted obtained 98.4% gold cyanidation recoveries. Since the highest gold recovery (77.6%) obtained

for the current study is still in the refractory range, further optimisation of the NaOH pre-leach pre-treatment is recommended for future work.

4.1.13.3 *Scanning Electron Microscopy (SEM) of tailings from cyanidation of pre-leach pre-treatment residue*

The cyanidation tailings were generated from pre-leach pre-treatment conditions of 3 M NaOH and 80°C on the ultrafine sample. SEM analysis on the tailings sample is illustrated in Figure 4.24.

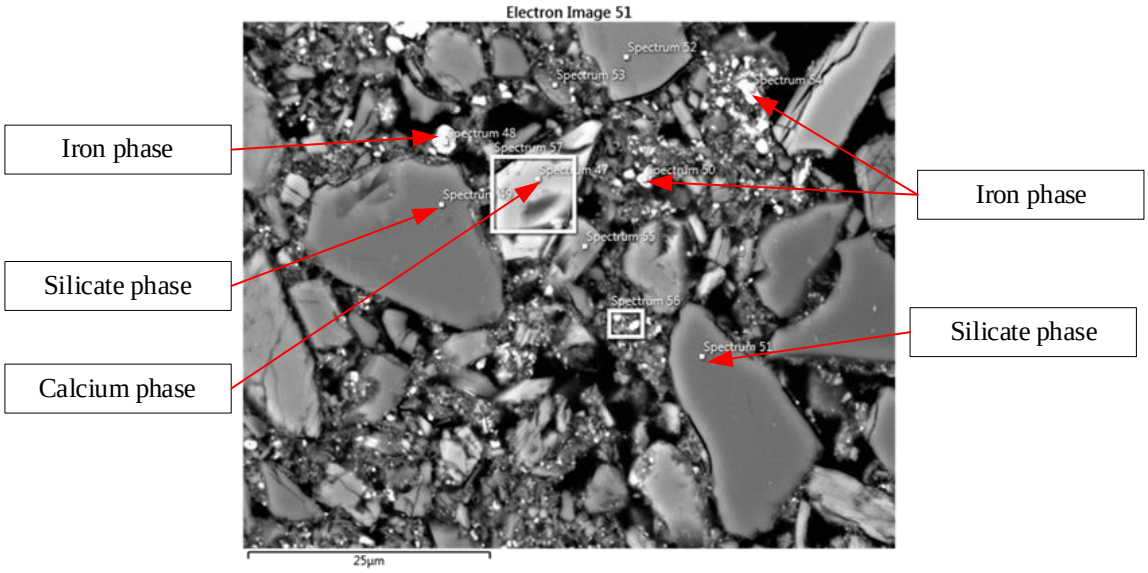

Figure 4.24: SEM of cyanidation tailings of NaOH pre-leached residue.

The electron image shows silicate (spectra 49, 51-53), calcium (spectrum 47) and iron (spectra 50 and 54) phases. Physical damage on the potential gold host matrix of silicates, and on other phases was observed to be significantly lower as compared to microwave techniques. This was mainly due to the differences in the treatment methods. Pre-leach pre-treatment is diffusion based hence matrix alteration was achieved by leaching impurity elements into solution rather than inducement of micro cracks.

Spectra compositions for the highlighted phases are depicted in Appendix M.

4.1.13.4 *Repeatability*

Repeatability was assessed using hot plate assisted pre-leach pre-treatment on the ultrafine sample at a NaOH concentration of 3 M. The temperature was maintained at 80^{O}C. Three runs were performed, and the results are shown in Figure 4.25 and Table 4.10. Further data on assays and leaching is presented in Appendix I.

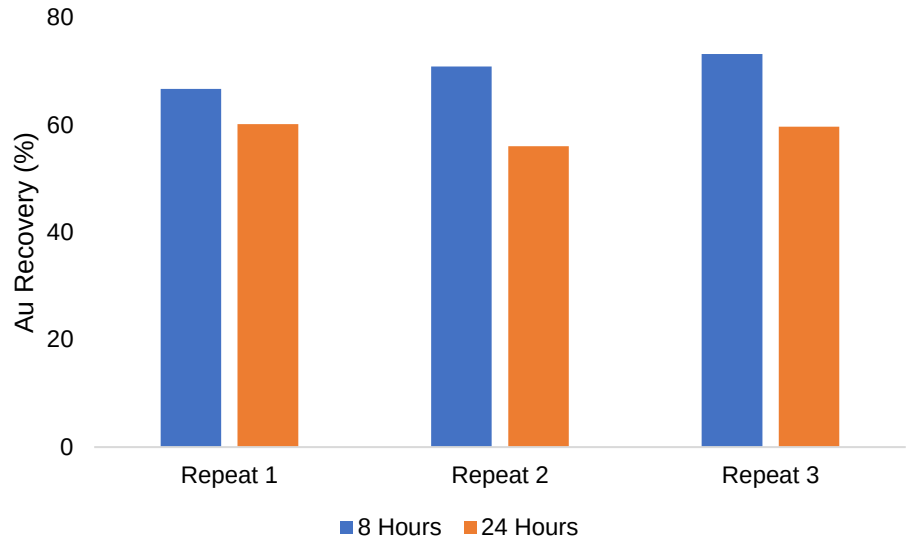

Figure 4.25: Repeats of cyanidation of pre-leach pre-treatment residues. Pre-leach conditions (80°C, Ultrafine, 3 M, 25% solids, 700 rpm). Cyanidation conditions (Ambient (uncontrolled room temperature), 2 kg/t NaCN, 25% solids, 192 rpm).

Table 4.10: Data on repeats of cyanidation of pre-leach pre-treatment residues.

Time (h)	**8**	**24**
Repeat 1 (%)	66.7	60.1
Repeat 2 (%)	70.9	56.0
Repeat 3 (%)	73.2	59.7
Average (%)	70.3	58.6
Standard Deviation (%)	3.29	2.25

The average cyanidation gold recoveries after 8 and 24 hours were 70.3 ± 3.29% and 58.6 ± 2.25% respectively. The error limits, 3.29% and 2.25%, for both times are relatively low which indicates a high repeatability of NaOH pre-leach pre-treatment and cyanidation of the residues. These results further confirmed that cyanide leaching beyond 8 hours resulted in precipitation of gold as the recoveries in all three repeats deteriorated after 24 hours.

4.1.14 Significance of the findings

Recent developments in the global economy and uncertainties have contributed to stimulating an increase in the gold price in the Coronavirus pandemic (COVID-19) economic environment. It is expected that the gold price will be strong, and in this regard pursuit of the project in the current pandemic window would be beneficial to the Group's gold margins.

Presently, the targeted gold production in the Pan African Resources (PAR) Group is pegged at 200 000 oz gold per annum (Pan African Resources, 2019a). The stockpile of the calcine tailings dam at New Consort is estimated to be 270 000 tonnes at an average gold head grade

of 2.96 ± 0.26 g/t. If a minimum gold recovery of 80% is achieved, it is envisaged that at least 11.3% of the PAR Group's projected gold output for that year will be achieved. At a proposed BTRP treatment rate of 1 200 000 tonnes/year (336 days) it is estimated that this stockpile will be exhausted in about 3 months. Calculations are shown in Appendix J.

The performance of the tests and expected economic contribution using a preliminary high level analysis to the Group's gold output for the period in which the material is processed, is summarized in Table 4.11. Equivalent gross revenues are based on the current gold price of $ 1 937.75/oz (as at October 11th, 2020).

Table 4.11: Simple high level possible economic contribution analysis from the test results.

Option	Treatment	Gold Recovery (%)	Expected gold output (oz)	Proportion of PAR's projected annual gold output (%)	Gross revenues at current gold price (US$)
1	Cyanidation of microwave roasted calcine	43.7	11 236.40	5.6	21 773 275.12
2	Microwave assisted leaching	56.9	14 610.11	7.3	28 310 734.58
3	Cyanidation of ultrafine milling	66.5	17 087.10	8.5	33 110 528.03
4	Sodium hydroxide pre-leach and cyanidation of ultrafine pre-leach residue	77.6	19 946.93	10.0	38 652 168.94

The projected growth in the Group's gold production capacity is contingent on the performance of the process economics of all four treatment options examined. The fourth option that reports the highest gold recovery is the most desirable and will be considered for further development should the economic feasibility prove to be favourable. It also does not require a large capital cost as compared to microwaves.

Presently, based on the output of the technical feasibility studies, the contribution to the Group has implications on the existent tailings reprocessing facility, the Barberton Tailings Reprocessing Plant (BTRP). There are three possibilities on the current production profile of the BTRP and are listed as follows:

1. Explore capability of existing mill at BTRP to perform ultrafine milling on the stockpile.

2. Consider possible upgrading of the existing circuit to include ultrafine milling if the current milling facilities cannot perform ultra-fine milling and include pre-leaching.

3. Alternatively, explore vessels in the existing plant that can be committed to pre-leaching, and focus on CAPEX for ultrafine milling if the existent milling facilities cannot perform ultrafine milling.

5.0 Mass balance

Theoretical gold mass balances were constructed for cyanidation of microwave roasted calcine, microwave assisted cyanidation, sodium hydroxide pre-leach pre-treatment and cyanidation of the pre-leach residue.

5.1 Assumptions

Several assumptions were made during the construction for the gold mass balances. These are:

1. Microwave roasted calcine remained unchanged.
2. Sulfide ions were continuously oxidized to thiosulfate ions during pre-leach pre-treatment.
3. Pre-leach pre-treatment gold losses were attributed to the thiosulfate ions only.
4. All gold recovery calculations were based on experimental data generated.
5. BTRP plant processes 148.8 t/h.
6. Water content in the liquor and tailings is 95% and 5% respectively.

5.2 Cyanidation of microwave roasted calcine.

The experimental conditions employed were 60 minutes microwave roasting of the as received sample. Cyanidation conditions were ambient temperature, 25% solids, 2 kg/t NaCN, pH 10.5 – pH 11 and 24 hours residence time. The process flowsheet and gold mass balance are presented in Figure 5.1 and Table 5.1 respectively. Further mass balance data are presented in Appendix N.

A gold cyanidation recovery of 43.7% was obtained after microwave roasting at the above-mentioned conditions. Further optimization and consideration of process economics will need to be considered.

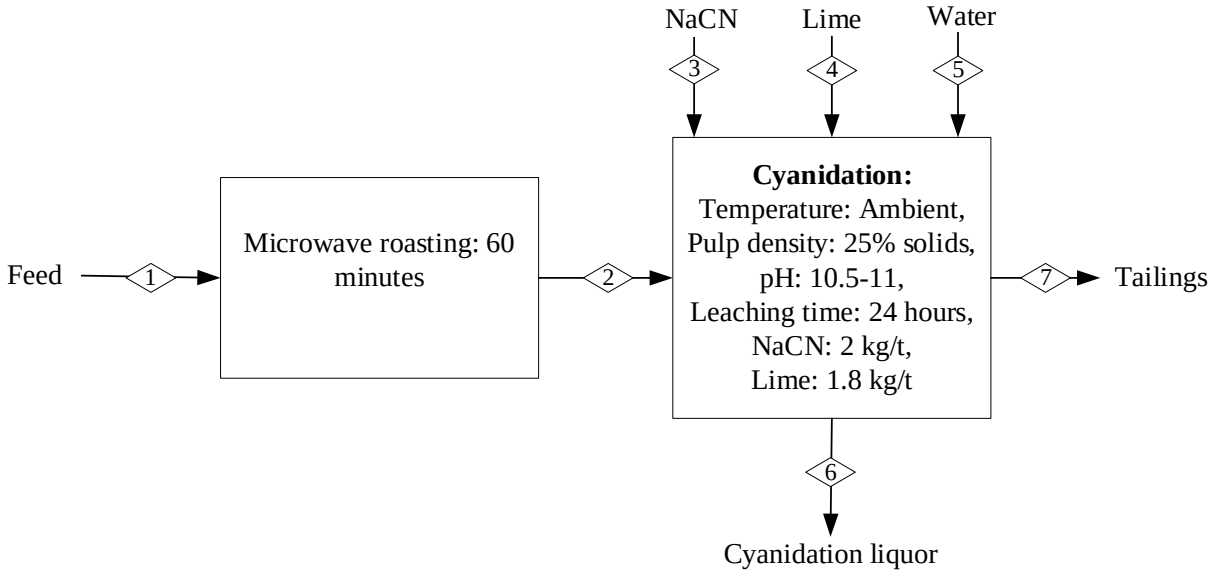

Figure 5.1: Simplified flowsheet diagram for gold recovery via microwave roasting and cyanidation.

Table 5.1: Gold mass balance for cyanidation of microwave roasted calcine.

Species	**1**	**2**	**3**	**4**	**5**	**6**	**7**
Feed (t/hr)	148.8	148.8					
Au (g/hr)	440.5	440.5				192.6	247.8
NaCN (t/hr)			0.2976			0.2975	
CaO (t/hr)				0.2678		0.2678	
H_2O (t/hr)					446.4	424.1	22.32
O_2 (t/hr)					0.003685	0.003677	
Tailings (t/hr)							148.8

5.3 Microwave assisted leaching

The experimental conditions employed were a residence time of 50 minutes, pH 10.5 – pH 11, liquids to solids ratio: 6:1, 1.8 kg/t lime and 8 kg/t NaCN. The process flowsheet and gold mass balance are presented in Figure 5.2 and Table 5.2 respectively. Other mass balance generating data are presented in Appendix O.

Microwave assisted cyanidation yielded 56.9% gold recovery. The main advantage of this process is the short residence time which is beneficial for possibly reducing the man-hours in the metallurgical plant. With more robust equipment, it can be projected that maximum recoveries can be achieved within 120 minutes.

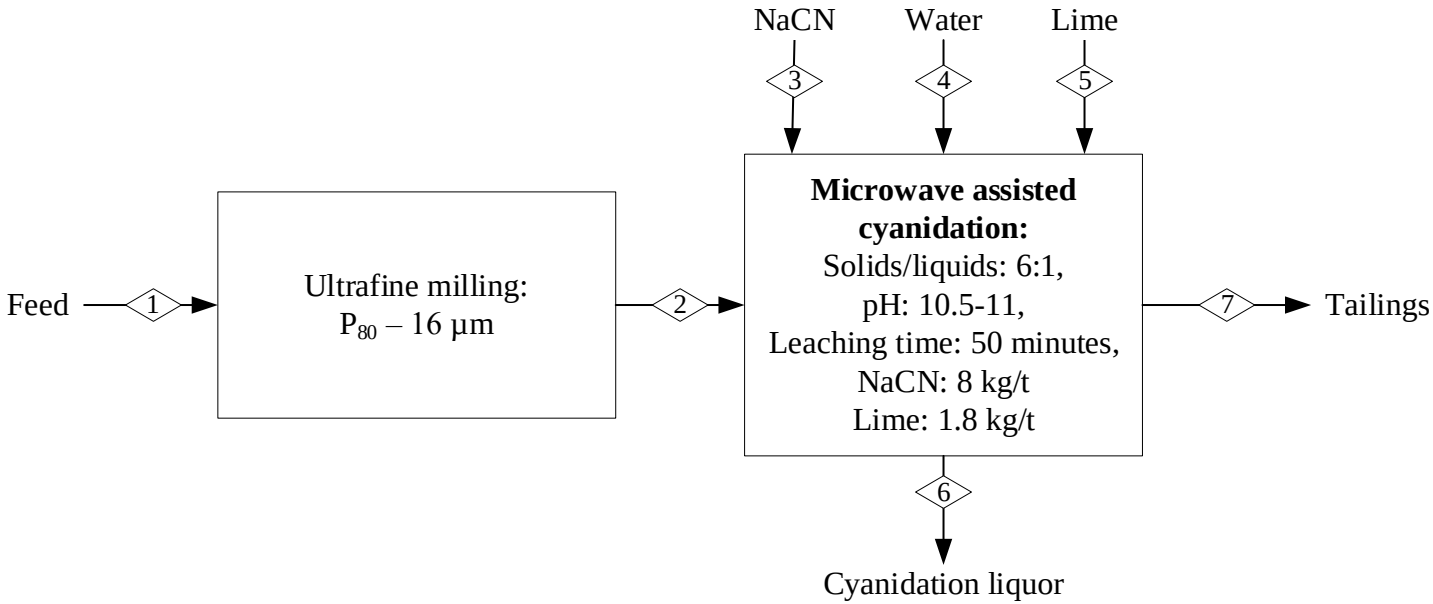

Figure 5.2: Simplified flowsheet for microwave assisted cyanidation.

Table 5.2: Gold mass balance for microwave assisted cyanidation.

Species	**1**	**2**	**3**	**4**	**5**	**6**	**7**
Feed (t/h)	148.8	148.8					
Au (g/h)	440.4	440.4				250.4	190.0
NaCN (t/h)			1.190			1.190	
CaO (t/h)					0.2678	0.2678	
H_2O (t/h)				892.8		848.2	44.64
O_2 (t/h)				0.007370		0.007360	
Tailings (t/h)							148.8

5.4 Sodium hydroxide pre-leach pre-treatment and cyanidation of pre-leach residue

Ultrafine milled sample was leached at ambient temperature for 4 hours at a sodium hydroxide concentration of 3 M, agitation speed of 700 rpm and 25% solids concentration. Cyanidation of the pre-leach pre-treatment residue was done for 8 hours at ambient temperature, 25% solids, 1.8 kg/t lime, 2 kg/t NaCN and pH 10.5 – pH 11. The process flowsheet and gold mass balance are presented in Figure 5.3 and Table 5.3 respectively. Other tables with more mass balance detail are displayed in Appendix P.

A total of 12 leaching hours (pre-leach pre-treatment + cyanidation) led to a 77.63% gold recovery. Since the process incorporated ultrafine milling and pre-leaching prior to cyanidation, process economics need to be investigated for viability. Adding to the direct cyanidation gold recovery on the ultrafine milled sample (~67%), pre-leaching unlocked about 11% more gold.

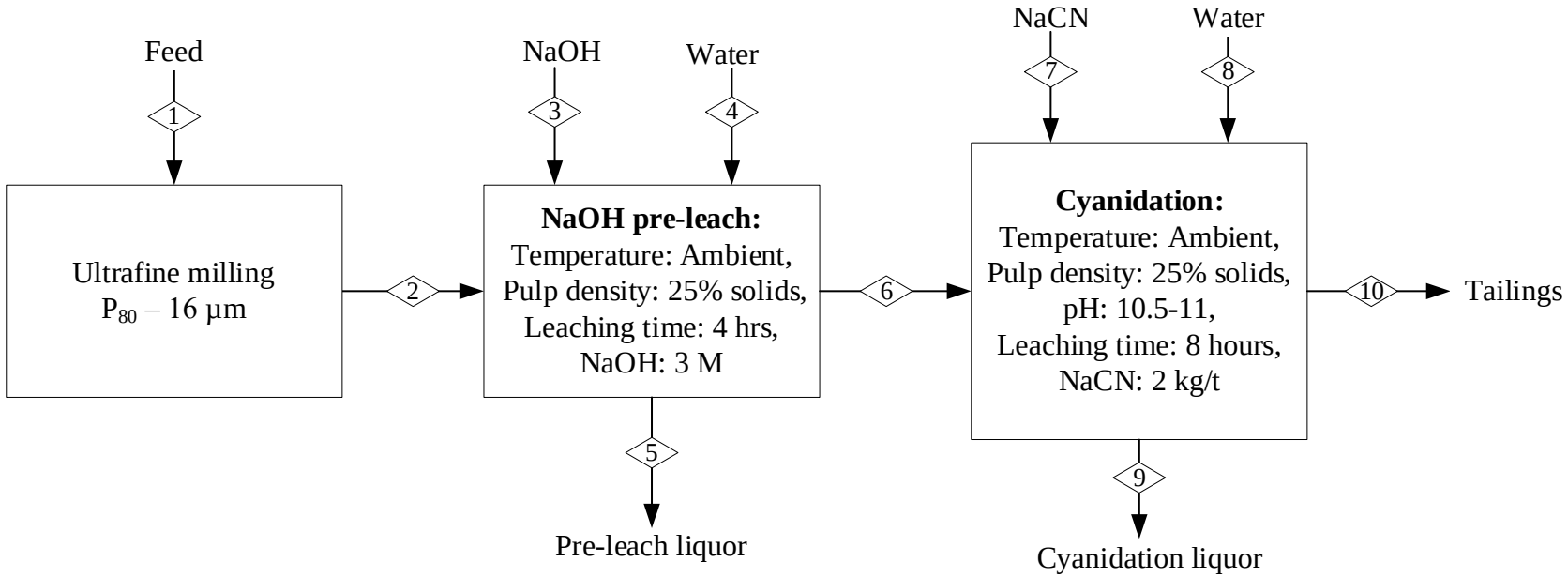

Figure 5.3: Simplified flowsheet for gold recovery via sodium hydroxide pre-leach pre-treatment and cyanidation.

Table 5.3: Gold mass balance for cyanidation of sodium hydroxide pre-leach pre-treatment residue.

Species	**1**	**2**	**3**	**4**	**5**	**6**	**7**	**8**	**9**	**10**
Feed (t/hr)	148.8	148.8								
pre-leach residue (t/h)						148.8				
NaOH (t/h)			53.57		53.57					
Au (g/h)	440.4	440.4			0.6166	439.8			341.4	98.39
NaCN (t/h)							0.2976		0.2974	
H_2O (t/h)				446.4	424.1			446.4	424.1	22.32
O_2 (t/h)				0.003685	0.003685				0.003671	
CN tailings										148.8

6.0 Conclusions

The goal of the research study sought to develop understanding for a feasible process to recover gold from refractory gold calcine tailings that are located in Barberton, Mpumalanga. To achieve the stated goal, three objectives were addressed as detailed in section 1.3.

Objective 1: Mineralogically characterize the refractory tailings heap material to determine the gold size, nature and association

Characterization of the calcine tailings from the New Consort mine was achieved. It was observed that the calcine tailings had a high gold head grade of 2.96 ± 0.26 g/t with silicates and hematite as main phases. Gold ranged in size from the submicron level to several micrometres in size, existing as both free and locked refractory gold. Refractoriness was found to be due to association of gold grains with arsenic and sulfur, which are cyanide consumers. Furthermore, the gold also appeared as encapsulated grains in quartz and talc minerals. Based on the observed mineralogy of the calcine tailings it was therefore shown that pre-treatment methods are necessary to facilitate unlocking of the gold for enhanced gold recoveries.

Objective 2: Develop a pre-treatment method prior to cyanide leaching for increased recoveries

Three different methods were explored, namely, ultrafine milling, microwave roasting pre-treatment and sodium hydroxide pre-leaching.

Mechanical breaking of the phases hosting the gold by ultrafine milling to P_{80} – 16 µm, proved beneficial as the direct cyanidation recovery was increased.

Microwave roasting pre-treatment for 60 minutes on the as received sample increased the gold cyanidation recovery. Water addition on the as received sample prior to microwave roasting reduced the roasting time by half while attaining an almost similar recovery to roasting for 60 minutes. Independent studies have shown that ultrafine milling in isolation is not effective to unlock submicroscopic gold. Therefore, ultrafine milling was combined with microwave roasting and sodium hydroxide pre-leach pre-treatment. Microwave roasting the ultrafine sample for 30 minutes followed by cyanidation did not perform as expected, it effected relatively limited increase in gold recovery. However, given the discussed limitations of microwave equipment and

experiment, use of an optimized setup has the potential to further upgrade gold cyanidation recoveries by better micro crack propagation.

Finally, sodium hydroxide pre-leach pre-treatment of the ultrafine sample was shown to be more effective than microwave roasting mainly due to the drawbacks of the microwaves setup. The highest recoveries were attained at ambient conditions at high NaOH concentrations on the ultrafine sample.

Objective 3: Develop a method to assist direct cyanidation for improved gold recoveries

A method was successfully developed to aid the direct cyanidation of the refractory calcine tailings. The method was based on the use of microwave energy. Microwave assisted cyanidation yielded a 56.7% gold recovery after leaching the ultrafine sample at 8 kg/t NaCN concentration for 50 minutes.

Based on the experimental findings, three process flowsheets were considered. The gold mass balance for each flowsheet was completed. The flowsheet which incorporated sodium hydroxide pre-leach pre-treatment was chosen as the best as it achieved the highest cyanidation gold recovery of 77.6%.

7.0 Recommendations

Results of the studies have demonstrated that gold can be recovered from the refractory calcine tailings. Further technical investigations will help compliment the work that was performed in this study, and make the initial findings more conclusive.

Optimization studies of direct cyanidation of the ultrafine tailings have potential to increase gold recoveries. Secondly, due to limitations in the microwave technology used for experiments, further investigation of microwave experiments with optimized equipment is recommended. High power density and short exposure times should be investigated to increase the probability of the formation of micro cracks. Temperature measurements to aid distinguishment between microwave effects on particles and general heating are also recommended in a suitable applicator.

Thirdly, optimisation work of the sodium hydroxide pre-leach pre-treatment step would lead to increased recoveries of locked submicron gold.

Furthermore, the results of the investigation strongly indicate that the preliminary pre-treatment processes can be developed further into more detailed process flow sheets. In this regard the detailed mass and energy balances need to be undertaken to ascertain the implications of the proposed processes on the recovery and purity of gold, water balance and effluent flows, and energy requirements. Further an analysis of performance of tests on the calcine tailings with carbon in pulp and elution should be undertaken to explore opportunities.

Finally, it is recommended, based on the possibility of pursuing the proposed possibilities discussed earlier, on the existent BTRP facility, to undertake a preliminary economic feasibility study on the project. The CAPEX and OPEX of the options studied and the net returns should be examined. Following comparison of the performance the most feasible option should be selected. However, this option should not negate environmental performance indicators in order to effectively address the sustainable growth. It is also important to note that there are possibilities too that can be considered to reduce capital expenditure. Considering this, blending ratios with other tailings at BTRP can also be investigated. This allows for the simplest modification to be undertaken on the existing process at BTRP. Investigation of blending the pre-treated tailings can be done with fresh feed material from other process streams.

8.0 References

Al-Harahsheh, M. & Kingman, S.W. 2004. Microwave-assisted leaching - A review. *Hydrometallurgy*. 73(3–4):189–203.

Ali, A. 2010. Understanding the Effects of Mineralogy, Ore Texture and Microwave Power Delivery on Microwave Treatment of Ores. Ph.D thesis. Stellenbosch University, Stellenbosch.

Ali, A. & Bradshaw, S. 2011. Confined particle bed breakage of microwave treated and untreated ores. *Minerals engineering*. 24(14):1625–1630.

Allan, G.C. & Woodcock, J.T. 2001. A review of the flotation of native gold and electrum. *Minerals Engineering*. 14(9):931–962.

Alp, İ., Celep, O. & Deveci, H. 2010. Alkaline sulfide pretreatment of an antimonial refractory Au-Ag ore for improved cyanidation. *Jom*. 62(11):41–44.

Amankwah, R.K. & Ofori-Sarpong, G. 2011. Microwave heating of gold ores for enhanced grindability and cyanide amenability. *Minerals Engineering*. 24(6):541–544.

Amankwah, R.K. & Pickles, C.A. 2009. Microwave roasting of a carbonaceous sulphidic gold concentrate. *Minerals Engineering*. 22(13):1095–1101.

Amaya, I., Bernal, D., Garnica, S., Reslen, M. & Correa, R. 2013. Improved roasting of some Colombian gold ores. *DYNA (Colombia)*. 80(178):70–77.

Anderson, C.G. & Twidwell, L.G. 2008. The alkaline sulfide hydrometallurgical separation, recovery and fixation of tin, arsenic, antimony, mercury and gold. *Proceedings of the 2008 Global Symposium on Recycling, Waste Treatment and Clean Technology, REWAS 2008*. (3):159–168.

Anderson, G.S. & McDonald, N.W. 2016. IsaMills at Kalgoorlie Consolidated Gold Mines - from the M3000 to the M10000 and Replacement of the Roasters at Gidji Processing Plant. In Perth *13th Ausimm mill operators' conference*. 29–38.

Anhaeusser, C.R. 1969. The stratigraphy, structure and gold mineralisation of the Jamestown and Sheba hills areas of the Barberton Mountain Land. Ph.D thesis (unpubl). University of Witwatersrand, Johannesburg.

Anhaeusser, C.R. 1972. The geology of the Jamestown Hills area of the Barberton Mountain Land, South Africa. *South African Journal of Geology*. 75(3):225–263.

Anhaeusser, C.R. 1986. *Archaean gold mineralisation in the Barberton Mountain Land. In Mineral Deposits of Southern Africa, vol 1, edit. C.R. Anhaeusser and S. Maske*. Johannesburg: Geological Society of South Africa.

Asamoah, R.K., Skinner, W. & Addai-Mensah, J. 2018. Leaching behaviour of mechano-chemically activated bio-oxidised refractory flotation gold concentrates. *Powder Technology*. 331:258–269.

Badri, R. & Zamankhan, P. 2013. Sulphidic refractory gold ore pre-treatment by selective and bulk flotation methods. *Advanced Powder Technology*. 24(2):512–519.

Barton, C.M. 1982. Geology and mineral resources of northwest Swaziland (Barberton Greenstone Belt). *Bull. geol. Surv. Swaziland*. 10:97pp.

Bas, A.D., Safizadeh, F., Zhang, W., Ghali, E. & Choi, Y. 2015. Active and passive behaviors of gold in cyanide solutions. *Transactions of Nonferrous Metals Society of China (English Edition)*. 25(10):3442–3453.

Batchelor, A.R., Jones, D.A., Plint, S. & Kingman, S.W. 2015. Deriving the ideal ore texture for microwave treatment of metalliferous ores. Minerals Engineering. 84(October 2017):116–129.

Batchelor, A.R., Buttress, A.J., Jones, D.A., Katrib, J., Way, D., Chenje, T., Stoll, D., Dodds, C., et al. 2017. Towards large scale microwave treatment of ores: Part 2 – Metallurgical testing. *Minerals Engineering*. 111:5–24.

Bhakta, P., Langhans, J.W. & Lei, K.P.V. 1989. *Alkaline oxidative leaching of gold-bearing arsenopyrite ores.* Reno.

Bosch, D.W. 1987. *Retreatment of Residues and Waste Rock. In The Extractive Metallurgy Of Gold In South Africa, vol 2, edit. G.G. Stanley*. Johannesburg: South African Institute of Mining and Metallurrgy.

Bradshaw, S.M. 1999. Applications of microwave heating in mineral processing. *South African Journal of Science*. 95(9):394–396.

Brock, B.B. & Pretorius, D.A. 1964. *An introduction to the stratigraphy and structure of the Rand Goldfield. The geology of Som Ore Deposits in Southern Africa. Haughton, S. H. (edit). vol. 1.* Johannesburg: Geological Society of South Africa.

Butterman, W.C. & Amey, E.B.I. 2005. Mineral Commodity Profiles — Gold. *Usgs*. 1–66.

Buttress, A.J., Katrib, J., Jones, D.A., Batchelor, A.R., Craig, D.A., Royal, T.A., Dodds, C. & Kingman, S.W. 2017. Towards large scale microwave treatment of ores: Part 1 – Basis of design, construction and commissioning. *Minerals Engineering*. 109:169–183.

Celep, O. & Yazici, E.Y. 2013. Ultra fine grinding of silver plant tailings of refractory ore using vertical stirred media mill. *Transactions of Nonferrous Metals Society of China (English Edition)*. 23(11):3412–3420.

Celep, O., Alp, I. & Deveci, H. 2011. Improved gold and silver extraction from a refractory antimony ore by pretreatment with alkaline sulphide leach. *Hydrometallurgy*. 105(3–4):234–239.

Celep, O., Alp, I., Paktunç, D. & Thibault, Y. 2011. Implementation of sodium hydroxide pretreatment for refractory antimonial gold and silver ores. *Hydrometallurgy*. 108(1–2):109–114.

Cho, K., Kim, H., Myung, E., Purev, O., Choi, N. & Park, C. 2020. Recovery of gold from the refractory gold concentrate using microwave assisted leaching. *Metals*. 10(5):1–17.

Corkhill, C. & Vaughan, D. 2009. Arsenopyrite oxidation - a review. *Applied Geochemistry*. 24(12):2342–2361.

Corrans, I.J. & Angove, J.E. 1991. Ultra fine milling for the recovery of refractory gold. *Minerals Engineering*. 4(7–11):763–776.

Crundwell, F.K. 2013. The dissolution and leaching of minerals: Mechanisms, myths and misunderstandings. *Hydrometallurgy*. 139:132–148.

Crundwell, F.K. 2014a. The mechanism of dissolution of minerals in acidic and alkaline solutions: Part III. Application to oxide, hydroxide and sulfide minerals. *Hydrometallurgy*. 149:71–81.

Crundwell, F.K. 2014b. The mechanism of dissolution of minerals in acidic and alkaline solutions: Part II Application of a new theory to silicates, aluminosilicates and quartz. *Hydrometallurgy*. 149:265–275.

Darban, A.K., Aazami, M., Meléndez, A.M., Abdollahy, M. & Gonzalez, I. 2011. Electrochemical study of orpiment (As2S3) dissolution in a NaOH solution. *Hydrometallurgy*. 105(3–4):296–303.

Das, A. & Sarkar, B. 2018. Advanced Gravity Concentration of Fine Particles: A Review.

Mineral Processing and Extractive Metallurgy Review. 39(6):359–394.

Dehghani, A., Ostad-rahimi, M., Mojtahedzadeh, S.H. & Gharibi, K.K. 2009. Recovery of gold from the Mouteh Gold Mine tailings dam. *The Journal of The Southern African Institute of Mining and Metallurgy*. 109(July):417–421.

Deschênes, G. 2005. Advances in the cyanidation of gold. *Developments in Mineral Processing*. 15(C):479–500.

Dunn, J.G. & Chamberlain, A.C. 1997. The recovery of gold from refractory arsenopyrite concentrates by pyrolysis-oxidation. *Minerals Engineering*. 10(9):919–928.

Dzombak, D.A., Ghosh, R.S. & Wong-Chong, G.M. 2006. *Cyanide in Water and Soil : Chemistry, Risk and Management*. Boca Raton: CRC/Taylor & Francis.

EcoPartners. 2010. *South African Mine Dumps. EcoPartners Report 2010*.

Ellis, S. 2003. Ultra Fine Grinding - A Practical Alternative to Oxidative Treatment of Refractory Gold Ores. In *Proceedings Eighth Mill Operators' Conference*. 11–17. [Online], Available: https://pdfs.semanticscholar.org/7367/fbb93ff8890719d5b1aa743b1495b6783d3e.pdf.

Ellis, S. & Gao, M. 2003. Development of ultrafine grinding at Kalgoorlie Consolidated Gold Mines. *Minerals and Metallurgical Processing*. 20(4):171–177.

Feather, C.E. 1987. *Geology and Mineralogy of the Principal Goldfields in South Africa. In The Extractive Metallurgy Of Gold In South Africa, vol 1, edit. G.G. Stanley*. Johannesburg: South African Institute of Mining and Metallurrgy.

Fernández, R.R., Collins, A. & Marczak, E. 2010. Gold recovery from high-arsenic-containing ores at Newmont's roasters. *Minerals and Metallurgical Processing*. 27(2):60–64.

Foster, R.P. & Piper, D.P. 1993. Archaean lode gold deposits in Africa: Crustal setting, metallogenesis and cratonization. *Ore Geology Reviews*. 8(3–4):303–347.

Fraser, K.S., Walton, R.H. & Wells, J.A. 1991. Processing of refractory gold ores. *Minerals Engineering*. 4(7–11):1029–1041.

González-Anaya, J.A., Nava-Alonso, F. & Pecina-Treviño, E.T. 2011. Gold recovery optimization of a refractory concentrate by ultrafine grinding - A laboratory study. *Minerals and Metallurgical Processing*. 28(2):95–101.

Gossman, G.I. 1987. *Pyrometallurgy of Gold. In The Extractive Metallurgy Of Gold In South*

Africa, vol 2, edit. G.G. Stanley. Johannesburg: South African Institute of Mining and Metallurgy.

Guo, P., Wang, S. & Zhang, L. 2019. Selective removal of antimony from refractory gold ores by ultrasound. *Hydrometallurgy*. 190:105161.

Habashi, F. 1967. *Kinetics and mechanism of gold and silver dissolution in cyanide solution*. Montana: Bureau of Mines and Geology.

Habashi, F. 2005. Gold - An historical introduction. In Vol. 15 *Developments in Mineral Processing*. xxv–xlvii.

Haque, K.E. 1987a. Gold leaching from Refractory Ores - Literature Survey. *Minerals Processing and Extractive Metallurgy Review*. 2:3:235–253.

Haque, K.E. 1987b. Microwave irradiation Pretreatment of a Refractory gold concentrate. In Proceedings of the International Symposium on Gold Metallurgy. Salter, R. S., Wyslouzil, D. M., McDonald, G.W. (eds). In Winnepeg, Canada: Pergamon Pr. 327–339.

Haque, K.E. 1999. Microwave energy for mineral treatment processes - A brief review. *International Journal of Mineral Processing*. 57(1):1–24.

Harbort, G., Hourn, M. & Murphy, A. 1996. IsaMill Ultrafine Grinding for a Sulphide Leach Process. In *Proceedings AusImm Eighth Mill Operators' Conference, Townsville, QLD, Australia*. 1–6.

Hearn, M.G. 1943. A study of the working properties of the chief gold producer of the Barberton District, Eastern Transvaal. D.Sc thesis (unpubl.). University of Witwatersrand, Johannesburg.

Helmstaedt, H. & Gurney, J.J. 2001. Formation of the Archean Kaapvaal Province revisited : Implications for the birth and growth of its diamondiferous root. *The Slave– Kaapvaal Workshop, Merrickville, Ontario*. (April 2015).

Hilson, G. & Monhemius, A.J. 2006. Alternatives to cyanide in the gold mining industry: what prospects for the future? *Journal of Cleaner Production*. 14(12–13):1158–1167.

Hu, N., Chen, W., Ding, D. Xin, Li, F., Dai, Z. Ran, Li, G. Yue, Wang, Y. Dong, Zhang, H., et al. 2017. Role of water contents on microwave roasting of gold bearing high arsenic sulphide concentrate. *International Journal of Mineral Processing*. 161:72–77.

Huang, J.H. & Rowson, N.A. 2002. Hydrometallurgical decomposition of pyrite and marcasite

in a microwave field. *Hydrometallurgy*. 64(3):169–179.

Iglesias, N. & Carranza, F. 1994. Refractory gold-bearing ores: a review of treatment methods and recent advances in biotechnological techniques. *Hydrometallurgy*. 34(3):383–395.

Ishikawa, K., Yoshioka, T., Sato, T. & Okuwaki, A. 1997. Solubility of hematite in LiOH, NaOH and KOH solutions. *Hydrometallurgy*. 45(1–2):129–135.

Jackson, E. (Eric). 1986. *Hydrometallurgical extraction and reclamation*. (Ellis Horwood series in metals and associated materials). Chichester, West Sussex: Ellis Horwood.

Janse van Rensburg, S. 2016. Guidelines for Retreatment of SA gold tailings: MINTEK's learnings. In Johannesburg *Proceedings of the 23rd WasteCon Conference*. 367–376. [Online], Available: https://iwmsa.co.za/sites/default/files/downloads/56. Janse van Rensburg%2C S.pdf.

Jeffrey, M.I. & Anderson, C.G. 2003. A fundamental study of the alkaline sulfide leaching of gold. *The European Journal of Mineral Processing and Environmental Protection*. 3(3):1303–868.

Jha, M.C. & Kramer, M.J. 1984. *Recovery of Gold from Arsenical Ores in Precious Metals: Mining, Extraction and Processing (V. Kydryk, D. Corrigann & W Liang, eds)*. Metallurgical Society of AIME.

Kappes, D.W. 2005. Heap leaching of gold and silver ores. In Vol. 15 *Developments in Mineral Processing*. 456–478.

Kim, E., Horckmans, L., Spooren, J., Vrancken, K.C., Quaghebeur, M. & Broos, K. 2017. Selective leaching of Pb, Cu, Ni and Zn from secondary lead smelting residues. *Hydrometallurgy*. 169(2017):372–381.

Komnitsas, C. & Pooley, F.D. 1989. Mineralogical characteristics and treatment of refractory gold ores. *Minerals Engineering*. 2(4):449–457.

Koslides, T. & Ciminelli, V.S.T. 1992. Pressure oxidation of arsenopyrite and pyrite in alkaline solutions. *Hydrometallurgy*. 30(1–3):87–106.

Krishnan, K.H., Mohanty, D.B. & Sharma, K.D. 2007. The effect of microwave irradiations on the leaching of zinc from bulk sulphide concentrates produced from Rampura-Agucha tailings. *Hydrometallurgy*. 89(3–4):332–336.

Li, H., Long, H., Zhang, L., Yin, S., Li, S., Zhu, F. & Xie, H. 2020. Effectiveness of microwave-

assisted thermal treatment in the extraction of gold in cyanide tailings. *Journal of Hazardous Materials*. 384:1–11.

Liebenburg, W.R. 1972. *Mineralogical features of gold ores in South Africa. In Gold metallurgy in South Africa. edit R. J. Adamson*. Johannesburg: Chamber of mines of South Africa.

Liebenburg, W.R. & Schweigart, H. 1966. *Mineralogy and chemical behaviour of some refractory gold ores from the Barberton Mountain Land, South Africa*. Johannesburg.

Limpitlaw, D. & Briel, A. 2014. Post-mining land use opportunities in developing countries - A review. *Journal of the Southern African Institute of Mining and Metallurgy*. 114(11):899–903.

Lorenzen, L. & van Deventer, J.S.J. 1992. Electrochemical interactions between gold and its associated minerals during cyanidation. *Hydrometallurgy*. 30(1–3):177–193.

Lowe, D.R. & Byerly, G.R. 1999. Stratigraphy of the west-central part of the Barberton Greenstone Belt, South Africa. *Special Paper of the Geological Society of America*. 329:1–36.

Lowe, D.R. & Byerly, G.R. 2007. An Overview of the Geology of the Barberton Greenstone Belt and Vicinity: Implications for Early Crustal Development. In Vol. 15 *Developments in Precambrian Geology*. 481–526.

Ma, S.J., Luo, W.J., Mo, W., Su, X.J., Liu, P. & Yang, J.L. 2010. Removal of arsenic and sulfur from a refractory gold concentrate by microwave heating. *Minerals Engineering*. 23(1):61–63.

Marsden, J. & House, I. 1992. *The Chemistry of Gold Extraction*. West Sussex: Ellis Horwood Limited.

Meng, Y.Q. 2005. New extraction process of carbonaceous refractory gold concentrate. *Transactions of Nonferrous Metals Society of China (English Edition)*. 15(5):1178–1184.

Mesa Espitia, S.L. & Lapidus, G.T. 2015. Pretreatment of a refractory arsenopyritic gold ore using hydroxyl ion. *Hydrometallurgy*. 153:106–113.

Metzner, G. 1993. Multivariable and Optimising Mill Control. In Sydney, Australia *International Mineral Processing Congr (IMPC)*.

Miller, P. & Brown, A. 2005. Bacterial oxidation of refractory gold concentrates.

Developments in Mineral Processing. 15(C):371–402.

Minerals Council South Africa. 2018. Facts and Figures Pocket Book 2018. (June).

Minerals Council South Africa. 2019. *Gold*. [Online], Available: https://www.mineralscouncil.org.za/sa-mining/gold [2019, June 14].

Minerals Council South Africa. 2020. *Illegal mining*. [Online], Available: https://www.mineralscouncil.org.za/work/illegal-mining [2020, April 11].

Muir, A., Mitchell, J.Ã., Flatman, S. & Sabbagha, C. 2005. Retreatment of gold residues. *Developments in Mineral Processing*. 15(05):753–785.

Mukendi, N.D., Handfield-Jones, R.V.R. & Akdogan, G. 2000. Microwave assisted leaching of refractory gold concentrates. In *International Congress on Mineral Processing and Extractive Metallurgy. Melbourne, Australia*. 197–199.

Munyai, M.R., Dirks, P.H.G.M. & Charlesworth, E.G. 2011. Archaean gold mineralisation during post-orogenic extension in the New Consort Gold Mine, Barberton greenstone belt, south Africa. *South African Journal of Geology*. 114(1):121–144.

Naicker, K., Cukrowska, E. & McCarthy, T.S. 2003. Acid mine drainage arising from gold mining activity in Johannesburg, South Africa and environs. *Environmental Pollution*. 122(1):29–40.

Nanthakumar, B., Pickles, C.A. & Kelebek, S. 2007. Microwave pretreatment of a double refractory gold ore. *Minerals Engineering*. 20(11):1109–1119.

Nattrass, N. 1995. The crisis in South African gold mining. *World Development*. 23(5):857–868.

Nicolaysen, L.O. 1962. Stratigraphic interpretation of age measurements in Southern Africa. Petrologic Studies: A Volume to Honour A. F. Buddington. *Geological Society of America*. 569–598.

Otto, A., Dziggel, A., Kisters, A.F.M. & Meyer, F.M. 2007. The New Consort Gold Mine, Barberton greenstone belt, South Africa: Orogenic gold mineralization in a condensed metamorphic profile. *Mineralium Deposita*. 42(7):715–735.

Pan African Resources. 2018. *Pan African Resources integrated annual report 2018. 29 October 2018.* [Online], Available: https://www.panafricanresources.com/investors/financial-reports/ [2020, April 14].

Pan African Resources. 2019a. *Pan African Resources integrated annual report 2019. 18 September 2019.* [Online], Available: https://www.panafricanresources.com/investors/financial-reports/ [2020, September 19].

Pan African Resources. 2019b. *Barberton mines*. [Online], Available: http://www.panafricanresources.com/operations-overview/barberton/ [2019, June 24].

Pan African Resources. 2020a. *Sustainable development report-2020*. [Online], Available: https://www.panafricanresources.com/investors/gri-and-sustainability/ [2020, October 21].

Pan African Resources. 2020b. *Pan African Resources integrated annual report 2020. 16 September 2020.* [Online], Available: https://www.panafricanresources.com/investors/financial-reports/ [2020, October 13].

Pan African Resources. 2020c. *Mineral resources and mineral reserves 2020 report.* [Online], Available: https://www.panafricanresources.com/wp-content/uploads/Pan-African-MRMR-report-2020.pdf [2020, October 23].

Pan African Resources. 2020d. *Mineral resources and mineral reserves 2020 report.*

Pearton, T. & Viljoen, M. 2017. Gold on the Kaapvaal craton, Outside the Witwatersrand basin, South Africa. *South African Journal of Geology*. 120(1):101–132.

Phillips, G.N. & Powell, R. 2015. Hydrothermal alteration in the Witwatersrand goldfields. *Ore Geology Reviews*. 65(P1):245–273.

Pickles, C.A. 2009a. Microwaves in extractive metallurgy: Part 1 - Review of fundamentals. *Minerals Engineering*. 22(13):1102–1111.

Pickles, C.A. 2009b. Microwaves in extractive metallurgy: Part 2 - A review of applications. *Minerals Engineering*. 22(13):1112–1118.

Pooley, F.D. 1987. Use of Bacteria to Enhance Recovery of Gold from Refractory Ores. In *Minprep 87, Int. Sym on Innovative Plant and Processes for Mineral Eng.* 31 March–2 April 1987, Doncaster : 1-14.

Rashotte, N. 2019. *Gold Mining in South Africa | An Overview for Gold Investors | INN*. [Online], Available: https://investingnews.com/daily/resource-investing/precious-metals-investing/gold-investing/gold-mining-in-south-africa/ [2019, December 29].

Robb, L.J. & Meyer, F.M. 1995. The Witwatersrand Basin, South Africa: Geological

framework and mineralization processes. *Ore Geology Reviews*. 10(2):67–94.

Robb, L.J. & Robb, V.M. 1998. *Gold in the Witwatersrand basin in The Mineral Resources of South Africa (M.G.C. Wilson and C.R. Anhaeusser, eds): Handbook*. 6th ed. Pretoria: ZAF, Council for Geoscience.

Robertson, M.. 1989. The structural geology and gold mineralisation of the Main Reef Complex, Sheba Gold Mine, Barberton Greenstone Belt. University of the Witwatersrand.

De Ronde, C.E.J., Spooner, E.T.C., De Wit, M.J. & Bray, C.J. 1992. Shear zone related Au-quartz deposits in the Barberton Greenstone Belt, South Africa: field and petrographic characteristics, fluid properties and light stable isotope geochemistry. *Economic Geology*. 87:366–402.

Sammut, D. 2016. *Patent No. WO 2016/134420 Al*. Australia: World Intellectual Property Organization.

Sanders, J.W., Rowland, T.W. & Mellody, M. 1994. Formation related gold production from the central rand group and the Ventersdorp supergroup, South Africa. In Johannesburg: Institute of mining and metallurgy *XV th CMMI Congress*. 47–53.

Schouwstra, R.P. & De Villiers, J.P.R. 1988. Gold mineralisation and associated wallrock alteration in Main Reef Complex at Sheba Mine, South Africa. *Transactions of the Institute of Mining and Metallurgy*. 97B:158–170.

Seccombe, A. 2018. *Pan African to shut costly Evander mine*. [Online], Available: https://www.businesslive.co.za/bd/companies/mining/2018-05-02-pan-african-resources-to-shut-8-shaft-at-evander-retrenching-1700/ [2020, October 13].

Snyders, C.A., Akdogan, G., Bradshaw, S.M., van Vreden, J.H. & Smith, R. 2018. The development of a caustic pre-leaching step for the recovery of Au from a refractory ore tailings heap. *Minerals Engineering*. 121(July 2017):23–30.

Swash, P.M. 1988. Mineralogical investigation of refractory gold ores and their beneficiation, with special reference to arsenical ores. *Journal of The South African Institute of Mining and Metallurgy*. 88(5):173–180.

Swash, P.M. & Ellis, P. 1986. The roasting of arsenical gold ores: a mineralogical perspective. In *GOLD 100, Proceedings of the International Conference on Gold. South African Institute of Mining and Metallurgy*. 2, 235-257.

Thomas, K.G. 2005. Pressure oxidation overview. In Vol. 15 *Developments in Mineral Processing*. 346–369.

Thomas, K.G. & Cole, A.P. 2005. Roasting developments - especially oxygenated roasting. In Vol. 15 *Developments in Mineral Processing*. 403–432.

Tucker, R.F., Viljoen, R.P. & Viljoen, M.J. 2016. A Review of the Witwatersrand Basin - The World��s Greatest Goldfield. *Episodes*. 39(2):105.

Tutu, H., McCarthy, T.S. & Cukrowska, E. 2008. The chemical characteristics of acid mine drainage with particular reference to sources, distribution and remediation: The Witwatersrand Basin, South Africa as a case study. *Applied Geochemistry*. 23(12):3666–3684.

Vermeulen, N.J. 2001. The composition and state of gold tailings. DPhil Thesis. University of Pretoria, Pretoria.

De Villiers, J.E. 1957. *The Mineralogy of the Barberton Gold Deposits*. Pretoria: Union of South Africa. Department of Mines.

Visser, D.J.L. 1956. The Geology of the Barberton area. *Geological Survey of South Africa*.

Voges, F.D. 1986. *The New Consort Gold Mine, Barberton Greenstone Belt. In Mineral Deposits of Southern Africa, vol 1, edit. C.R. Anhaeusser and S. Maske*. Johannesburg: Geological Society of South Africa.

Wang, X., Qin, W., Jiao, F., Yang, C., Cui, Y., Li, W., Zhang, Z. & Song, H. 2019. Mineralogy and pretreatment of a refractory gold deposit in Zambia. *Minerals*. 9(7):1–16.

Ward, J.H.. & Wilson, M.G.C. 1998. *Gold outside the Witwatersrand basin in The Mineral Resources of South Africa (M.G.C. Wilson and C.R. Anhaeusser, eds): Handbook*. 6th ed. ZAF, Council for Geoscience.

Weissenstein, K. & Sinkala, T. 2011. Soil pollution with heavy metals in mine environments, impact areas of mine dumps particularly of gold- and copper mining industries in Southern Africa. *Arid Ecosystems*. 1(1):53–58.

Werdmuller, V.W. 1986. *The Central Rand in Witwatersrand gold - 100 years (E.S.A. Antrobus, ed).* Geological Society of South Africa.

Wesołowski, M. (1984) ‘Thermal decomposition of talc: A review’, *Thermochimica Acta*, 78(1–3), pp. 395–421. doi: 10.1016/0040-6031(84)87165-8.

De Wit, M.J., De Ronde, C.E.J., Tredoux, M., Roering, C., Hart, R.J., Armstrong, R.A., Green, R.W.E., Peberdy, E., et al. 1992. Formation of an Archaean continent. *Nature*. 357(6379):553–562.

Woodcock, J.T., Sparrow, G.J. & Bradhurst, D.H. 1989. Possibilities for using microwave energy in the extraction of gold. In *Proceedings of the 1st Australian Symposium on Microwave Power applications. Wollongong, Australia*.

Woollacott, L.. & Eric, R.. 1994. *Mineral and metal extraction: an overview*. Johannesburg: South African Institute of Mining and Metallurgy.

World Health Organization. 2005. *Electromagnetic Fields And Public Health: Microwave Ovens*. [Online], Available: https://www.who.int/peh-emf/publications/facts/info_microwaves/en/ [2020, February 25].

Xia, D.K. & Pickles, C.A. 2000. Microwave caustic leaching of electric arc furnace dust. *Minerals Engineering*. 13(1):79–94.

Yalcin, E. & Kelebek, S. 2011. Flotation kinetics of a pyritic gold ore. *International Journal of Mineral Processing*. 98(1–2):48–54.

Yannopoulos, J.C. 1991. *The Extractive Metallurgy of Gold*. New York: Van Nostrand Reinhold.

Zhang, G., Wang, S., Zhang, L. & Peng, J. 2016. Ultrasound-intensified Leaching of Gold from a Refractory Ore. *ISIJ International*. 56(4):714–718.

9.0 Appendices

9.1 Appendix A: Water addition investigation for microwave roasting experiment

A series of experiments were done to determine the experimental water addition (3%, 6%, 12% and 15%) value to be used in the microwave roasting experiments. Four experiments were carried out and the water addition which gave the highest temperature value was chosen. Figure 9.1 shows the results of the experiment.

Procedure

Four 600ml beakers were loaded with 50g as received samples. Volumes of 1.5, 3.0, 6.0 and 7.5ml representing (3, 6, 12 and 15%) respectively were poured into the beakers, and mixed thoroughly for even distribution of the water content. After mixing, the samples were placed into 100ml Joan beakers, and microwaved for 15 minutes each in the presence of a 300ml water load. The temperature was measured by a thermocouple, and recorded at the end of each roasting test. Figure 9.1 illustrates the findings of the water addition investigation. The results indicated that a water content of 6% gave the highest temperature of 164.5°C. Thus, a water content of 6% was chosen to aid microwave roasting of the as received sample.

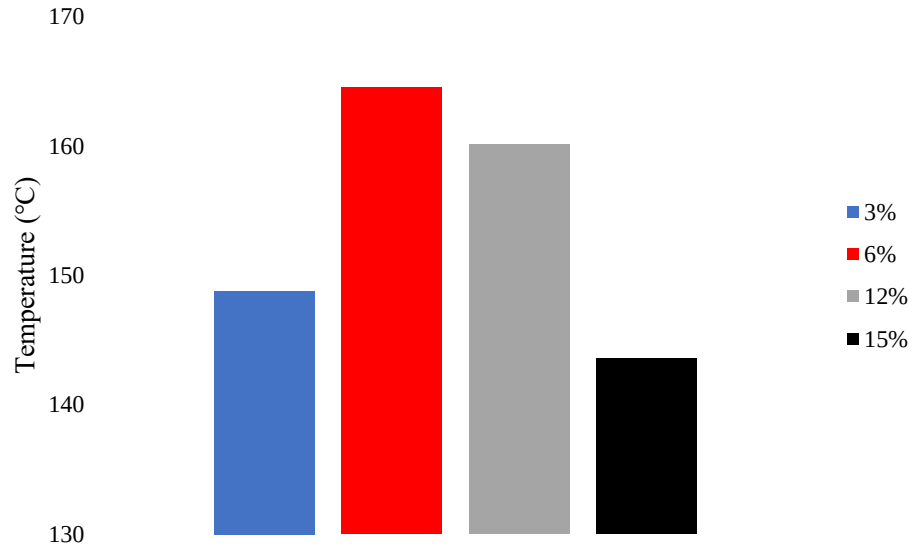

Figure 9.1: Results of water addition investigation.

9.2 Appendix B: Data for Particle Size Distribution on the as received sample

Data for Particle Size Distribution on the as received sample (Table 9.1).

Table 9.1: Particle Size Distribution of the as received sample.

Cumulative vol finer (%)	Particle diameter (µm)
0.1	0.3
0.5	0.4
1.3	0.5
2.1	0.6
2.7	0.7
3.4	0.8
4.0	0.9
4.7	1.0
11.1	2.0
16.8	3.0
21.9	4.0
26.3	5.0
29.9	6.0
33.0	7.0
35.7	8.0
38.0	9.0
40.2	10.0
56.7	20.0
61.9	25.0
66.6	30.0
73.6	40.0
78.6	50.0
82.8	60.0
86.3	70.0
89.1	80.0
91.2	90.0
92.7	100.0
96.8	150.0
98.2	200.0
98.8	250.0
99.4	300.0

9.3 Appendix C: Quantitative Evaluation of Minerals by Scanning Electron Microscopy (QEMSCAN)

Bulk mineralogy graph Figure 9.2.

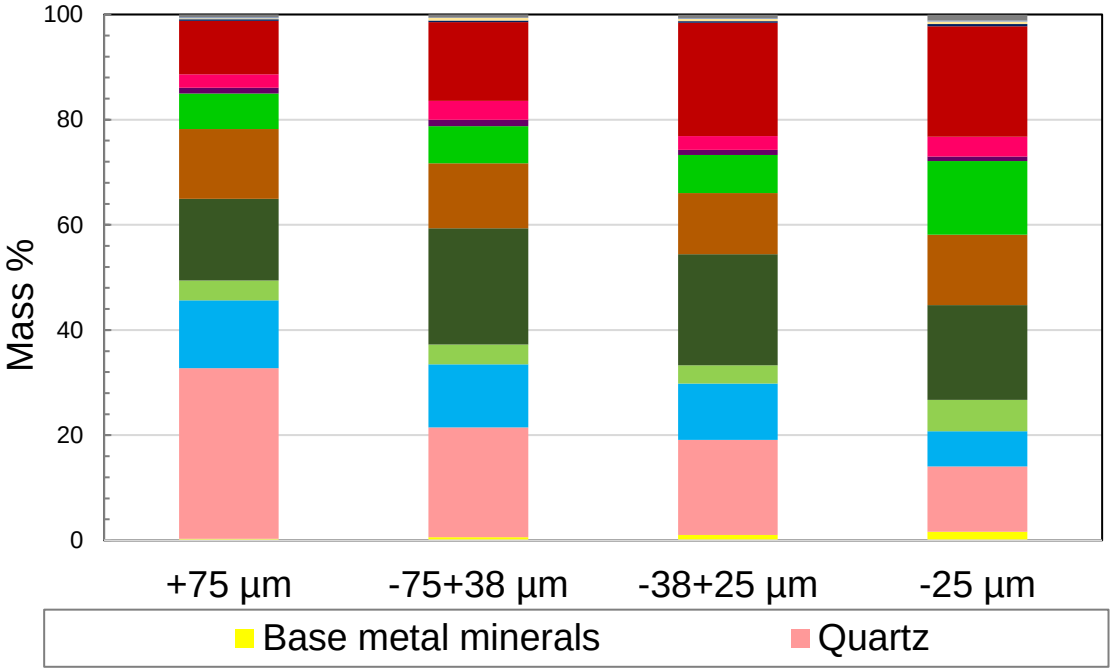

Figure 9.2: Bulk mineralogy graph.

Base metal proportions graph (Figure 9.3).

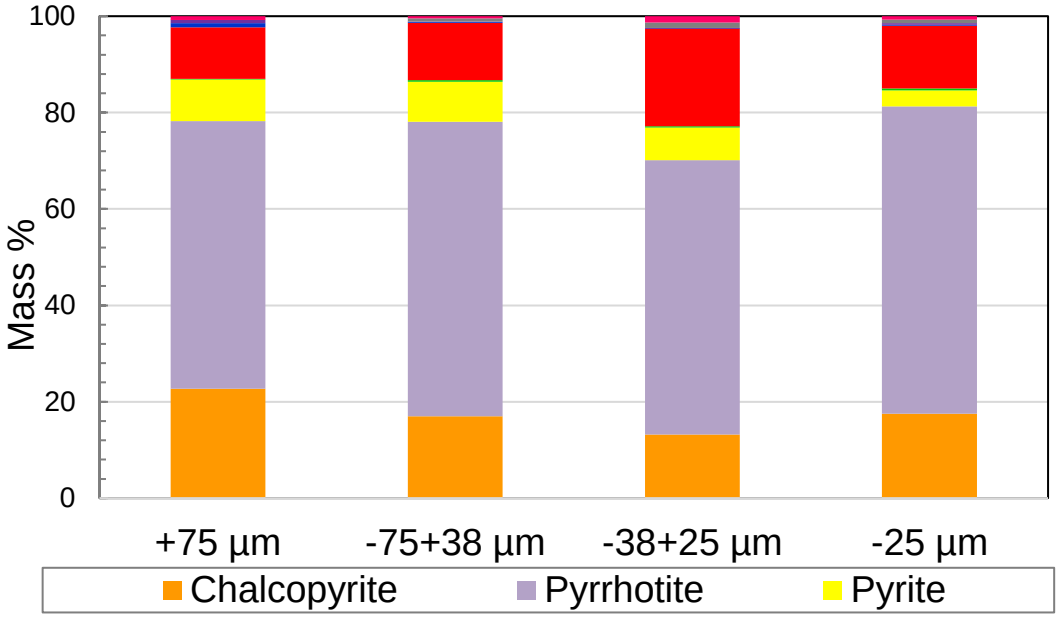

Figure 9.3: Base metal proportions graph.

9.4 Appendix D: Direct cyanidation of as received sample

Samples grades for as received sample (Table 9.2).

Table 9.2: Samples grade for as received sample (direct cyanidation).

Cyanidation run	Measured tailings grade (g/t)	Calculated feed grade (g/t)
Run 1	2.40	2.76
Run 2	2.07	2.29

Run1 and 2 cyanidation data (Table 9.3).

Table 9.3: Runs 1 and 2 cyanidation.

Run 1				
leach time (h)	0	1	2	24
Au (ug/L)	0	26.99	69.20	155.29
Recovery	0	3.1	7.9	17.7
Run 2				
leach time (h)	0	1	2	24
Au (ug/L)	0	52.01	67.12	119.92
Recovery	0	7.3	9.5	16.9

9.5 Appendix E: Particle Size Distribution on the ultrafine sample

Particle Size Distribution on the ultrafine sample (Table 9.4).

Table 9.4: Particle Size Distribution on the ultrafine sample.

Cumulative vol finer (%)	Particle diameter (µm)
0.7	0.1
5.3	0.2
8.4	0.3
10.1	0.4
11.5	0.5
13.1	0.6
14.8	0.7
16.5	0.8
18.3	0.9
19.9	1.0
33.0	2.0
42.4	3.0
50.0	4.0
55.8	5.0
60.2	6.0
63.4	7.0
66.1	8.0
68.4	9.0
70.5	10.0
85.5	20.0
89.6	25.0
92.6	30.0
96.0	40.0
97.6	50.0
98.5	60.0
98.9	70.0
99.0	80.0
99.0	90.0
99.1	100.0
99.7	150.0

9.6 Appendix F: Direct cyanidation of ultrafine sample

Samples grades for direct cyanidation of ultrafine sample (Table 9.5).

Table 9.5: Samples grade (direct cyanidation of ultrafine sample).

Cyanidation run	Measured tailings grade (g/t)	Calculated feed grade (g/t)
Run 1	2.35	5.83
Run 2	2.35	5.55

Run 1 and 2 cyanidation data (Table 9.6).

Table 9.6: Runs 1 and 2.

Run1					
leach time (h)	0	1	2	8	24
Au (ug/L)	0	506.25	738.35	1111.05	1213.01
Recovery	0	28.0	40.9	61.5	67.1
Run 2					
leach time (h)	0	1	2	8	24
Au (ug/L)	0	481.40	784.07	1097.80	1126.10
Recovery	0	28.2	45.9	64.2	65.9

9.7 Appendix G: Cyanidation microwave roasted samples

Samples grades for cyanidation of microwave roasted samples (Table 9.7).

Table 9.7: Samples grades.

Cyanidation run	Measured tailings grade (g/t)	Calculated head grade (g/t)
AR, 60 min	2.25	3.60
AR, 30 min, +6% water	2.83	4.61
AR, 30 min	2.62	2.86
UF, 30 min	2.06	3.73
Repeat run 1	1.82	4.75
Repeat run 2	1.76	4.46
Repeat run 3	2.16	5.28

AR- As received, UF- ultrafine

Cyanidation of microwave roasted as received samples (Table 9.8).

Table 9.8: Data for cyanidation microwave roasted as received samples (30 min, 30 min+6% water and 60 min.)

30 min				
leach time (h)	0	1	8	24
Au (ug/L)	0	115.56	147.63	173.12
Recovery	0	12.1	15.5	18.2
30min, +6% Water				
leach time (h)	0	1	8	24
Au (ug/L)	0	65.69	510.51	653.78
Recovery	0	4.3	33.2	42.6
60min				
leach time (h)	0	1	8	24
Au (ug/L)	0	223.48	411.68	524.64
Recovery	0	18.6	34.3	43.7

Cyanidation of microwave roasted ultrafine sample (Table 9.9).

Table 9.9: Data for cyanidation microwave roasted ultrafine sample.

30min				
leach time (h)	0	1	8	24
Au (ug/L)	0	402.18	764.86	849.31
Recovery	0	32.4	61.6	68.4

Cyanidation repeats of microwave roasted samples (Table 9.10).

Table 9.10: Data for repeats of cyanidation of microwave roasted samples (30 min, ultrafine)

Run 1				
leach time (h)	0	1	8	24
Au (ug/L)	0	510.27	882.45	940.05
Recovery	0	36.8	63.6	67.8
Run 2				
leach time (h)	0	1	8	24
Au (ug/L)	0	514.48	918.80	1017.04
Recovery	0	34.7	62.0	68.7
Run 3				
leach time (h)	0	1	8	24
Au (ug/L)	0	464.83	991.61	1087.73
Recovery	0	28.3	60.4	66.3

9.8 Appendix H: Microwave assisted cyanidation

Samples grades for microwave assisted cyanidation (Table 9.11).

Table 9.11: Samples grades for microwave assisted cyanidation.

Cyanidation run	Measured tailings grade (g/t)	Calculated head grade (g/t)
2kg/t NaCN, AR	3.54	3.14
2kg/t NaCN, Ultrafine	2.83	2.91
4kg/t NaCN, AR	3.22	3.44
4kg/t NaCN, Ultrafine	4.81	7.03
8kg/t NaCN, AR	3.08	3.61
8kg/t NaCN, Ultrafine	3.15	6.37
Repeat Run 1	3.05	7.79
Repeat Run 2	2.29	5.66
Repeat Run 3	1.71	4.12

AR - As received,

Microwave assisted cyanidation (Table 9.12).

Table 9.12: Data for microwave assisted cyanidation.

2kg/t NaCN, AR				
leach time (h)	0	10	30	50
Au (ug/L)	0	13.87	12.83	14.31
Recovery	0	3.1	2.9	3.2
2kg/t NaCN, Ultrafine				
leach time (h)	0	10	30	50
Au (ug/L)	0	21.41	36.76	62.20
Recovery	0	5.2	8.9	15.0
4kg/t NaCN, AR				
leach time (h)	0	10	30	50
Au (ug/L)	0	65.31	94.30	116.16
Recovery	0	11.4	16.4	20.3
4kg/t NaCN, Ultrafine				
leach time (h)	0	10	30	50
Au (ug/L)	0	254.20	325.95	462.48
Recovery	0	21.7	27.8	39.5
8kg/t NaCN, AR				
leach time (h)	0	10	30	50
Au (ug/L)	0	70.04	114.86	173.85
Recovery	0	11.7	19.1	28.9
8kg/t NaCN, Ultrafine				
leach time (h)	0	10	30	50
Au (ug/L)	0	274.49	367.50	603.35
Recovery	0	25.9	34.6	56.9

Repeats of microwave assisted cyanidation (Table 9.13).

Table 9.13: Repeats of microwave assisted cyanidation (ultrafine, NaCN 8kg/t).

Run 1		
leach time (h)	0	50
Au (ug/L)	0	849.24
Recovery	0	65.4
Run 2		
leach time (h)	0	50
Au (ug/L)	0	602.98
Recovery	0	63.9
Run 2		
leach time (h)	0	50
Au (ug/L)	0	432.11
Recovery	0	62.9

9.9 Appendix I: Sodium hydroxide pre-leach pre-treatment

Samples grades for NaOH pre-leach pre-treatment (Table 9.14).

Table 9.14: Pre-leach samples grades.

Pre-leach run	**Measured tailings grade (g/t)**	**Calculated feed grade (g/t)**
Amb, AR, 1M	5.14	5.30
Amb, AR, 3M	3.84	3.90
Amb, UF, 1M	3.61	3.79
Amb, UF, 3M	4.20	4.49
80℃, AR, 3M	3.56	3.83
80℃, AR, 1M	2.99	3.09
80℃, UF, 3M	3.65	4.31
80℃, UF, 1M	3.49	3.59

Amb-25℃, AR - As received, UF-Ultrafine

Gold leached during NaOH pre-leach pre-treatment (Table 9.15).

Table 9.15: Gold leached during NaOH pre-leach runs.

Amb, AR, 1 M		
leach time (h)	0	4
Au (ug/L)	0	1.29
Recovery	0	0.07
Amb, AR, 3 M		
leach time (h)	0	4
Au (ug/L)	0	1.30
Recovery	0	0.10
Amb, UF, 1M		
leach time (h)	0	4
Au (ug/L)	0	2.26
Recovery	0	0.18
Amb, UF, 3 M		
leach time (h)	0	4
Au (ug/L)	0	2.10
Recovery	0	0.14
80°C, AR, 1 M		
leach time (h)	0	4
Au (ug/L)	0	13.50
Recovery	0	1.30
80°C, AR, 3 M		
leach time (h)	0	4
Au (ug/L)	0	3.22
Recovery	0	0.25
80°C, UF, 1 M		
leach time (h)	0	4
Au (ug/L)	0	0.00
Recovery	0	0.00
80°C, UF, 3 M		
leach time (h)	0	4
Au (ug/L)	0	70.88
Recovery	0	4.65

Amb-25°C, AR - As received, UF-Ultrafine

Cyanidation samples grades for sodium hydroxide pre-leach pre-treatment (Table 9.16).

Table 9.16: Cyanidation samples grades.

Cyanidation run	**Measured tailings grade (g/t)**	**Calculated feed grade (g/t)**
Amb, AR, 1M	2.66	5.30
Amb, AR, 3M	2.39	3.90
Amb, UF, 1M	1.68	3.79
Amb, UF, 3M	1.96	4.49
80℃, AR, 3M	2.55	3.83
80℃, AR, 1M	2.36	3.09
80℃, UF, 3M	1.88	4.31
80℃, UF, 1M	1.64	3.59
Repeat run 1	1.35	3.17
Repeat run 2	1.37	2.73
Repeat run 3	2.73	3.12

Amb-25℃, AR - As received, UF-Ultrafine

Cyanidation of NaOH pre-leach pre-treatment residues (Table 9.17).

Table 9.17: Cyanidation of NaOH pre-leach residue.

Amb, AR, 1 M			
leach time (h)	0	8	24
Au (ug/L)	0	452.59	911.51
Recovery	0	25.6	51.6
Amb, AR, 3 M			
leach time (h)	0	8	24
Au (ug/L)	0	356.17	526.92
Recovery	0	27.4	40.5
Amb, UF, 1 M			
leach time (h)	0	8	24
Au (ug/L)	0	723.93	590.85
Recovery	0	72.0	58.7
Amb, UF, 3 M			
leach time (h)	0	8	24
Au (ug/L)	0	930.24	860.51
Recovery	0	77.6	71.8
80°C, AR, 1 M			
leach time (h)	0	8	24
Au (ug/L)	0	253.64	265.31
Recovery	0	24.6	25.8
80°C, AR, 3 M			
leach time (h)	0	8	24
Au (ug/L)	0	282.01	442.12
Recovery	0	22.1	34.6
80°C, UF, 1 M			
leach time (h)	0	8	24
Au (ug/L)	0	572.83	671.96
Recovery	0	47.9	56.2
80°C, UF, 3 M			
leach time (h)	0	8	24
Au (ug/L)	0	536.58	505.05
Recovery	0	59.9	56.4

Amb-25°C, AR - As received, UF-Ultrafine

Cyanidation repeats of NaOH pre-leach pre-treatment residues (Table 9.18).

Table 9.18: Repeats of cyanidation of NaOH pre-leach residue (ultrafine, 3 M, 80°C).

Run 1			
leach time (h)	0	8	24
Au (ug/L)	0	685.75	618.20
Recovery	0	66.7	60.1
Run 2			
leach time (h)	0	8	24
Au (ug/L)	0	606.83	479.69
Recovery	0	70.9	56.0
Run 3			
leach time (h)	0	8	24
Au (ug/L)	0	731.17	595.93
Recovery	0	73.2	59.7

9.10 Appendix J: Calculation of the projected contribution of the calcine tailings to the PAR Group

Calculating possible contribution of the calcine tailings to PAR Group's projected gold output:

Assuming a minimum of 80% gold recovery: 0.8*2.96 g/t*270 000 t *(1 oz/28.3495231 g)

= 22 552.76 oz

Given that the Group's target is 200 000 oz, it implies the contribution from the calcine tailings that year will be: (22 555.76 oz /200 000 oz) *100 = 11.3%

Time taken to process the calcine tailings dump: 270 000 t/100 000 t/month = 2.7 months

9.11 Appendix K: SEM spectra for cyanidation tailings of microwave roasted calcine

Table 9.19 presents the individual spectra analysis of the electron image for cyanidation tailings of microwave roasted calcine.

Table 9.19: SEM individual spectra analysis of the electron image 15.

Spectrum Label	Spectrum 65	Spectrum 66	Spectrum 67	Spectrum 68	Spectrum 69	Spectrum 70	Spectrum 71	Spectrum 72	Spectrum 73	Spectrum 74	Spectrum 75	Spectrum 76	Spectrum 77
O	38.15	22.85	23.75	43.20	23.45	41.77	52.19	33.78	41.48	52.13	29.11	39.45	31.14
Na	0.62	0.00	0.34	0.46	0.00	1.54	0.00	0.40	0.38	0.00	0.28	0.74	0.21
Mg	6.95	0.07	0.52	9.03	0.56	6.62	0.51	3.80	10.86	1.20	6.95	10.61	3.82
Al	3.49	0.05	0.80	2.49	0.49	5.53	0.44	2.75	1.92	0.63	2.33	5.52	2.81
Si	17.97	0.56	1.30	24.79	1.18	21.71	44.50	13.33	22.10	43.81	5.39	17.09	9.15
S	0.06	0.17	0.01	0.03	0.00	0.06	0.05	0.00	0.00	0.17	0.00	0.00	0.20
Ca	2.74	0.11	0.36	8.12	0.17	5.48	0.24	3.09	5.61	0.26	0.96	1.86	2.07
Fe	29.76	76.16	71.71	11.68	73.81	17.28	1.98	42.58	17.02	1.74	52.27	24.56	50.58
As	0.27	0.00	1.19	0.00	0.26	0.00	0.09	0.26	0.62	0.00	2.71	0.17	0.00
Ag	0.00	0.03	0.00	0.20	0.08	0.00	0.00	0.01	0.00	0.05	0.00	0.00	0.00
Total	100.00	100.00	100.00	100.00	100.00	100.00	100.00	100.00	100.00	100.00	100.00	100.00	100.00

9.12 Appendix L: SEM spectra for microwave assisted cyanidation tailings

Table 9.20 presents the individual spectra analysis of the electron image for cyanidation tailings of microwave assisted leaching.

Table 9.20: SEM individual spectra analysis of the electron image 45.

Spectrum Label	Spectrum 24	Spectrum 25	Spectrum 26	Spectrum 27	Spectrum 28	Spectrum 29	Spectrum 30	Spectrum 31	Spectrum 32	Spectrum 33	Spectrum 34
O	47.61	48.63	24.63	28.29	28.28	39.26	24.56	42.63	34.68	52.45	26.17
Na	0.10	0.04	0.24	0.12	0.24	0.00	0.16	0.32	1.01	1.71	0.25
Mg	0.01	0.00	0.10	11.15	5.66	16.32	0.54	13.03	9.75	0.39	5.26
Al	0.22	0.05	0.20	0.22	0.73	9.93	0.34	2.06	6.40	0.07	1.18
Si	0.00	0.04	0.47	6.87	2.37	25.42	1.20	27.13	19.20	0.38	6.96
S	0.00	0.00	0.02	0.04	0.23	0.00	0.16	0.00	0.16	0.00	0.23
Ca	51.28	50.53	0.25	0.54	0.72	0.00	0.39	9.49	2.30	0.74	1.13
Fe	0.72	0.65	73.40	51.22	51.57	9.07	72.34	5.22	25.87	42.02	57.22
As	0.02	0.06	0.25	1.30	10.00	0.00	0.12	0.00	0.47	2.24	1.51
Ag	0.04	0.00	0.00	0.00	0.00	0.00	0.19	0.00	0.00	0.00	0.08
Au	0.00	0.00	0.44	0.23	0.19	0.00	0.00	0.13	0.16	0.00	0.00
Total	100.00	100.00	100.00	100.00	100.00	100.00	100.00	100.00	100.00	100.00	100.00
Spectrum Label	Spectrum 35	Spectrum 36	Spectrum 37	Spectrum 38	Spectrum 39	Spectrum 40	Spectrum 41	Spectrum 42	Spectrum 43	Spectrum 44	Spectrum 45
O	28.21	22.99	26.50	27.65	25.59	1.55	38.86	40.71	48.75	42.14	49.04
Na	0.29	0.00	0.00	0.28	0.69	0.17	0.37	0.60	0.00	0.39	0.07
Mg	3.57	6.43	2.60	2.85	3.94	0.02	2.84	9.30	0.00	11.83	0.90
Al	2.91	2.77	2.09	2.02	2.64	0.10	18.78	2.22	0.00	2.22	0.67
Si	5.31	10.66	5.96	7.58	8.49	0.33	27.60	25.97	50.71	26.98	41.97
S	0.10	0.24	0.03	0.05	0.00	0.00	0.00	0.00	0.00	0.00	0.08
Ca	0.29	2.90	0.63	0.96	0.92	0.05	1.70	9.14	0.10	9.54	2.37
Fe	58.35	53.16	61.36	57.60	57.49	97.61	9.81	11.92	0.30	6.83	4.59
As	0.69	0.62	0.57	0.48	0.24	0.17	0.05	0.00	0.11	0.00	0.32
Ag	0.19	0.23	0.00	0.43	0.00	0.00	0.00	0.14	0.03	0.08	0.00
Au	0.10	0.00	0.25	0.10	0.00	0.00	0.00	0.00	0.00	0.00	0.00
Total	100.00	100.00	100.00	100.00	100.00	100.00	100.00	100.00	100.00	100.00	100.00

9.13 Appendix M: SEM spectra for cyanidation tailings of pre-leach pre-treatment residue

Table 9.21 presents the individual spectra analysis of the electron image for cyanidation tailings of NaOH pre-leach residue.

Table 9.21: SEM individual spectra analysis of the electron image 51.

Spectrum Label	Spectrum 47	Spectrum 48	Spectrum 49	Spectrum 50	Spectrum 51	Spectrum 52	Spectrum 53	Spectrum 54	Spectrum 55	Spectrum 56	Spectrum 57
O	48.76	25.47	44.18	2.31	44.65	42.93	32.28	24.78	43.48	30.90	48.11
Na	0.34	0.13	5.12	0.00	6.41	0.06	0.02	0.12	0.05	0.93	0.44
Mg	0.23	1.05	0.03	0.58	0.08	13.54	3.65	0.86	17.57	8.32	0.85
Al	0.34	0.58	14.74	0.33	13.18	0.57	20.84	0.53	0.00	3.84	0.37
Si	0.79	1.65	28.99	0.64	31.53	28.10	36.87	1.32	28.68	18.27	2.07
S	0.00	0.05	0.00	0.15	0.00	0.01	0.00	0.01	0.06	0.10	0.00
Ca	48.63	0.53	6.49	0.41	3.79	9.59	0.00	0.32	0.37	4.20	46.33
Fe	0.76	70.44	0.46	95.03	0.36	5.00	6.24	71.89	9.79	33.09	1.83
As	0.14	0.08	0.00	0.06	0.00	0.00	0.10	0.00	0.00	0.00	0.00
Ag	0.00	0.00	0.00	0.25	0.00	0.22	0.00	0.17	0.00	0.33	0.00
Au	0.00	0.00	0.00	0.23	0.00	0.00	0.00	0.00	0.00	0.03	0.00
Total	100.00	100.00	100.00	100.00	100.00	100.00	100.00	100.00	100.00	100.00	100.00

9.14 Appendix N: Mass balance: cyanidation of microwave roasting pre-treatment

Table 9.22 presents gold mass balance determination for cyanidation of microwave roasted calcine.

Table 9.22: Gold mass balance determination for cyanidation of microwave roasted calcine.

			Reactants					Products	
	Reaction 1		Au	NaCN	O_2	H_2O	=	$Na(Au(CN)_2)$	NaOH
		Stoichiometric coefficients	4.00000	8.00000	1.00000	2.00000		4.00000	4.00000
		Molecular weight (g/mol)	196.967	49.0072	31.9980	18.0153		271.990	39.9970
		Mass(g/hr)	440.448						
Step 1	100% conversion	Mole (mol/hr)	2.23616	4.47231	0.559039	1.118078		2.23616	2.23616
Step 2	Check	Mass (g/hr)	440.448	219.175	17.8881	20.1425		608.212	89.4395
						697.654			697.652
		Gold Recovery (%)	43.7300						

Step 3	Actual		Reactants					Products	
			Au	NaCN	O_2	H_2O	=	$Na(Au(CN)_2)$	NaOH
		Stoichiometric coefficients	4.00000	8.00000	1.00000	2.00000		4.00000	4.00000
		Molecular weight (g/mol)	196.967	49.0072	31.9980	18.0100		271.990	40.0000
		Mass(g/hr)	192.608						
		Mole (mol/hr)	0.977871	1.95574	0.244468	0.488936		0.977871	0.977871
		Mass (g/hr)	192.608	95.8454	7.82248	8.80573		265.971	39.1148

9.15 Appendix O: Mass balance: microwave assisted leaching

Table 9.23 presents gold mass balance determination for microwave assisted cyanidation.

Table 9.23: Gold mass balance determination for microwave assisted cyanidation.

Microwave Assisted leaching			Reactants					Products	
	Reaction 1		Au	NaCN	O_2	H_2O	=	$Na(Au(CN)_2)$	NaOH
		Stoichiometric coefficients	4.00000	8.00000	1.00000	2.00000		4.00000	4.00000
		Molecular weight (g/mol)	196.967	49.0072	31.9980	18.0100		271.990	40.0000
		Mass(g/hr)	440.448						
Step 1	100% conversion	Mole (mol/hr)	2.23616	4.47231	0.559039	1.118078		2.23616	2.23616
Step 2	Check	Mass (g/hr)	440.448	219.175	17.8881	20.1366		608.212	89.4462
						697.64822			697.6583464
		Gold Recovery (%)	56.8600						

Step 3	Actual		Reactants					Products	
			Au	NaCN	O_2	H_2O	=	$Na(Au(CN)_2)$	NaOH
		Stoichiometric coefficients	4.00000	8.00000	1.00000	2.00000		4.00000	4.00000
		Molecular weight (g/mol)	196.967	49.0072	31.9980	18.0100		271.990	40.0000
		Mass(g/hr)	250.439						
		Mole (mol/hr)	1.271478	2.54296	0.317870	0.635739		1.271478	1.271478
		Mass (g/hr)	250.439	124.6232	10.17119	11.44966		345.829	50.8591

9.16 Appendix P: Mass balance: sodium hydroxide pre-leach pre-treatment and cyanidation of pre-leach residue

Sodium hydroxide pre-leach pre-treatment and cyanidation of pre-leach residue

Table 9.24 highlights gold mass balance determination for sodium hydroxide pre-leach.

Table 9.24: Gold mass balance for sodium hydroxide pre-leach.

			Reactants			Products
	Gold loss reaction	(thiosulfate loss)	Au^{+}	$S_2O_3^{2-}$	=	$Au(S_2O_3^{2-})_2$
		stoichiometric coefficients	1.00000	2.00000		1.00000
		molecular weight g/mol	196.967	112.130		421.227
		mass (g/h)	440.448			
step 1	100% conversion	mole (mol/h)	2.23616	4.47231		2.23616
step 2	check	mass g/h	440.448	501.480		941.928
				941.928		941.928
		Gold recovery (%)	0.140000			

			Reactants		=	Products
step 3	Actual					
			Au^{+}	$S_2O_3^{2-}$		$Au(S_2O_3^{2-})_2$
		stoichiometric coefficients	1.00000	2.00000		1.00000
		molecular weight g/mol	196.967	112.130		421.227
		mass (g/h)	439.831			
		mole (mol/h)	2.23303	4.46605		2.23303
		mass g/h	439.831	500.778		940.610
				940.610		940.610

Cyanidation of pre-leach pre-treatment residue.

Table 9.25 highlights gold mass balance determination for cyanidation of sodium hydroxide pre-leach pre-treatment residue.

Table 9.25: Gold mass balance for cyanidation of sodium hydroxide pre-leach residue.

Cyanidation of NaOH pre-leach residue			Reactants					Products	
	Reaction 1		Au	NaCN	O_2	H_2O	=	$Na(Au(CN)_2)$	NaOH
		Stoichiometric coefficients	4.00000	8.00000	1.00000	2.00000		4.00000	4.00000
		Molecular weight (g/mol)	196.967	49.0072	31.9980	18.0100		271.990	40.0000
		Mass(g/hr)	439.831						
Step 1	100% conversion	Mole (mol/hr)	2.23303	4.46605	0.558256	1.116513		2.23303	2.23303
Step 2	Check	Mass (g/hr)	439.831	218.869	17.8631	20.1084		607.361	89.3210
						696.67151			696.68162
		Gold Recovery (%)	77.6300						

Step 3	Actual		Reactants					Products	
			Au	NaCN	O_2	H_2O	=	$Na(Au(CN)_2)$	NaOH
		Stoichiometric coefficients	4.00000	8.00000	1.00000	2.00000		4.00000	4.00000
		Molecular weight (g/mol)	196.967	49.0072	31.9980	18.0100		271.990	40.0000
		Mass(g/hr)	341.920						
		Mole (mol/hr)	1.73593	3.47186	0.433982	0.867964		1.73593	1.73593
		Mass (g/hr)	341.920	170.146	13.88656	15.6320		472.155	69.4371